



Pacific Northwest
NATIONAL LABORATORY

Proudly Operated by Battelle Since 1965

A Critical Review of the Impacts of Leaking CO₂ Gas and Brine on Groundwater Quality

September 2015

NP Qafoku^{1,*}
L Zheng^{2,*}
DH Bacon^{1,*}

AR Lawter¹
CF Brown¹

1 Pacific Northwest National Laboratory

2 Lawrence Berkeley National Laboratory

*NPQ, LZ and DB provided equal contributions to this report



Prepared for the U.S. Department of Energy
under Contract DE-AC05-76RL01830

DISCLAIMER

This report was prepared as an account of work sponsored by an agency of the United States Government. Neither the United States Government nor any agency thereof, nor Battelle Memorial Institute, nor any of their employees, makes **any warranty, express or implied, or assumes any legal liability or responsibility for the accuracy, completeness, or usefulness of any information, apparatus, product, or process disclosed, or represents that its use would not infringe privately owned rights.** Reference herein to any specific commercial product, process, or service by trade name, trademark, manufacturer, or otherwise does not necessarily constitute or imply its endorsement, recommendation, or favoring by the United States Government or any agency thereof, or Battelle Memorial Institute. The views and opinions of authors expressed herein do not necessarily state or reflect those of the United States Government or any agency thereof.

PACIFIC NORTHWEST NATIONAL LABORATORY
operated by
BATTELLE
for the
UNITED STATES DEPARTMENT OF ENERGY
under Contract DE-AC05-76RL01830

Printed in the United States of America

Available to DOE and DOE contractors from the
Office of Scientific and Technical Information,
P.O. Box 62, Oak Ridge, TN 37831-0062;
ph: (865) 576-8401
fax: (865) 576-5728
email: reports@adonis.osti.gov

Available to the public from the National Technical Information Service
5301 Shawnee Rd., Alexandria, VA 22312
ph: (800) 553-NTIS (6847)
email: orders@ntis.gov <<http://www.ntis.gov/about/form.aspx>>
Online ordering: <http://www.ntis.gov>



This document was printed on recycled paper.

(8/2010)

A Critical Review of the Impacts of Leaking CO₂ Gas and Brine on Groundwater Quality

NP Qafoku¹
L Zheng²
DH Bacon¹

AR Lawter¹
CF Brown¹

1 Pacific Northwest National Laboratory

2 Lawrence Berkeley National Laboratory

*NPQ, LZ and DB provided equal contributions to this report

September 2015

Prepared for
the U.S. Department of Energy
under Contract DE-AC05-76RL01830

Pacific Northwest National Laboratory
Richland, Washington 99352

Acknowledgments

The U.S. Department of Energy's (DOE's) Office of Fossil Energy has established the National Risk Assessment Partnership (NRAP) Project. This multiyear project harnesses the breadth of capabilities across the DOE national laboratory system to develop a defensible, science-based quantitative methodology for determining risk profiles at carbon dioxide (CO₂) storage sites. As part of this effort, scientists from Lawrence Berkeley National Laboratory (LBNL), Lawrence Livermore National Laboratory (LLNL), Los Alamos National Laboratory (LANL), Pacific Northwest National Laboratory (PNNL), and the National Energy Technology Laboratory (NETL) are working to evaluate the potential for aquifer impacts should CO₂ or brine leak from deep subsurface storage reservoirs. The research presented in this report was completed as part of the groundwater protection task of the NRAP Project. NRAP funding was provided to PNNL under DOE contract number DE-AC05-76RL01830.

Contents

Acknowledgments.....	iii
1.0 Introductory Remarks	1.1
2.0 Objectives	2.1
3.0 Geochemical Data Required to Assess and Predict Aquifer Responses to CO ₂ and Brine Leakage.....	3.1
3.1 Threshold Values & Average Groundwater Concentrations.....	3.1
3.1.1 High Plains Aquifer.....	3.1
3.1.2 Edwards Aquifer	3.2
3.1.3 Other Aquifers.....	3.3
3.2 Solid Phase Properties: Mineralogy	3.7
3.2.1 High Plains Aquifer.....	3.7
3.2.2 Edwards Aquifer	3.10
3.3 Other Aquifers.....	3.11
3.3.1 Carbonate Aquifers	3.15
3.3.2 Sandstone and Unconsolidated Sand and Gravel Aquifers	3.16
3.3.3 Comparison of Different Aquifers	3.17
3.4 Relevant Processes and Reactions.....	3.17
3.4.1 Surface Reactions	3.18
3.4.2 Dissolution/Precipitation	3.25
3.4.3 Redox Reactions.....	3.28
3.5 Development of Conceptual and Reduced Order Models	3.28
4.0 Potential Risk for Groundwater Pollution Due to CO ₂ Gas and Brine Intrusion.....	4.1
4.1 The Effects on TDS and pH	4.1
4.1.1 High Plains Aquifer.....	4.1
4.1.2 Edwards Aquifer	4.2
4.2 Changes in Major, Minor, and Trace Element Concentration.....	4.4
4.2.1 High Plains Aquifer.....	4.4
4.2.2 Edwards Aquifer	4.7
4.2.3 Other Aquifers.....	4.11
4.3 Changes in Organic Contaminant Concentrations	4.12
4.3.1 High Plains Aquifer.....	4.12
4.3.2 Edwards Aquifer	4.18
4.3.3 Reservoirs as a Source Term for Organic Compounds	4.21
5.0 Conclusive Remarks	5.1
5.1 Crucial Site-Specific Data.....	5.1
5.2 Potential Risk to Groundwater	5.2
5.3 Future Efforts	5.3

6.0 References 6.1

Figures

3.1	Comparison of Background Values of pH for the High Plains Aquifer and Shallow, Urban Unconfined Portion of the Edwards Aquifer used in NRAP Studies with Ranges for Various Aquifer Types in the U.S	3.5
3.2	Comparison of Background Values of TDS for the High Plains Aquifer and Shallow, Urban Unconfined Portion of the Edwards Aquifer used in NRAP Studies with Ranges for Various Aquifer Types in the U.S	3.5
3.3	Comparison of Background Values of Arsenic for the High Plains Aquifer and Shallow, Urban Unconfined Portion of the Edwards Aquifer used in NRAP Studies with Ranges for Various Aquifer Types in the U.S	3.6
3.4	Comparison of Background Values of Barium for the High Plains Aquifer and Shallow, Urban Unconfined Portion of the Edwards Aquifer used in NRAP Studies with Ranges for Various Aquifer Types in the U.S	3.6
3.5	Comparison of Background Values of Lead for the High Plains Aquifer and Shallow, Urban Unconfined Portion of the Edwards Aquifer used in NRAP Studies with Ranges for Various Aquifer Types in the U.S	3.7
3.6	SEM/EDS for (a) CNG 8, (b) CNG 60, (c) CNG 150, and (d) CAL 121 91.....	3.9
3.7	SEM/EDS for Edwards Samples: (a) Set A #1, (b) Set A #7, and (c) Set B # 2	3.11
3.8	Schematic of the CO ₂ and Brine Leakage Model Parameters and Profiles in the Generalized Model.....	3.30
4.1	Simulated and Observed Breakthrough Curves of pH for the Column Test of Sample CNG60.....	4.2
4.2	Major Ion Modeling Results Compared to Column Experiment Results	4.4
4.3	Simulated and Observed Breakthrough Curves of Ca for the Column Test of Sample CNG60	4.6
4.4	Simulated and Observed Breakthrough Curves of As for the Column Test of Sample CNG60	4.6
4.5	As Modeling Results Compared to Column Experiment Results and Aquifer Concentrations	4.8
4.6	Ba Modeling Results Compared to Experimental Results and Aquifer Concentrations	4.8
4.7	Cr Modeling Results Compared to Experimental Results and Aquifer Concentrations.....	4.9
4.8	Cu Modeling Results Compared to Experimental Results and Aquifer Concentrations	4.9
4.9	Pb Modeling Results Compared to Experimental Results and Aquifer Concentrations	4.10
4.10	Sb Modeling Results Compared to Experimental Results and Aquifer Concentrations	4.10
4.11	Se Modeling Results Compared to Experimental Results and Aquifer Concentrations.....	4.11
4.12	Cross Section Views of the Spatial Distribution of pH at 50, 200 years. (a) at y=2600 m, (b) at x = 2000 m, and (c) at z = -202.5 m.....	4.15
4.13	Cross Section Views of the Spatial Distribution of Total Aqueous Benzene Concentration at 200 Years: (a) at y=2600 m, (b) at x = 2000 m, and (c) at z = -202.5 m.....	4.15
4.14	An Iso-Surface at Benzene Concentration of 3.84e-10 mol/L.....	4.16
4.15	Cross Section Views of the Spatial Distribution of Total Aqueous Naphthalene Concentration at 200 Years: (a) at y=2600 m, (b) at x = 2000 m, and (c) at z = -202.5 m	4.16
4.16	An Iso-Surface at Naphthalene Concentration of 1.53e-9 mol/L	4.17
4.17	Cross Section Views of the Spatial Distribution of Total Aqueous Phenol Concentration at 200 Years: (a) at y=2600 m, (b) at x = 2000 m, and (c) at z = -202.5 m.....	4.17
4.18	An Iso-Surface at Naphthalene Concentration of 3.19e-11 mol/L	4.18
4.19	Cumulative Density Function of Aquifer Volume Exceeding Organic No-Impact Thresholds during 200 Years of Well Leakage	4.20

Tables

3.1	Initial Aquifer Concentrations Used in the Simulations, Estimated Mean Aquifer Values, and No-Impact Thresholds	3.2
3.2	Initial Values, Tolerance Limits, and Regulatory Standards for each Variable	3.3
3.3	Aquifer Name Abbreviations.....	3.4
3.4	A Summary of Recent Studies Conducted in Different Aquifers.....	3.12
3.5	Surface Protonation and Complexation Reactions on Goethite.....	3.19
3.6	Surface Protonation and Complexation Reactions on HFO	3.20
3.7	Surface Protonation and Complexation Reactions of Cations on Illite	3.21
3.8	Surface Protonation and Complexation Reactions of Cations on Kaolinite	3.21
3.9	Surface Protonation and Complexation Reactions of Cations on Montmorillonite	3.22
3.10	Surface Protonation and Complexation Reactions of Anions on Calcite	3.22
3.11	Cation Exchange Reactions and Selectivity Coefficients, Using the Gaines-Thomas Convention.	3.23
3.12	Compilation of Published K_d for Benzene Between Soil and Water.....	3.23
3.13	K_{oc} for Benzene, Phenol, and Naphthalene.....	3.24
3.14	Degradation Rate Constant for Benzene, Phenol, and Naphthalene.....	3.25
3.15	Kinetic Mineral Reactions and Neutral Mechanism Rates for the Edwards Aquifer at 25°C	3.25
3.16	Equilibrium Constants of the Major Rock-Forming Minerals for the High Plains Aquifer	3.26
3.17	Kinetic Properties for Minerals Considered in the Model.....	3.27
3.18	Proposed Parameter Ranges for Generalized CO ₂ and Brine Leakage Models.....	3.30
3.19	Sodium, Trace Metals and Organics Concentrations Considered in the Groundwater Simulations and ROM	3.31
3.20	Parameter Definition and Ranges for Hydrologic Simulations and Emulations	3.31
3.21	Input Parameters of the Development of the Scaling Functions	3.31
4.1	Mineral Reactions.....	4.3
4.2	Aqueous Complexation Reactions.....	4.3
4.3	Summary of Column Experiment Trace Metal Concentrations at the End of Each Experimental Stage, Relative to Aquifer Maximum Concentrations and MCL Regulatory Limits	4.7
4.4	Organics Concentrations in Brine Considered in the Reactive Transport Model.....	4.13
4.5	Distribution Coefficient and Degradation Constant for Organic Compounds.....	4.13
4.6	Flow and Chemical Parameters used in Simulations that Model Results.....	4.14
4.7	Input Parameters for Organic Adsorption and Biodegradation	4.18
4.8	Organic Concentration Ranges in Brine	4.19
4.9	Initial Values, Tolerance Limits, and Regulatory Standards for Each Variable.....	4.19

1.0 Introductory Remarks

Geological carbon sequestration (GCS) is a global carbon emission reduction strategy involving the capture of CO₂ emitted from fossil fuel burning power plants, as well as the subsequent injection of the captured CO₂ gas into deep saline aquifers or depleted oil and gas reservoirs. A critical question that arises from the proposed GCS is the potential impacts of CO₂ injection on the quality of drinking-water systems overlying CO₂ sequestration storage sites.

Although storage reservoirs are evaluated and selected based on their ability to safely and securely store emplaced fluids, leakage of CO₂ from storage reservoirs is a primary risk factor and potential barrier to the widespread acceptance of geologic CO₂ sequestration (OR Harvey et al. 2013; Y-S Jun et al. 2013; DOE 2007). Therefore, a systematic understanding of how CO₂ leakage would affect the geochemistry of potable aquifers, and subsequently control or affect elemental and contaminant release via sequential and/or simultaneous abiotic and biotic processes and reactions is vital.

Two possible scenarios for CO₂ leakage have been identified: a sudden, fast, and short-lived release of CO₂, as seen in the case of a well failure during injection or a sudden blowout (S Holloway, Pearce, J.M., Hards, V.L., Ohsumi, T., Gale, J. 2007; P Jordan, Benson, S. 2009; L Skinner 2003), or a slower, more gradual leak, occurring along undetected faults, fractures, or well linings (A Annunziatellis et al. 2008; S Bachu 2008; MA Celia and JM Nordbotten 2009; K Damen et al. 2005; JL Lewicki et al. 2007; JM Nordbotten et al. 2005; GW Scherer et al. 2011); however, well related leaks appear to be declining thanks to improved construction and operation (RL Newmark et al. 2010).

Upon entering an aquifer, a portion of the CO₂ gas will dissolve into the groundwater, which will cause a subsequent decrease in aqueous pH (RC Trautz et al. 2013) due to the formation and disassociation of carbonic acid (OR Harvey et al. 2013). The reduced pH can then cause an increase in the mobilization of major (Ca, Mg, K, Na, etc) and minor (Fe, Al, Ba, etc.) elements as well as potential contaminants via desorption and/or dissolution reactions. Changes in other water quality parameters, such as alkalinity, salinity, and total dissolved solids (TDS), may also occur.

Properties of the aquifer and the network of processes and reactions may also impact a system's behavior and response, and may also have an impact on potential risks associated with CO₂ sequestration. Brine can be brought upward into an overlying groundwater aquifer with increased pressure due to CO₂ injection (CM Oldenburg and AP Rinaldi 2011). Salinity of the brine, as well as presence of contaminants, such as As and Cd, can vary and can increase negative effects of CO₂ leakage.

Over the last decade, a number of studies have been undertaken to assess the impacts of potential CO₂ leakage from deep storage reservoirs on the quality of overlying freshwater aquifers. These studies include natural analogs (Pd Caritat et al. 2013; JL Lewicki, J Birkholzer and C-F Tsang 2007; EH Keating et al. 2010), field in-situ CO₂ injection (YK Kharaka et al. 2010; B Nisi et al. 2013; A Peter et al. 2012; RC Smyth et al. 2009; RC Trautz et al. 2013), and experimental column and batch studies (P Humez et al. 2013; MG Little and RB Jackson 2010; J Lu et al. 2010; G Montes-Hernandez et al. 2013; G Wang et al. 2015; Y Wei et al. 2011). However, the results of the studies are contradictory as some indicate CO₂ leaks pose a serious risk (AG Cahill et al. 2013; YK Kharaka et al. 2010; MG Little and RB Jackson 2010; J Lu et al. 2010; S Wang and PR Jaffe 2004; Y Wei, M Maroto-Valer and MD Steven 2011; L Zheng et al. 2009; CQ Vong et al. 2011), some indicate low levels of risk (E Frye et al. 2012; K Kirsch et al. 2014; PJ Mickler et al. 2013; EH Keating et al. 2010), and others have found some possible benefits (such as the removal of As, U, V, and Cr) related to CO₂ leakage into groundwater (J Lu et al. 2010; RC Smyth et al. 2009). Clearly, the scientific community has not yet reached an agreement on the important issue of

deciding whether the impacts from the leakage of CO₂ into groundwater are negative, insignificant, or positive.

This report summarizes data and findings that are already published in the literature over the last several years. In addition, a summary of the results collected over the last four years from batch and column experiments conducted at the Pacific Northwest National Laboratory and the associated modeling efforts conducted at PNNL and Lawrence Berkley National Laboratory (LBNL) will be presented and discussed.

The experiments were conducted with materials from two representative aquifer types that commonly overlie potential CO₂ sequestration reservoirs: the Edwards Aquifer in TX, representative of unconfined limestone aquifers, and the High Plains Aquifer in KS, representative of typical unconsolidated sand and gravel aquifers. Column experiments in which CO₂ charged synthetic groundwater flows through a column packed with material from the aquifers were conducted to simulate the impact of a gradual leak of CO₂ on a shallow aquifer. Batch experiments were conducted to simulate sudden, short-lived CO₂ release. A reactive transport model was then developed using solid phase characterization data of the aquifer materials to interpret the observed concentration changes in the effluent water, attempting to shed light on the chemical reactions, water-rock interaction mechanisms, and key parameters that control the concentration changes of some constituents.

Although the effects of water-rock interactions may be site-specific, the results from the experimental and modeling efforts will help in developing a systematic understanding of how CO₂ leakage is likely to influence pertinent geochemical processes (e.g., dissolution/precipitation, sorption/desorption). A three-dimensional multiphase flow and reactive transport simulation of CO₂ leakage from an abandoned wellbore into a generalized model of the shallow, unconfined portion of the Edwards Aquifer was also developed to determine potential impacts on groundwater quality.

In addition to the work that focused on aquifer composition, further experiments have been conducted to observe the effects of gaseous impurities and inorganic contaminants on aquifer response. Specifically, CH₄, present with CO₂, was used to represent possible impurities in the gas stream. Additionally, As and Cd spikes were added to the synthetic groundwater used in batch and column experiments based on the maximum As and Cd levels predicted to reach the aquifer from the brine source term within the reservoir, according to modeling simulations by D Bacon (2013). Supplementary experiments were performed to investigate the effect of autotrophic methanogenesis, stimulated by CO₂, on the mobility of metals. Collectively, these tests were conducted to study the effect of gas, trace metal, and biological variations likely to be found in GCS sites.

2.0 Objectives

The objectives of this report are to:

- identify the set of geochemical data required to assess and predict aquifer responses to CO₂ and brine leakage, and
- present and discuss potential risks for groundwater degradation due to CO₂ gas and brine exposure.

Specifically, this report will discuss the following issues:

- Aquifer responses:
 - Changes in aqueous phase (groundwater) chemical composition
 - Changes in solid phase chemistry and mineralogy
 - Changes in the extent and rate of reactions and processes and possible establishment of a new network of reactions and processes affecting or controlling overall mobility of major, minor, and trace elements
 - Development of conceptual and reduced order models (ROMs) to describe and predict aquifer responses
- The degree of impact:
 - Significant or insignificant changes in pH and major, minor, and trace element release that depend on the following controlling variables:
 - Leaking plume characteristics
 - Gas composition (pure CO₂, CO₂-CH₄-H₂S mixtures)
 - Brine concentration and composition (trace metals)
 - Aquifer properties:
 - Initial aqueous phase conditions
 - Mineralogy: minerals controlling sediments' response (e.g., calcite, Si bearing minerals, etc.)
- Overview of relevant hydrogeological and geochemical processes related to the impact of CO₂ gas and brine on groundwater quality
- The fate of the elements released from sediments or transported with brine:
 - Precipitation/incorporation into minerals (calcite and other minerals)
 - Adsorption
 - Electron transfer reactions
 - The role of natural attenuation
- Whether or not the release of metals following exposure to CO₂ harmful
 - Risk assessment.

3.0 Geochemical Data Required to Assess and Predict Aquifer Responses to CO₂ and Brine Leakage

3.1 Threshold Values & Average Groundwater Concentrations

In order to determine whether CO₂ and brine leakage has an impact on groundwater quality, a protocol was established for determining statistically significant changes in groundwater concentrations of regulated contaminants (GV Last et al. 2013). The effort examined selected portions of two aquifer systems: the urban shallow-unconfined aquifer system of the Edwards-Trinity Aquifer System (being used to develop the ROM for carbon-rock aquifers), and a portion of the High Plains Aquifer (an unconsolidated and semi-consolidated sand and gravel aquifer being used to develop the ROM for unconsolidated aquifers).

No-impact threshold values were determined for cadmium, lead, arsenic, pH, TDS, and select organic compounds that could be used to identify potential areas of contamination predicted by numerical models of carbon sequestration storage reservoirs. No-impact threshold values were later determined for chromium specifically to support the ROM being developed by Lawrence Livermore National Laboratory for the High Plains Aquifer. These threshold values are based on an interwell approach for determining background groundwater concentrations as recommended in the U.S. Environmental Protection Agency's document titled, "Unified Guidance for Statistical Analysis of Groundwater Monitoring Data at RCRA Facilities (2009)".

The resulting no-impact threshold values can be used to inform a "no change" scenario with respect to groundwater impacts, rather than use a maximum concentration limit or secondary drinking-water standard that in some cases could be significantly higher than existing concentrations in the aquifer. These no-impact threshold values are intended for use in helping to predict areas of potential impact. They are not intended for use as alternate regulatory limits.

Development of "generic" no-impact threshold values that could be used for a number of locations appears unlikely. Instead, the threshold values must be based on site-specific groundwater quality data. However, the scarcity of existing data, proximity of the data to the target model domain, potential spatial heterogeneity, and temporal trends make the development of statistically robust data sets and the use of valid statistical assumptions challenging. In some cases, the calculated no-impact threshold values may exceed regulatory standards. Other approaches, such as the hybrid intrawell-interwell approach also examined in the study by Last et al. 2013, may provide alternate mechanisms for calculating no-impact threshold limits. Examples are presented in the following sections to demonstrate the development and use of threshold values in two representative aquifers.

3.1.1 High Plains Aquifer

The hydrology ROMs and chemical scaling functions generated in the Generation III ROM are specific to thresholds that represent no net degradation to the groundwater quality. The impact thresholds defined for pH, TDS, trace metals, and select organics in Table 3.1 represent concentrations above (or below for pH) the background water chemistry that could be used to assess impact from brine and/or CO₂ leakage into the aquifer. Each threshold was calculated as the 95%-confidence, 95%-coverage tolerance from data collected in a 2010 U.S. Geological Survey (USGS) groundwater survey of 30 wells within the High Plains Aquifer from an area outside of the lithology model site.

This data set was chosen because spatial and temporal data were not available from wells located within the model domain. We considered benzene, naphthalene, and phenol as representative of benzene, toluene, ethylbenzene, and xylene-volatile aromatic compounds typically found in petroleum (BTEX), poly-aromatic hydrocarbons (PAH), and phenol organic compounds that could be present in the leaking brine (L Zheng et al. 2010). Table 3.1 also includes regulatory standards referring to concentrations that exceed primary or secondary maximum contaminant levels designated by the U.S. EPA (2009). Primary drinking-water standards are for trace metals, such as As, Ba, Cd, Cr, Cu, Pb, and BTEX organics among others, and are legally enforced for the protection of public health by limiting the levels of contaminants in drinking water. Secondary drinking-water standards are for elements such as Fe, Mn, and Zn. Usually, they are non-enforceable guidelines regulating contaminants that may cause cosmetic or aesthetic effects in drinking water. Currently PAHs and phenols are unregulated.

Table 3.1. Initial Aquifer Concentrations Used in the Simulations, Estimated Mean Aquifer Values, and No-Impact Thresholds

Parameter	Initial Value Used in Third-Generation Simulations	Mean of Selected and Adjusted 2010 Data ^b	“No-Impact” Threshold ^c	U.S. EPA Regulatory Standard
pH	7.6 ^a	7.5 ^c	7.0	6.5
TDS	570 mg/L ^{a,d}	440 mg/L ^d	1,300 mg/L ^{d,e}	500 mg/L ^e
Arsenic	1.50 µg/L	1.50 µg/L	9.30 µg/L	10.00 µg/L
Barium	43.00 µg/L ^b	43.00 µg/L ^b	140.00 µg/L	2,000 µg/L
Cadmium	0.06 µg/L	0.06 µg/L	0.25 µg/L	5 µg/L
Chromium	1.00 µg/L	1.00 µg/L	3.90 µg/L	100 µg/L
Iron	5.40 µg/L ^b	5.40 µg/L ^b	43.00 µg/L ^b	300 µg/L
Lead	0.09 µg/L	0.09 µg/L	0.63 µg/L	15 µg/L
Manganese	0.35 µg/L ^d	0.35 µg/L ^d	7.00 µg/L ^d	50 µg/L
Benzene	0	<0.03 µg/L ^d	0.03 µg/L ^g	5 µg/L
Naphthalene	0	<0.20 µg/L ^d	0.20 µg/L ^g	700 µg/L
Phenol	0	<0.003 µg/L ^f	0.003 µg/L ^g	10,000 µg/L ^h

(a) Based on Carroll et al., 2009.

(b) Geometric mean except for pH.

(c) 95%-confidence, 95%-coverage tolerance limit based on log values except for pH.

(d) Rounded to two significant digits.

(e) Threshold value exceeds regulatory standard; using the regulatory standard may result in widespread false positives under field conditions.

(f) As 4-Chloro-2-methylphenol.

(g) Detection limit for the 2010 U.S. Geologic Survey National Water-Quality Assessment Program (NAWQA) sample data.

(h) Recommended Water Quality Criteria for Human Health, consumption of Water + Organism (74 FR 27535);

<http://water.epa.gov/scitech/swguidance/standards/criteria/current/index.cfm#hhtable>.

3.1.2 Edwards Aquifer

As part of the USGS National Water-Quality Assessment (NAWQA) Program (2014), the USGS collected and analyzed groundwater samples from 1996 to 2006 from the San Antonio segment of the Edwards Aquifer of central Texas, a productive karst aquifer developed in Cretaceous-age carbonate rocks (M Musgrove et al. 2010). The National Water-Quality Assessment Program studies provide an

extensive data set of groundwater geochemistry and water quality, consisting of 249 groundwater samples collected from 136 sites (wells and springs), including 1) wells completed in the shallow, unconfined, and urbanized part of the aquifer in the vicinity of San Antonio (shallow/urban unconfined category); 2) wells completed in the unconfined (outcrop area) part of the regional aquifer (unconfined category); and 3) wells completed in springs discharging from the confined part of the regional aquifer (confined category).

Ninety water samples from the shallow, unconfined portion of the Edwards Aquifer in Texas (Musgrove et al., 2010) were used to examine methodologies for establishing baseline data sets and statistical protocols for determining statistically significant changes between background concentrations and predicted concentrations that would be used to represent a contamination plume in the modeling presented in this report (Last et al., 2013). No-impact threshold values were determined for As, Ba, Cd, Pb, benzene, naphthalene, phenol, pH, and TDS that could be used to identify potential areas of contamination predicted by numerical models of carbon sequestration storage reservoirs (Table 3.2). Initial values of these concentrations were also determined using selected statistical methods. For comparison, the EPA maximum contaminant levels (MCLs) are also shown.

Table 3.2. Initial Values, Tolerance Limits, and Regulatory Standards for each Variable

Analyte	Initial Value	“No-Impact” Threshold	Maximum Contaminant Level	Units
Arsenic	0.31	0.55	10	µg/L
Barium	38	54	2000	µg/L
Cadmium	0	0.04	5	µg/L
Lead	0.064	0.15	15	µg/L
Benzene	0	0.016	5	µg/L
Naphthalene	0	0.4	0.20	µg/L
Phenol	0	0.005	10000	µg/L
pH	6.9	6.6	6.5	-log[H ⁺]
TDS	330	420	500	mg/L

3.1.3 Other Aquifers

As part of the NAWQA Program, water samples were collected during 1991–2004 from domestic wells (private wells used for household drinking water) across the United States (U.S.) for analysis of drinking-water contaminants, where contaminants are considered, as defined by the Safe Drinking Water Act, to be all substances in water. The concentrations of major ions, trace elements, nutrients, radon, and organic compounds (pesticides and volatile organic compounds) were measured in as many as 2,167 wells. The wells were located within major hydrogeologic settings of 30 regionally extensive aquifers used for water supply in the U.S. One sample was collected from each well prior to any in-home treatment. Concentrations were compared to water quality benchmarks for human health, either EPA MCLs for public water supplies or USGS Health-Based Screening Levels (HBSLs).

Measurements of pH, TDS, and selected trace metals and organic compounds for eight aquifers were compared to the High Plains and Edwards Aquifers considered in the National Risk Assessment Partnership (NRAP) studies. To simplify comparison, abbreviations for the aquifer names are listed in Table 3.3. Median and 90th percentile values (10th percentile for pH) reported in LA DeSimone (2009) are compared to the initial and no-impact threshold values for the NRAP study aquifers.

All of the aquifers have median pH values ranging from 6.8 to 8.1 (Figure 3.1). Only two aquifers have 10th percentile values that are less than the regulatory limit of 6.5: the Coastal Lowlands sand aquifer (5.1) and New England crystalline-rock aquifer (5.9).

All of the aquifers have median TDS values less than the regulatory limit of 500 mg/L, with the exception of the Lower Tertiary and Upper Cretaceous sandstone aquifers (Figure 3.2). However, many have 90th percentile values above the regulatory limit, with some above 1000 mg/L (HP, BR, LT).

All of the aquifers have median As concentrations less than the regulatory limit of 10 µg/L (Figure 3.3), but many have 90th percentile values above the regulatory limit (BR, GC, M, SPb, and NEx). All of the aquifers have median and 90th percentile Ba concentrations below the regulatory limit of 2000 µg/L (Figure 3.4). Most aquifers have undetectable levels of Cd, and so the 90th percentile values are set to the detection limit. All of the aquifers have very low median concentrations of Pb (Figure 3.5) and most have 90th percentile concentrations of less than 1, well below the regulatory limit of 15 µg/L.

Only summary data for benzene, naphthalene, and phenol were provided in LA DeSimone (2009). Benzene was detected (> 0.2 µg/L) in 2 out of 1,948 samples. Naphthalene was detected (> 0.2 µg/L) in 2 out of 1,928 samples. Phenol was not detected (> 0.2 µg/L) in any of the 919 samples analyzed. This indicates that these organic compounds are not normally present in drinking-water aquifers, except due to contamination.

Table 3.3. Aquifer Name Abbreviations

Abbreviation	Description
HP	NRAP High Plains sand and gravel aquifer
Eu	NRAP Edwards shallow, urban carbonate-rock aquifer
BR	Basin and Range basin-fill sand and gravel aquifers
Gc	Central glacial sand and gravel aquifers
CL	Coastal lowlands sand aquifer system
LT	Lower Tertiary and Upper Cretaceous sandstone aquifers
M	Mississippian sandstone and carbonate-rock aquifers
F	Floridan carbonate-rock aquifer system
SPb	Snake River Plain basaltic-rock aquifers
NEx	New England crystalline-rock aquifers

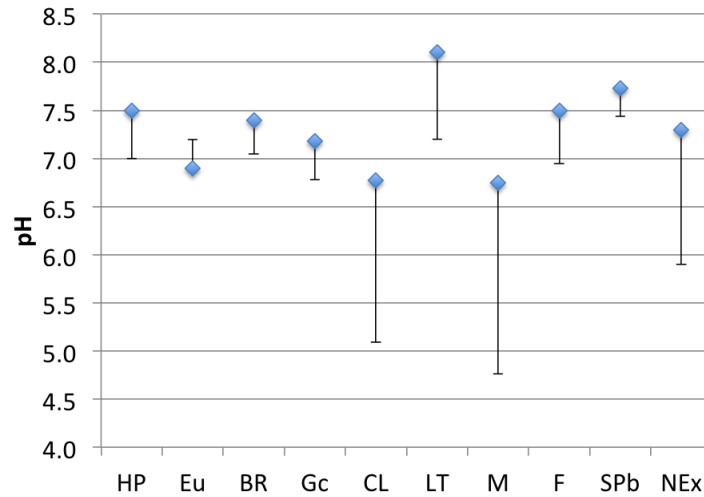


Figure 3.1. Comparison of Background Values of pH for the High Plains Aquifer and Shallow, Urban Unconfined Portion of the Edwards Aquifer used in NRAP Studies with Ranges for Various Aquifer Types in the U.S. Symbols represent median value and error bars the 10th percentile.

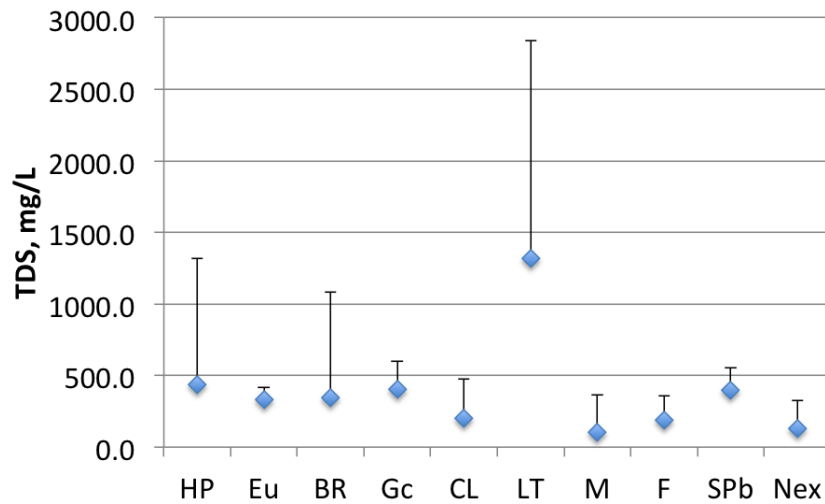


Figure 3.2. Comparison of Background Values of TDS for the High Plains Aquifer and Shallow, Urban Unconfined Portion of the Edwards Aquifer used in NRAP Studies with Ranges for Various Aquifer Types in the U.S. Symbols represent median value and error bars the 90th percentile.

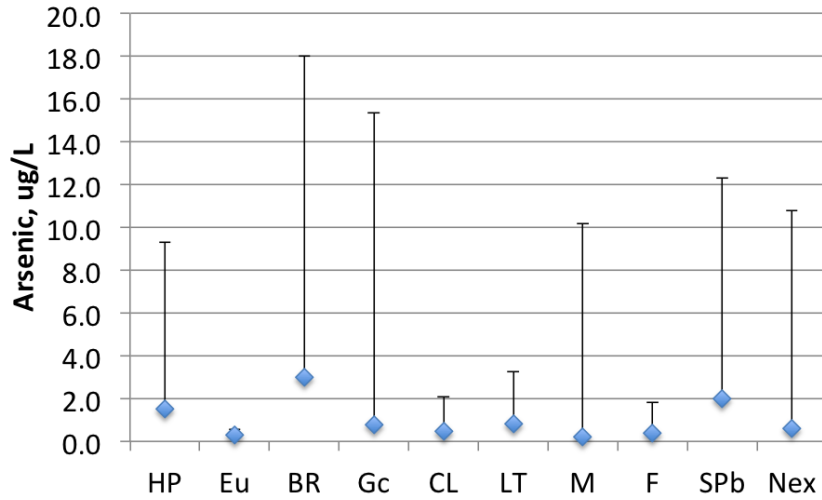


Figure 3.3. Comparison of Background Values of Arsenic for the High Plains Aquifer and Shallow, Urban Unconfined Portion of the Edwards Aquifer used in NRAP Studies with Ranges for Various Aquifer Types in the U.S. Symbols represent median value and error bars the 90th percentile.

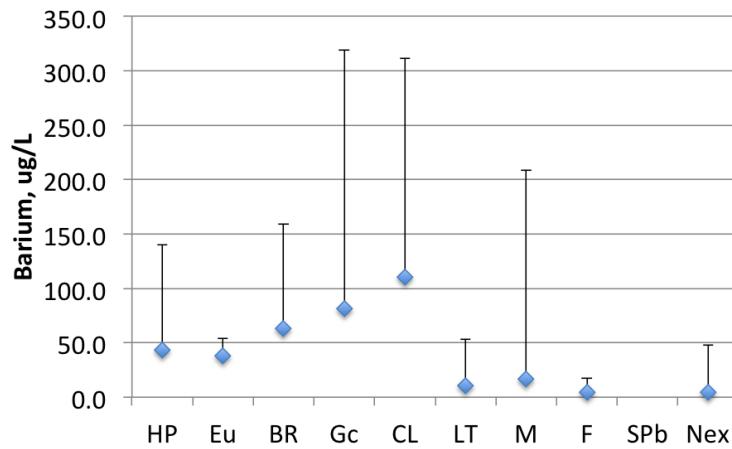


Figure 3.4. Comparison of Background Values of Barium for the High Plains Aquifer and Shallow, Urban Unconfined Portion of the Edwards Aquifer used in NRAP Studies with Ranges for Various Aquifer Types in the U.S. Symbols represent median value and error bars the 90th percentile.

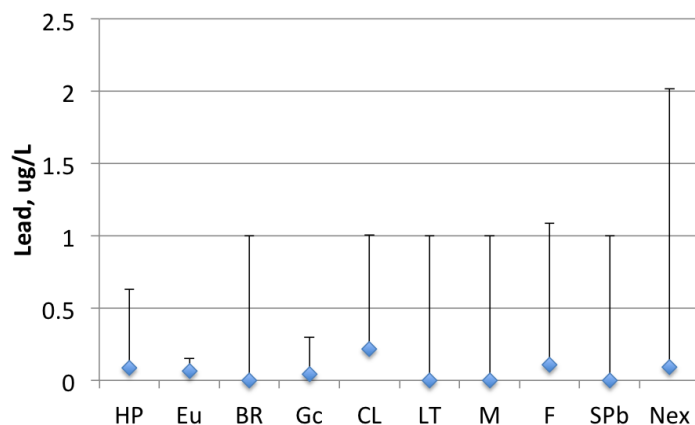


Figure 3.5. Comparison of Background Values of Lead for the High Plains Aquifer and Shallow, Urban Unconfined Portion of the Edwards Aquifer used in NRAP Studies with Ranges for Various Aquifer Types in the U.S. Symbols represent median value and error bars the 90th percentile.

3.2 Solid Phase Properties: Mineralogy

Mineralogical properties of the aquifer are important determinants of the way the aquifer will respond to the exposure of leaking CO₂ (and other gases) and brine from the deep subsurface reservoirs. We studied the mineralogy of two representative aquifers; a summary of the results is presented below.

3.2.1 High Plains Aquifer

The mineralogy of the High Plains Aquifer was determined in a set of samples obtained from the Kansas Geological Survey. These sediment samples were used in a series of batch and column experiments (N Qafoku et al. 2013). The sediments originated from three different wells (named CNG [latitude 37.0635, longitude -101.7193], CAL 121 [latitude 37.7736, longitude 100.8187], and CAL 122 [latitude 37.7368, longitude 100.7588]), all located in the central High Plains Aquifer area in Kansas. Four of the samples came from well CNG (CNG 8, CNG 60, CNG 110, and CNG 150), two samples came from well CAL 121 (CAL 121 150 and CAL 121 91), and two samples came from well CAL 122 (CAL 122 4 and CAL 122 29).

Sediment samples from Kansas were received as loose, sandy materials. Texture determination found the samples of the CAL well were classified as “sand” while the samples from the CNG well were classified as a “sandy loam” (CNG-8) and “loamy sand” (CNG 60 and CNG 110).

Quantitative XRD analyses (QXRD) showed that calcite contents of the sediments varied from zero to ~4% (N Qafoku et al. 2013). QXRD results also showed that the sediments contained appreciable amounts of feldspars, montmorillonite, quartz, and mica. QXRD analysis of the silt and clay fractions separated from these sediments confirm the presence of small amounts of carbonate minerals (calcite and/or dolomite) in all samples except one (H Shao et al. 2015). This is important because small-sized calcite particles undergo fast dissolution after sediment exposure to CO₂ gas, buffering the pH of the aqueous phase.

In addition to the QXRD analyses, a series of scanning electron microscope (SEM) inspections and energy dispersive spectrometry (EDS) measurements were performed to characterize the morphology of

the mineral particles and determine their chemical composition (Figure 3.6). EDS results showed a low amount of Ca and high concentration of Si for CNG 60. The SEM images showed the samples had rough surfaces (i.e., a high reactive surface area and potentially high adsorption and dissolution rates). EDS results, in agreement with previous QXRD data, suggested the presence of feldspars and/or micas in the High Plains Aquifer CNG sediments. Additional SEM/EDS related analyses and figures are presented in H Shao et al. (2015), A Lawter et al. (2016), and A Lawter et al. (2016).

Microwave digestion analyses were conducted to determine the elemental composition of the aquifer sediments. In addition, 8M nitric acid extractions were conducted to determine the identity of different inorganic elements and potential contaminants that may be released from the sediments during CO₂ injection. The results indicate that the solid phase of the sediments contains varied amounts of trace metals that are of environmental concern, such as As, Ba, Cd, Cr, and Pb, which are regulated with primary MCLs, and Fe, Mn, and Zn, which are regulated with secondary MCLs. Potentially, appreciable amounts of several contaminants (e.g., As) could be released from the sediments when contacted with CO₂ saturated groundwater (H Shao et al. 2015; N Qafoku et al. 2013).

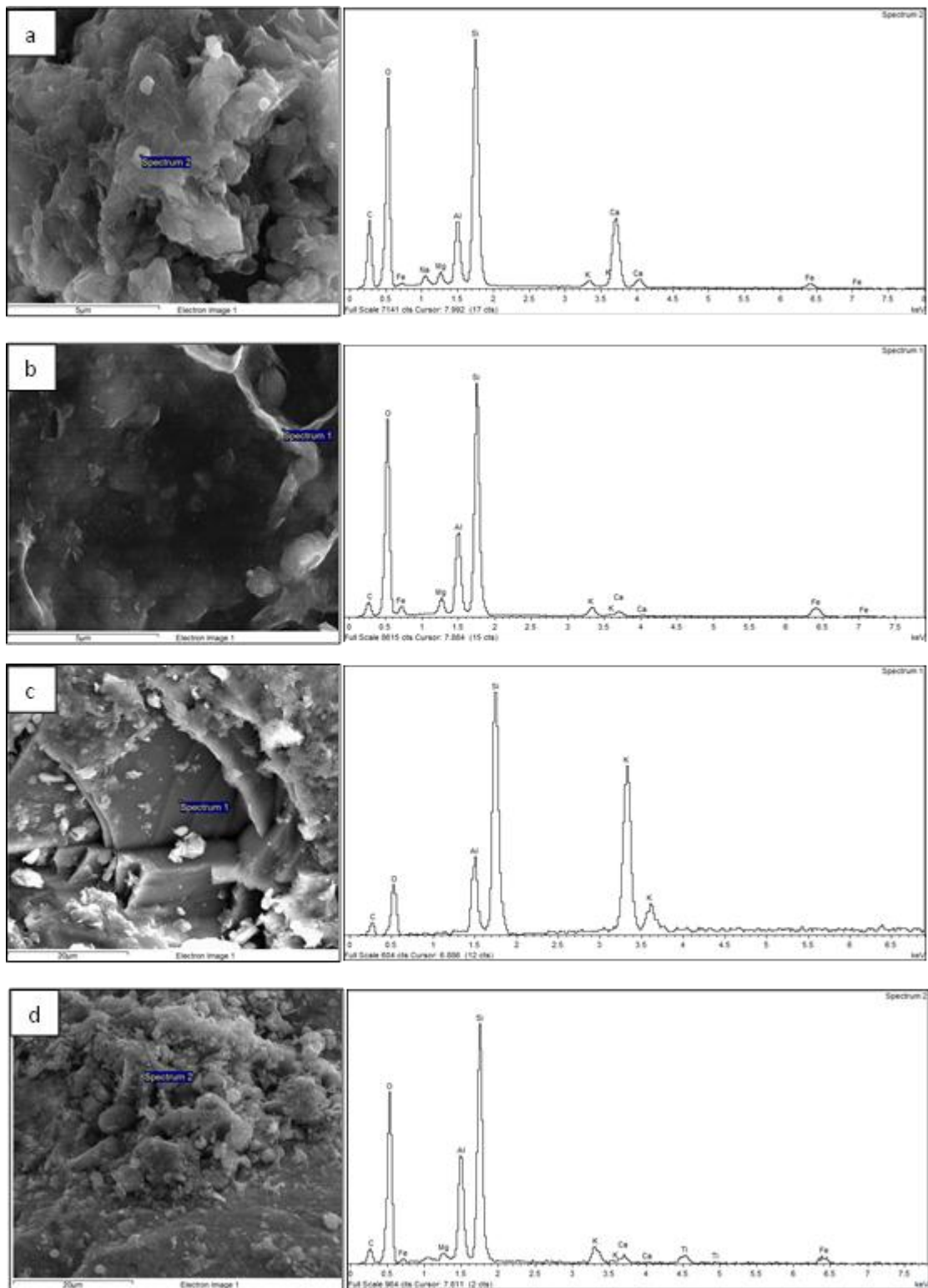


Figure 3.6. SEM/EDS for (a) CNG 8, (b) CNG 60, (c) CNG 150, and (d) CAL 121 91

3.2.2 Edwards Aquifer

Two sets (of seven samples each) from the unconfined section of the Edwards Aquifer were used in a series of batch and column experiments; they are referred to as Set A (weathered rock) and Set B (unweathered rock). The samples were received as mostly large rocks, but were ground to <2mm before use in experiments and characterization. XRD analyses conducted on the Edwards Aquifer showed samples from Set B were exclusively dominated by calcite, while samples from Set A (weathered rock) were dominated by calcite, but also contained quartz, and montmorillonite.

SEM micrographs and EDS chemical analysis measurements were used to describe the morphology of calcite, the predominant mineral in these samples, and to locate other minerals determined by XRD. For example, calcite and quartz were both present in the relatively weathered rocks (Set A). The rough surfaces of calcite explain the fast rate of dissolution observed in batch experiments in response to CO₂ gas exposure.

Phyllosilicates were also located in weathered samples (in one location, a 2:1 concentration ratio for Al and Si was found, which is a typical ratio for 2:1 phyllosilicates and montmorillonite). SEM and EDS results for Sample 2 from Set B (which is a representative of the unweathered rock samples) found only calcite (Figure 3.7). Additional information and figures related to the SEM/EDS analyses are presented in recent papers published by the NRAP group at PNNL and LBNL (G Wang et al. 2016; D Bacon et al. 2016).

As with the High Plains sediments, 8M nitric acid extractions were conducted on the Edwards Aquifer sediments. The main objective for conducting the 8M acid extractions was to understand the types of potential contaminants present in the sediments, which may (or may not) be mobilized when these solid materials are exposed to a CO₂ gas stream or CO₂ saturated synthetic groundwater (SGW). Results of these extractions show the materials contained potentially releasable contaminants, including As, Cd, Cr, Pb, and Zn (N Qafoku et al. 2013).

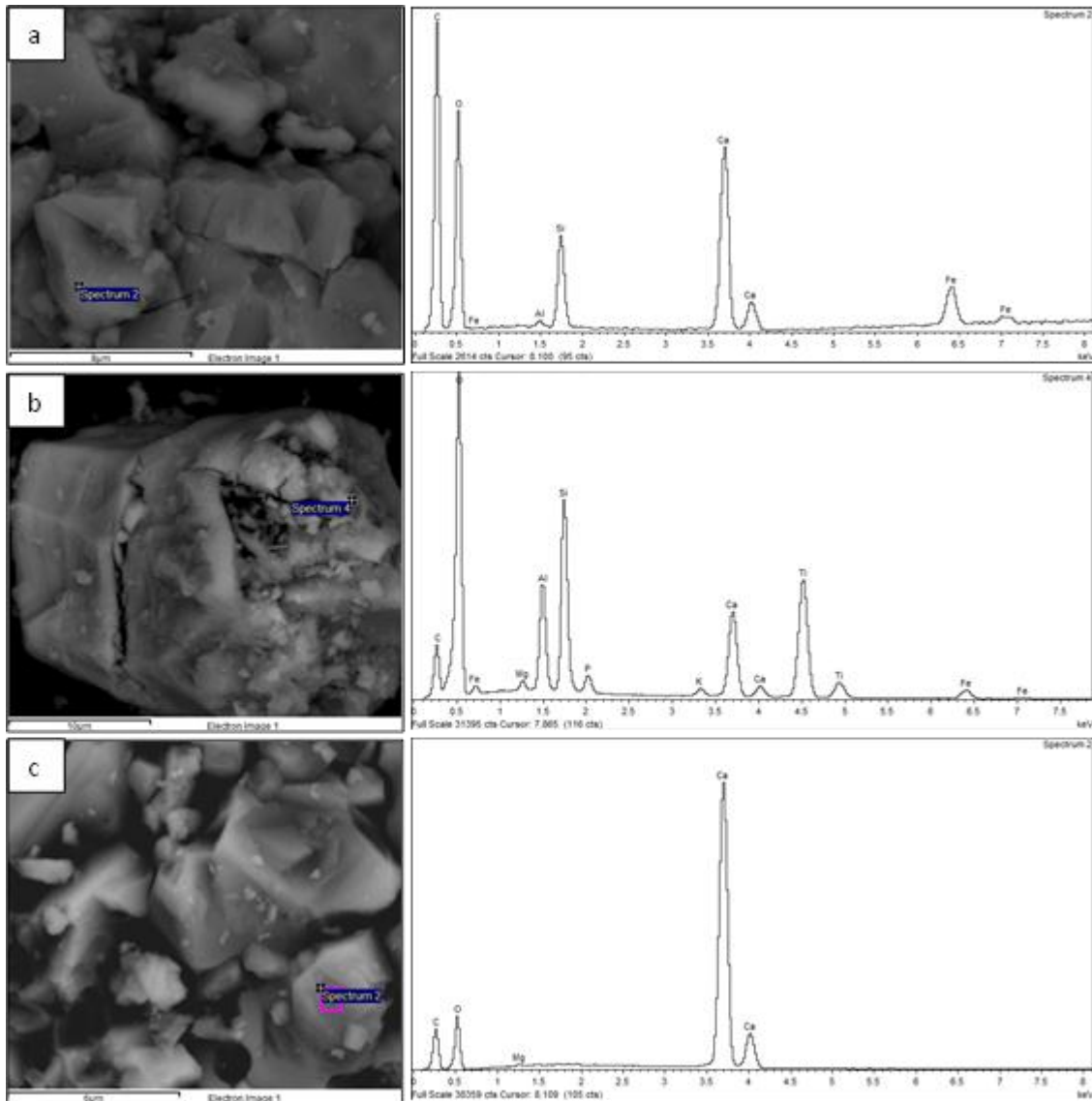


Figure 3.7. SEM/EDS for Edwards Samples: (a) Set A #1, (b) Set A #7, and (c) Set B # 2

3.3 Other Aquifers

Several other sites have been studied, such as the Montana State University-Zero Emission Research and Technology site (MSU-ZERT, Bozeman, MT), a natural analog site in Chimayo, NM, and Scurry Area Canyon Reef Operators Committee (SACROC) oil field in Scurry County, TX. The sites studied most extensively are all sandstone or unconsolidated sand and gravel aquifers; carbonate aquifers have received much less attention, although the abundance of carbonate aquifers and specific concerns related to these sites make carbonate sites important.

The importance of mineralogy (and especially calcite content) in the sediment is clearly stated in recent studies (E Frye et al. 2012; A Wunsch et al. 2014; A Wunsch et al. 2013; AG Cahill and R Jakobsen 2013; MG Little and RB Jackson 2010; J Lu et al. 2010; EH Keating et al. 2010). On one side, calcite may buffer the pH of the aquifer, decreasing the extent of mineral dissolution and release of contaminants. For example, in a column study conducted with artificial lake and river sediments (created

by mixing purchased calcite, quartz sand, and illite minerals), E Frye et al. (2012) observed that the mineralogical properties of aquifer materials significantly influenced the response of groundwater quality to the intrusion of CO₂. They found that calcite content as low as 10% can mitigate the effect of pH reduction and may result in zero Cd desorption from Cd laden illite (E Frye et al. 2012). Studies also show that carbonates buffer the system to avoid further decreases in pH (AG Cahill et al. 2013; MG Little and RB Jackson 2010). In an analog study conducted in New Mexico, USA, EH Keating et al. (2010) reported that despite relatively high levels of dissolved CO₂, trace element mobility was not significant due to the high buffering capacity of the groundwater aquifer they studied.

On the other side, K Kirsch et al. (2014) found that the contaminants released in their laboratory experiment were directly correlated with calcite dissolution, leading them to conclude that calcite dissolution is the source of the contaminants. A batch experiment conducted by J Lu et al. (2010) also suggests aquifers containing carbonate rocks are of particular concern due to the presence of Ba, Mn, and Sr in carbonates, in addition to increased alkalinity which followed carbonate dissolution. A summary of additional sites that have been subject to recent investigations is presented in Table 3.4.

Table 3.4. A Summary of Recent Studies Conducted in Different Aquifers

Project Site	Paper	Details/Results
ZERT - Food grade CO ₂ injected 1-2 m below the water table for 30 days at MSU-ZERT in Bozeman, MT.	(H Viswanathan et al. 2012)	PCA (principal component analysis) of the 80 water samples mentioned below; used to simulate the processes responsible for increased dissolved constituents using a multicomponent reaction path model
	(JA Apps et al. 2011)	Water samples taken before, during and after injection; geochemical model used to simulate processes likely to be responsible for dissolved constituents
	(YK Kharaka et al. 2010)	Field study: collected 80 water samples from the site before/during/after injection. Rapid and systematic changes in pH, alk, Ec; major increases in Ca, Mg, Fe and Mn, CO ₂ caused increase of BTEX, metals, lower pH, and other solutes; significantly below MCLs
High Plains:		
Ogallala aquifer, TX (Southern High Plains)	(MG Little and RB Jackson 2010)	Lab experiments; compared results with materials from aquifers in MD/VA and IL; Al, Mn, Fe, Zn, Cd, Se, Ba, Tl, and U approached or exceeded MCL's
Central High Plains	(A Lawter et al. 2015)	Batch and column (lab) studies

Project Site	Paper	Details/Results
	(L Zheng et al. 2016)	using HP sediments and SGW Modeling done to determine likely processes controlling geochemical changes observed in Lawter et al (2015)
	(H Shao et al. 2015)	Laboratory column and batch studies using As/Cd spiked SGW
	(A Lawter et al. 2016)	Laboratory batch and column studies using 1% CH ₄ and As/Cd spiked SGW
	(SA Carroll et al. 2014)	Model simulated CO ₂ leakage to predict plume size, potential impacts, detection, time scale, and “no-impact” thresholds
<u>Chimayo, NM</u> - natural analog site (field study)	(EH Keating et al. 2013)	A 3-D reactive transport model which captures the essential geochemical reactions that control CO ₂ /aquifer interactions at the site and which may determine trace metal concentrations
	(EH Keating et al. 2013)	Compared to Springerville, AZ where CO ₂ leaks through brine but salinity is not increased; in Chimayo, salinity is significantly increased. Used multiphase transport simulations to show which conditions favor increased salinity
	(EH Keating et al. 2010)	Found high levels of CO ₂ did not have a major effect on pH or trace metal mobility, but the addition of brakish waters did have a major effect on the aquifer
<u>Springerville, AZ</u>	(E Keating et al. 2014)	Site also studied in some Chimayo, NM papers, this paper found dissolved CO ₂ upward movement was much greater than buoyant free gas movement
<u>SACROC</u> - 35 year CO ₂ enhanced oil recovery site sitting under Dockum aquifer in TX (sandstone and conglomerate)	(KD Romanak et al. 2012)	Geochemical characterization of Dockum aquifer followed by hypothetical leakage model

Project Site	Paper	Details/Results
	(RC Smyth et al. 2009)	Also studied Cranfield, MS EOR site. Laboratory batch experiments were conducted, then field studies to see if any CO ₂ might have been leaking (no degradation of water sources was identified)
<u>Edwards</u>	(SA Carroll et al. 2014)	Model simulated CO ₂ leakage to predict plume size, potential impacts, detection, time scale, and “no-impact” thresholds
	(D Bacon et al. 2015)	Modeling of the results from the batch and column studies presented in the paper by Wang et al., 2014
	(G Wang et al. 2015)	Edwards Aquifer batch and column studies conducted (lab)
	(N Qafoku et al. 2013)	PNNL report covering Edwards and High Plains batch and column studies conducted during or before 2013
<u>Frio Formation, TX</u>		
Saline sandstone aquifer	(YK Kharaka et al. 2006; YK Kharaka et al. 2006)	Study of changes to the reservoir brine after CO ₂ injection in a saline storage reservoir. Rapid changes in pH and carbonate dissolution suggest conditions that may create pathways upward into overlying aquifers
	(YK Kharaka et al. 2009)	Monitoring was done to observe migration of injected CO ₂ from the lower Frio formation into a section 15m above the injection section 6 months after injection. However, 15 months after injection found no additional CO ₂ in the upper Frio formation and no CO ₂ leakage was detectable in the overlying groundwater
<u>Plant Daniel, MS (EPRI site):</u> Field-scale test site at Plant Daniel Power plant	(RC Trautz et al. 2013)	Groundwater sampling after injection of CO ₂ showed a decrease in pH (~3 units) but pulse-like behavior for alkalinity and conductivity. No inorganics regulated by the EPA exceeded MCLs during testing. A reactive transport model was then tested using the obtained data, with good agreement for pH, Ca, Mg, K, and Sr, and lesser agreement

Project Site	Paper	Details/Results
	(C Varadharajan et al. 2013)	for Mn, Ba, Cr, and Fe Sediment characterization of the Plant Daniel site combined with laboratory studies to determine to compare results with field studies and determine the cause of elemental changes
<u>Cranfield, MS</u>	(SD Hovorka et al. 2011)	Summary of completed, continuing, and future studies conducted at the Cranfield site
	(CB Yang et al. 2013)	A push-pull test was conducted to determine the effect of CO ₂ on the aquifer. XRD and SEM characterization of the site are also included
	(J-P Nicot et al. 2013)	Well logs were used to assess the risk related to CO ₂ leakage from wells within the Cranfield EOR site. The risk assessment concluded that no more than two, but likely none, of the wells were likely to leak CO ₂

3.3.1 Carbonate Aquifers

Few studies have been conducted with carbonate aquifers, although some studies have included sediments with varying amounts of carbonate materials. The results from three such studies (two focused on aquifers and one on sediments with variable carbonate content) are summarized below.

A Wunsch et al. (2014) and A Wunsch et al. (2013) use laboratory experiments to study metal release from limestones and dolomites, respectively. These carbonate aquifer materials were placed in batch reactors with a 1:5 solid to solution ratio, with $p\text{CO}_2$ ranging from 0.01 to 1 bar. Results of the limestone experiments showed an increase in Ca following an increase in $p\text{CO}_2$, then stabilizing with time. Ba, Sr, Co, and As followed the Ca trend, as did Mg in one of the limestone samples. Pb, Tl, Si, and U were also released from one or both limestone samples, but did not follow the same trend as Ca, and sulfates continually increased for the duration of the experiment. The pH initially decreased during the first 1-2 days of each stage of the experiment, then increased for the remainder, ranging from an initial pH of approximately 9.5 to less than 6.5. The same pH trend was seen in the dolomite batch study, with pH reaching a low of <5.6. In the dolomite experiments, both Ca and Mg concentrations began to increase immediately. Concentrations of As, Ba, Co, Cs, Ge, Mn, Mo, Ni, Rb, Sb, Sr, Tl, and Zn were also elevated in at least one of the dolomite leachate samples. The two studies concluded that carbonates were the source of several contaminants found in the aqueous samples. After opening the reactors at the conclusion of the experiment, however, many of these contaminants were removed from solution with the return to atmospheric conditions. These studies show the potential for contaminant release from carbonate aquifers, despite the potential for high buffering capacities in these aquifers, as well as the importance of site-specific studies (A Wunsch et al. 2014; A Wunsch et al. 2013).

Pd Caritat et al. (2013) studied two limestone aquifers at a sequestration demonstration site in Victoria, Australia at the Otway project site. Groundwater composition was monitored before, during, and after the

injection of CO₂, but no significant changes related to CO₂ leakage were detected during the three years of monitoring. To aid in the detection of a leak, and to distinguish the injected CO₂ from natural CO₂, tracers were added twice during injection. These tracers were not detected in the atmospheric, soil, or aquifer samples collected from the site (J Underschultz et al. 2011).

AG Cahill et al. (2013) used eight different sediments in a laboratory batch experiment to determine contaminant release from sediments with carbonate content varying from 0 to 100 percent. The silicate dominated sediments were found to be more prone to acidification, but less likely to release elevated amounts of contaminants due to a low amount of easily dissolved minerals. Carbonate dominated samples (TIC > 2%) were found to release greater concentrations of elements, although the carbonate systems were able to buffer against greater pH decreases. Results from the AG Cahill et al. (2013) study show the distinctive potential issues with several different aquifer types, demonstrating the importance of evaluating each possible aquifer type.

3.3.2 Sandstone and Unconsolidated Sand and Gravel Aquifers

Sandstone aquifers have received more attention than carbonate aquifers; a summary of the findings in recent studies is presented below.

SACROC is an oil field near Cranfield, MS, where CO₂ has been used for enhanced oil recovery (EOR) for over 35 years. Geochemical characterization has been conducted on the Dockum aquifer, a minor sandstone and conglomerate aquifer overlying the SACROC injection area. The characterization was followed by a hypothetical leakage model to show expected reactions in the aquifer due to CO₂ leakage (KD Romanak et al. 2012).

The hypothetical leakage model showed dedolomitization as the dominant process in this system; calcite dissolution cannot be assumed. KD Romanak et al. (2012) conclude that current parameters used in leakage detection are site-specific, but the use of dissolved inorganic carbon as a parameter may reduce the need for site-specific parameters, as they found the DIC response to be similar across many modeled environments. Laboratory batch studies indicated several constituents would increase and pH would decrease if CO₂ were to leak into the overlying Dockum aquifer. However, a field study of several wells located inside and outside the SACROC oil field shows no degradation of groundwater resources due to CO₂ injection. While some elemental concentrations exceeded EPA MCLs, this occurred more outside the SACROC area than inside the oil field (RC Smyth et al. 2009).

At the MSU-ZERT site in Bozeman, MT, food grade CO₂ was injected below the water table for 30 days. The water table is located beneath the topsoil, in a sandy gravel deposit (L Zheng et al. 2012). Water samples were collected before, during, and after injection. Analysis of the samples showed that although pH, alkalinity, and several constituents changed within the groundwater during injection, none of the changes exceeded EPA MCL's (YK Kharaka et al. 2010). Modeling was done to determine the processes responsible for the increased dissolved constituents (JA Apps et al. 2011; L Zheng et al. 2012).

Chimayo, NM is the location of a natural analog site where shallow wells release CO₂ into a drinking-water aquifer. Field studies coupled with modeling have been used to study the impact of CO₂ gas on the aquifer, as well as the transport of brine with CO₂ along fault zones (EH Keating et al. 2013; EH Keating, JA Hakala, et al. 2013; EH Keating et al. 2010). The Chimayo, NM site was compared with a site in Springerville, AZ, another natural analog site where brine is present but, in this case, the salinity of the affected aquifer was not significantly increased. Reactive transport models were used to determine what conditions favor the transport of brine with CO₂, and found the width of the leakage pathway to be a major factor (i.e., narrow pathways increase co-transport) (EH Keating et al. 2013).

3.3.3 Comparison of Different Aquifers

Many of the previous studies have focused on sandstone or unconsolidated sand and gravel aquifers with variable carbonate content (LH Spangler et al. 2010; C Varadharajan et al. 2013; B Dafflon et al. 2013; AG Cahill and R Jakobsen 2013; K Kirsch et al. 2014; S Carroll et al. 2009; YK Kharaka et al. 2010; C Yang et al. 2014; EH Keating et al. 2010; L Zheng et al. 2012). A study by AG Cahill et al. (2013) considered samples with >2% total inorganic carbon to be “carbonate dominated,” and concluded that these samples released greater amounts of trace elements but decreased pH less than silicate dominated samples. Using Cd laden illite, E Frye et al. (2012) determined carbonate content as low as 10% mitigated the effect of CO₂ injection; no Cd was desorbed.

Fewer studies have been conducted with carbonate aquifer materials in relation to CO₂ sequestration, and given their prevalence as sources of potable water overlying potential sequestration reservoirs within the continental U.S., there is a need to better understand their response to potential CO₂ gas intrusions. B Nisi et al. (2013) established geochemical and isotopic data for spring and surface waters located at a CO₂ injection site that included some limestone units. However, the manuscript was written prior to CO₂ injection and does not provide insight to consequences of CO₂ leakage interactions with carbonate materials. The demonstration site studied by Pd Caritat et al. (2013) did involve research post-injection, but no leakage into the overlying limestone aquifer was detected. In two laboratory batch experiments, both limestone and dolomite aquifer materials were tested for metal release by A Wunsch et al. (2014) and A Wunsch et al. (2013), respectively, with conclusions that calcite is the primary source for several released contaminants; regulatory limits were exceeded for As, Mn, and Ni in one or both studies.

Other studies focused on the effect of carbonate materials in smaller amounts (i.e., carbonate minerals are present but the aquifer is not dominated by carbonates). These studies give insight to the effect of carbonates on aquifer response to CO₂ exposure. One such study, G Montes-Hernandez, F Renard and R Lafay (2013), used synthetic goethite and calcite in batch experiments. The results showed the presence of these two minerals prevented remobilization of Cu(II), Cd(II), Se(IV), and As(V), and increased adsorption of Se(IV) and As(V), although As(III) was partially remobilized with the presence of CO₂.

AG Cahill et al. (2013) used batch experiments to study differences in water chemistry changes for chalk, calcareous sand, and siliceous sand, concluding that carbonate materials had the greatest change in chemistry but the least change in pH. According to this study, the greater change in pH in the siliceous sand represented a greater risk for mobilization of toxic elements, although less toxic elements released from carbonates could also present a risk to water quality. S Wang and PR Jaffe (2004) used numerical simulations and geochemical transport modeling to predict the solubilization of trace metals, with a focus on Pb in galena-quartz and galena-calcite systems, concluding the higher alkalinity and pH of the calcite system significantly reduced the detrimental effects of the presence of CO₂.

Other studies on trace element release in carbonate aquifers, although not studied in the context of CO₂ sequestration risk evaluation, have been conducted with an emphasis on As mobility. While the calcite content can buffer the change in pH, As can be incorporated into the crystal lattice of carbonates such as limestone and calcite (F Di Benedetto et al. 2006; P Costagliola et al. 2013; Y Yokoyama et al. 2012), causing As to be released as the carbonate minerals dissolve (O Lazareva et al. 2014; J Arthur et al. 2002).

3.4 Relevant Processes and Reactions

The way groundwater in shallow aquifers responds to the leakage of CO₂ and brine is controlled by coupled transport (advection and diffusion) and chemical reactions. In this section, we list possible

reactions that could affect the fate of the pH, TDS, trace metals, and organic compounds in the aquifer, keeping in mind that it is likely that only a subset of these reactions will be important for a particular aquifer.

While the increase in concentration of dissolved constituents raises concerns, a lot of effort has been invested in understanding the controlling chemical processes and source minerals via model interpretation of laboratory experiments (e.g., H Viswanathan et al. (2012)) and field tests (L Zheng et al. 2012), hopefully facilitating the development of numerical models with better predictability.

The chemical processes potentially responsible for the mobilization of trace elements include the dissolution of carbonates (YK Kharaka et al. 2006; AE McGrath et al. 2007; JT Birkholzer et al. 2008), sulfides (S Wang and PR Jaffe 2004; JA Apps et al. 2010; L Zheng et al. 2009), and iron oxyhydroxide minerals (YK Kharaka et al. 2006; YK Kharaka et al. 2009), as well as surface reactions such as adsorption/desorption and ion exchange (YK Kharaka et al. 2006; JA Apps et al. 2010; L Zheng et al. 2009; YK Kharaka et al. 2009).

The release of alkali and alkaline earth metals, including Na, K, Ca, Mg, Sr, and Ba, which are most commonly observed both in laboratory and field experiments, is thought to be controlled by the dissolution of calcite and Ca-driven cation exchange reactions (L Zheng et al. 2012). The reaction path and kinetic model study conducted by RT Wilkin and DC Digiulio (2010) further indicates that the geochemical response of an aquifer to CO₂ leakage is closely related to the aquifer mineralogy. It is thus expected that differences in geology (the type of aquifer), mineralogy (the type of minerals), and groundwater chemistry (the ion composition and pH) at any particular site could all lead to different responses to CO₂ leakage. For this reason, as noted by JA Apps et al. (2010), field tests integrated with modeling studies are necessary to further assess hydrogeochemical processes potentially affecting groundwater quality upon a CO₂ release. In general, there are three type of reactions, as discussed in the following sections.

3.4.1 Surface Reactions

3.4.1.1 Surface Reactions for Trace Metals

In a typical aquifer sediment, Fe oxides and hydroxides [such as, goethite, hydrous ferric oxide (HFO)] and clay minerals (such as illite, kaolinite, montmorillonite) are important adsorbents. Other minerals could also have some adsorption capacity, but become less relevant when Fe oxides and hydroxides and clay minerals are present in the sediment (which is the case in almost all soils and sediments).

L Zheng et al. (2012) summarized the adsorption/desorption reactions H⁺ (surface protonation), Cd, Cu, Pb, As, Ca, Fe, Ba, Cr, Sb, and aqueous carbonate on goethite, HFO, illite, kaolinite, and montmorillonite. There are two popular methods to model adsorption/desorption reactions: a linear sorption isotherm via a distribution coefficient (K_d) or as a surface complexation model (SCM). SCM is currently used in the NRAP to model adsorption/desorption reactions. The surface complexation reactions for the trace metals that are included in the Gen III ROM, namely As, Pb, Cd, and Ba, are listed in Table 3.5-Table 3.10. Note that surface protonation reactions are also included in these tables. These reactions play an important role in buffering pH when pH buffering by calcite dissolution is minimal. Table 3.10 lists the adsorption/desorption reactions for arsenate and arsenite on calcite, which is an important process that controls the fate of As in carbonate aquifers.

Table 3.5. Surface Protonation and Complexation Reactions on Goethite

Reactions	Log k_{int}	Site Density (mol/m ²)	Surface Area (m ² /g)	Amount of Solid (g/kg water)	Type of SCM Model	Reference
$goe^1_{OH_2^+} = goe^1_{OH} + H^+$	-7.38	3.9-8	80	10	DLM	(PJ Swedlund et al. 2009)
$goe^1_{O^-} + H^+ = goe^1_{OH}$	10.74	3.9-8	80	10	DLM	
$goe^2_{OH_2^+} = goe^2_{OH} + H^+$	-7.38	3.8e-6	80	10	DLM	(PJ Swedlund, JG Webster and GM Miskelly 2009)
$goe^2_{O^-} + H^+ = goe^2_{OH}$	10.74	3.8e-6	80	10	DLM	
$goe^1_{OCd^+} + H^+ = goe^1_{OH} + Cd^{+2}$	-1.29	3.9-8	80	2	DLM	(PJ Swedlund, JG Webster and GM Miskelly 2009)
$goe^2_{OCd^+} + H^+ = goe^2_{OH} + Cd^{+2}$	1.83	3.8e-6	80	2	DLM	
$goe^1_{OPb^+} + H^+ = goe^1_{OH} + Pb^{+2}$	-4.78	3.9-8	80	10	DLM	(PJ Swedlund, JG Webster and GM Miskelly 2009)
$goe^2_{OPb^+} + H^+ = goe^2_{OH} + Pb^{+2}$	-1.52	3.8e-6	80	10	DLM	
$goe^2_{H_2AsO_3} + H_2O = goe^2_{OH} + H_3AsO_3$	-5.19 ^a	3.32e-6	54	0.5	DLM	(S Dixit and JG Hering 2003)
$goe^2_{HAsO_3^-} + H_2O + H^+ = goe^2_{OH} + H_3AsO_3$	2.34 ^a	3.32e-6	54	0.5	DLM	
$goe^2_{H_2AsO_4} + H_2O = goe^2_{OH} + AsO_4^{+3} + 3H^+$	-31.0	3.32e-6	54	0.5	DLM	(S Dixit and JG Hering 2003)
$goe^2_{HAsO_4^-} + H_2O = goe^2_{OH} + AsO_4^{+3} + 2H^+$	-26.81	3.32e-6	54	0.5	DLM	
$goe^2_{AsO_4^{-2}} + H_2O = goe^2_{OH} + AsO_4^{+3} + H^+$	-20.2	3.32e-6	54	0.5	DLM	

(a) note that in Dixit and Hering (2003), the reactions were written in terms of AsO_3^{-3}

Table 3.6. Surface Protonation and Complexation Reactions on HFO

Reactions	Log k_{int}	Site Density (mol/m ²)	Surface Area (m ² /g)	Amount of Solid (g/kg water)	Type of SCM Model	Reference
$HFO^1_{-OH_2^+} = HFO^1_{-OH} + H^+$	-7.29	8.5e-8	600	0.1	DLM	(DA Dzombak and FMM
$HFO^1_{-O^-} + H^+ = HFO^1_{-OH}$	8.93	8.5e-8	600	0.1	DLM	Morel 1990)
$HFO^2_{-OH_2^+} = HFO^2_{-OH} + H^+$	-7.29	3.4e-6	600	0.1	DLM	(DA Dzombak and FMM
$HFO^2_{-O^-} + H^+ = HFO^2_{-OH}$	8.93	3.4e-6	600	0.1	DLM	Morel 1990)
$HFO^1_{-OCd^+} + H^+ = HFO^1_{-OH} + Cd^{+2}$	-0.47	8.5e-8	600	0.1	DLM	(DA Dzombak and FMM
$HFO^2_{-OCd^+} + H^+ = HFO^2_{-OH} + Cd^{+2}$	2.9	3.4e-6	600	0.1	DLM	Morel 1990)
$HFO^1_{-OPb^+} + H^+ = HFO^1_{-OH} + Pb^{+2}$	-4.65	8.5e-8	600	0.1	DLM	(DA Dzombak and FMM
$HFO^2_{-OPb^+} + H^+ = HFO^2_{-OH} + Pb^{+2}$	-0.3	3.4e-6	600	0.1	DLM	Morel 1990)
$HFO^1_{-OBa^+} + H^+ = HFO^1_{-OH} + Ba^{+2}$	-5.46	8.5e-8	600	0.1	DLM	(DA Dzombak and FMM
$HFO^2_{-OBa^+} + H^+ = HFO^2_{-OH} + Ba^{+2}$	7.20	3.4e-6	600	0.1	DLM	Morel 1990)
$HFO^1_{-H_2AsO_3} + H_2O = HFO^1_{-OH} + AsO_3^{-3} + 3H^+$	-38.76	3.32e-6	54	0.5	DLM	(S Dixit and JG
$HFO^1_{-HAsO_3^-} + H_2O + H^+ = HFO^1_{-OH} + AsO_3^{-3} + 2H^+$	-31.87	3.32e-6	54	0.5	DLM	Hering 2003)
$HFO^1_{-H_2AsO_4} + H_2O = HFO^1_{-OH} + AsO_4^{+3} + 3H^+$	-29.88	3.32e-6	54	0.5	DLM	(S Dixit and JG
$HFO^1_{-HAsO_4^-} + H_2O = HFO^1_{-OH} + AsO_4^{+3} + 2H^+$	-24.43	3.32e-6	54	0.5	DLM	Hering 2003)
$HFO^1_{-AsO_4^{-2}} + H_2O = HFO^1_{-OH} + AsO_4^{+3} + H^+$	-18.10	3.32e-6	54	0.5	DLM	

Table 3.7. Surface Protonation and Complexation Reactions of Cations on Illite

Reactions	Log k_{int}	Site Density (mol/m ²)	Surface Area (m ² /g)	Amount of Solid (g/kg water)	Type of SCM Model with Capacitance	Reference
ill_OH ₂ ⁺ = ill_OH + H ⁺	-8.02	2.27e-6	66.8	0.03	CCM, \mathcal{K} =2.0 F/m ²	(X Gu and LJ Evans 2007)
ill_O ⁻ + H ⁺ = ill_OH	8.93	2.27e-6	66.8	0.03	CCM, \mathcal{K} =2.0 F/m ²	
ill_Na + H ⁺ = ill_H + Na	1.58	1.3e-6	66.8	0.03	CCM, \mathcal{K} =2.0 F/m ²	
ill_OCd ⁺ + H ⁺ = ill_OH + Cd ⁺²	3.62	2.27e-6	66.8	0.03	CCM, \mathcal{K} =2.0 F/m ²	
(ill_) ₂ Cd + 2H ⁺ = 2ill_H + Cd ⁺²	-0.63	1.3e-6	66.8	0.03	CCM, \mathcal{K} =2.0 F/m ²	(X Gu and LJ Evans 2007)
ill_CdOH + 2H ⁺ = ill_H + Cd ⁺² + H ₂ O	6.49	1.3e-6	66.8	0.03	CCM, \mathcal{K} =2.0 F/m ²	
ill_OPb ⁺ + H ⁺ = ill_OH + Pb ⁺²	0.70	2.27e-6	66.8	0.03	CCM, \mathcal{K} =2.0 F/m ²	
(ill_) ₂ Pb + 2H ⁺ = 2ill_H + Pb ⁺²	-1.37	1.3e-6	66.8	0.03	CCM, \mathcal{K} =2.0 F/m ²	(X Gu and LJ Evans 2007)
ill_PbOH + 2H ⁺ = ill_H + Pb ⁺² + H ₂ O	3.65	1.3e-6	66.8	0.03	CCM, \mathcal{K} =2.0 F/m ²	
ill_H ₂ AsO ₃ + H ₂ O = ill_OH + H ₃ AsO ₃	-2.12	3.83e-6	22.6	40	CCM, \mathcal{K} =1.06 F/m ²	(S Goldberg 2002)
ill_HAsO ₃ ⁻ + H ₂ O + H ⁺ = ill_OH + H ₃ AsO ₃	5.66	3.83e-6	22.6	40	CCM, \mathcal{K} =1.06 F/m ²	
ill_AsO ₄ ⁻² + H ₂ O + 2H ⁺ = ill_OH + H ₃ AsO ₄	5.21	3.83e-6	22.6	40	CCM, \mathcal{K} =1.06 F/m ²	(S Goldberg 2002)

Table 3.8. Surface Protonation and Complexation Reactions of Cations on Kaolinite

Reactions	Log k_{int}	Site Density (mol/m ²)	Surface Area (m ² /g)	Amount of Solid (g/kg water)	Type of SCM Model	Reference
kao_OH ₂ ⁺ = kao_OH + H ⁺	-4.63	2.24e-6	22.42	7.8	CCM, \mathcal{K} =1.2 F/m ²	
kao_O ⁻ + H ⁺ = kao_OH	7.54	2.24e-6	22.42	7.8	CCM, \mathcal{K} =1.2 F/m ²	(X Gu and LJ Evans 2008)
Kao_Na ⁺ + H ⁺ = Kao_H + Na ⁺	2.02	3.57e-7	22.42	7.8	CCM, \mathcal{K} =1.2 F/m ²	
Kao_OCd ⁺ + H ⁺ = Kao_OH + Cd ⁺²	3.23	2.24e-6	22.42	7.8	CCM, \mathcal{K} =1.2 F/m ²	
(Kao_) ₂ Cd + 2H ⁺ = 2Kao_H + Cd ⁺²	-1.22	3.57e-7	22.42	7.8	CCM, \mathcal{K} =1.2 F/m ²	(X Gu and LJ Evans 2008)
Kao_OPb ⁺ + H ⁺ = Kao_OH + Pb ⁺²	0.64	2.24e-6	22.42	7.8	CCM, \mathcal{K} =1.2 F/m ²	
(Kao_) ₂ Pb + 2H ⁺ = 2Kao_H + Pb ⁺²	-2.36	3.57e-7	22.42	7.8	CCM, \mathcal{K} =1.2 F/m ²	(X Gu and LJ Evans 2008)
kao_HAsO ₃ ⁻ + H ₂ O + H ⁺ = kao_OH + H ₃ AsO ₃	5.43	3.83e-6	21.6	40	CCM, \mathcal{K} =1.06 F/m ²	(S Goldberg 2002)
kao_AsO ₄ ⁻² + H ₂ O + 2H ⁺ = kao_OH + H ₃ AsO ₄	4.69	3.83e-6	21.6	40	CCM, \mathcal{K} =1.06 F/m ²	(S Goldberg 2002)

Table 3.9. Surface Protonation and Complexation Reactions of Cations on Montmorillonite

Reactions	Log k_{int}	Site Density (mol/m ²)	Surface Area (m ² /g)	Amount of Solid (g/kg water)	Type of SCM Model and Capacitance	Reference
mon_OH ₂ ⁺ = mon_OH + H ⁺	-6.04	4.41e-6	46	1.5	CCM, \mathcal{K} = 3.2 F/m ²	
mon_O ⁻ + H ⁺ = mon_OH	6.63	4.41e-6	46	1.5	CCM, \mathcal{K} = 3.2 F/m ²	(X Gu et al. 2010)
mon_Na ⁺ + H ⁺ = mon_H + Na ⁺	-0.18	1.53e-5	46	1.5	CCM, \mathcal{K} = 3.2 F/m ²	
mon_OCd ⁺ + H ⁺ = mon_OH + Cd ⁺²	2.93	4.41e-6	46	1.5	CCM, \mathcal{K} = 3.2 F/m ²	(X Gu, LJ Evans and SJ Barabash 2010)
(mon_) ₂ Cd + 2H ⁺ = 2mon_H + Cd ⁺²	-2.37	1.53e-5	46	1.5	CCM, \mathcal{K} = 3.2 F/m ²	(X Gu, LJ Evans and SJ Barabash 2010) (S Goldberg 2002)
mon_OPb ⁺ + H ⁺ = mon_OH + Pb ⁺²	-0.49	4.41e-6	46	1.5	CCM, \mathcal{K} = 3.2 F/m ²	(X Gu, LJ Evans and SJ Barabash 2010) (S Goldberg 2002)
(mon_) ₂ Pb + 2H ⁺ = 2mon_H + Pb ⁺²	-2.56	1.53e-5	46	1.5	CCM, \mathcal{K} = 3.2 F/m ²	(S Goldberg 2002)
mon_H ₂ AsO ₃ + H ₂ O = mon_OH + H ₃ AsO ₃	-1.19	3.83e-6	68.9	40	CCM, \mathcal{K} = 1.06 F/m ²	(S Goldberg 2002)
mon_HAsO ₃ ⁻ + H ₂ O + H ⁺ = mon_OH + H ₃ AsO ₃	3.92	3.83e-6	68.9	40	CCM, \mathcal{K} = 1.06 F/m ²	(S Goldberg 2002)
mon_HAsO ₄ ⁻ + H ₂ O + H ⁺ = mon_OH + H ₃ AsO ₄	4.52	3.83e-6	68.9	40	CCM, \mathcal{K} = 1.06 F/m ²	(S Goldberg 2002)

Table 3.10. Surface Protonation and Complexation Reactions of Anions on Calcite

Reactions	Log k_{int}	Site Density (mol/m ²)	Surface Area (m ² /g)	Amount of Solid (g/kg water)	Type of SCM Model	Reference
cal_CO ₃ H ⁰ = cal_CO ₃ ⁻ + H ⁺	-5.1	8.22e-6	0.22	200	DLM	
cal_CO ₃ H ⁰ + Ca ²⁺ = cal_CO ₃ Ca ⁺ + H ⁺	-1.7	8.22e-6	0.22	200	DLM	
cal_CaCO ₃ ⁻ + H ₂ O = cal_CaOH ²⁺ + CO ₃ ²⁻	-5.25	7.99e-6	0.22	200	DLM	
cal_CaCO ₃ ⁻ + HCO ₃ ⁻ = cal_CaHCO ₃ ⁰ + CO ₃ ²⁻	-3.929	7.99e-6	0.22	200	DLM	
cal CaCO ₃ ⁻ + H ₂ AsO ₄ ⁻ = cal_CaHAsO ₄ ⁰ + H ⁺ + CO ₃ ²⁻	-8.97	7.99e-6	0.22	200	DLM	(HU Sjø et al. 2008)
cal CaCO ₃ ⁻ + CaHAsO ₄ ⁰ = cal_CaAsO ₄ Ca ⁰ + H ⁺ + CO ₃ ²⁻	-9.81	7.99e-6	0.22	200	DLM	
cal_sCaCO ₃ ⁻ + H ₂ O = cal_sCaOH ²⁺ + CO ₃ ²⁻	-5.25	2.3e-7	0.22	200	DLM	
cal_sCaCO ₃ ⁻ + HCO ₃ ⁻ = cal_sCaHCO ₃ ⁰ + CO ₃ ²⁻	-3.929	2.3e-7	0.22	200	DLM	
cal_sCaCO ₃ ⁻ + H ₂ AsO ₄ ⁻ = cal_sCaHAsO ₄ ⁰ + H ⁺ + CO ₃ ²⁻	-7.98	2.3e-7	0.22	200	DLM	
cal_sCaCO ₃ ⁻ + CaHAsO ₄ ⁰ = cal_sCaAsO ₄ Ca ⁰ + H ⁺ + CO ₃ ²⁻	-7.22	2.3e-7	0.22	200	DLM	

Several experimental and modeling studies (L Zheng et al. 2012; RC Trautz et al. 2013; L Zheng et al. 2016) revealed that cation exchange reactions control the fate of the alkali and alkaline earth metals. Among them, Ba is of particular importance because it is more of an environmental concern. The cation exchange reactions that are typically involved when CO₂ leaks into a shallow aquifer are listed in Table 3.11.

Table 3.11. Cation Exchange Reactions and Selectivity Coefficients, Using the Gaines-Thomas Convention (CJA Appelo and D Postma 1994)

Cation Exchange Reaction	$K_{Na/M}$
$Na^+ + X-H = X-Na + H^+$	1
$Na^+ + X-K = X-Na + K^+$	0.2
$Na^+ + 0.5X-Ca = X-Na + 0.5Ca^{+2}$	0.4
$Na^+ + 0.5X-Mg = X-Na + 0.5Mg^{+2}$	0.6
$Na^+ + 0.5X-Ba = X-Na + 0.5Ba^{+2}$	0.2
$Na^+ + 0.5X-Sr = X-Na + 0.5Sr^{+2}$	0.15
$Na^+ + X-Li = X-Li + Li^+$	0.08

3.4.1.2 Surface Reactions for Organic Compounds

Because linear adsorption isotherms are widely used to model the transport of organic compounds in aquifers, the NRAP groundwater model uses the same approach and the key parameter is the distribution coefficient, K_d . The distribution coefficient between soil and water is defined as:

$$K_d = \frac{m_i^s / m^s}{m_i^{H_2O} / m^{H_2O}} \quad (3.1)$$

where m_i^s and $m_i^{H_2O}$ is the mass of organic species i in the sediments and water respectively, and m^s and m^{H_2O} is the mass of sediments and water, respectively. Note that K_d in Equation 3.1 is dimensionless. Alternatively, K_d can also take units of mL/g or L/kg if expressed as a ratio of concentrations (i.e., mg/kg_{soil} divided by mg/L_{water}). Table 3.12 lists some published K_d values for benzene, which are highly variable. Also shown in Table 3.12 is the weight fraction of organic carbon in sediments, f_{oc} , calculated based on a K_{oc} of 79 ($\log K_{oc}=1.9$); the definition of f_{oc} and K_{oc} will be discussed later.

Table 3.12. Compilation of Published K_d for Benzene Between Soil and Water

Reference	K_d (mL/g)	f_{oc}	Comments
(T Larsen et al. 1992)	0.05-0.65	0.00063-0.0082	Measured for aquifer samples which are located at various places in Denmark and have a great variety
(RB Donahue et al. 1999)	0.1-1.0	0.0013-0.013	Measured for Regina clay in Canada
(J-S Jean et al. 2002)	0.16-0.5	0.0021-0.0063	Measured in a laboratory experiment for artificial medium-size sand
(SB Hawthorne and DJ Miller 2003)	28-59	0.35-0.75	Measured for manufactured gas plant soils (contaminated by organic compounds)

The large range of measured K_d values is primarily due to the dependence of K_d on the organic matter content of soils, which is quite variable. In other words, K_d is sediment specific, and the same K_d value is not necessarily applicable to a range of different soil types. Although the value of K_d depends on the properties of sediments, the hydrophobic partitioning theory as reviewed by SW Karickhoff et al. (1979) implies that the partitioning of a specific compound between water and organic carbon, as expressed by K_{oc} , is largely independent of the organic content of the solid material. K_d can be calculated from K_{oc} by the equation:

$$K_d = f_{oc} \times K_{oc} \quad (3.2)$$

where $f_{oc} = m_{oc}^s / m^s$ is the mass fraction of organic carbon in sediments, defined as the mass of organic carbon in sediments, m_{oc}^s , divided by the mass of sediments. K_{oc} may be thought of as the ratio of the amount of chemical adsorbed per unit weight of organic carbon in the soil to the concentration of the chemical in solution at equilibrium:

$$K_{oc} = \frac{m_i^s / m_{oc}^s}{m_i^{H_2O} / m^{H_2O}} \quad (3.3)$$

K_{oc} is usually related to K_{ow} by:

$$\log K_{oc} = a \log K_{ow} + b \quad (3.4)$$

where K_{ow} is the octanol/water partition coefficient. SW Karickhoff, DS Brown and TA Scott (1979) reported the following equation from least squares fitting for $\log K_{oc}$ versus $\log K_{ow}$.

$$\log K_{oc} = 1.0 \cdot \log K_{ow} - 0.21 \quad (3.5)$$

D Mackay et al. (1992) reported that the $\log K_{oc}$ ranges from 1.09 to 2.53 with a median around 1.8–2.0.

Table 3.13. K_{oc} (L/kg) for Benzene, Phenol, and Naphthalene

Organic Compound	Max	Min	Geometric Mean
Benzene	100	31	62
Phenol			28.8 ^a
Naphthalene	1950	830	1191

(a) calculated rather than measured

Oxidation of the organics was calculated with the first-order degradation kinetics:

$$\frac{dC}{dt} = -KC \quad (3.6)$$

where C is the concentration of the organic compound and K is the first-order rate constant which was treated as a variable parameter.

The K_{oc} for benzene, phenol, and naphthalene is included in Table 3.13 and the degradation rate constants for these same organic compounds are included in Table 3.14.

Table 3.14. Degradation Rate Constant (1/day) for Benzene, Phenol, and Naphthalene (ZA Saleem 1999)

Organic Compound	Max	Min	Median
Benzene	0.071	0	0
Phenol	0.2	0	0.032
Naphthalene	0.03	0	0

3.4.2 Dissolution/Precipitation

The dissolution/precipitation of minerals in aquifer sediments is critical for how aquifers respond to incoming CO₂ and brine. First, the dissolution of minerals, typically carbonate minerals such as calcite, is the major pH buffering process.

Second, the dissolution of minerals could lead to the release of trace metals directly or indirectly. For example, the dissolution of some sulfide minerals (e.g., galena or arsenopyrite) could be responsible for the increase of lead and arsenic concentration (L Zheng et al. 2009; JA Apps et al. 2010; S Wang and PR Jaffe 2004) and the dissolution of calcite could lead to the release of some impurities in calcite, such as Sr and Ba (J Lu et al. 2010). The dissolution of calcite could also cause indirect release of Cs and Ba by triggering Ca-driven cation exchange reactions (L Zheng et al. 2012). It is noteworthy that not only the fast reacting minerals such as calcite play a significant role, but also the slow reacting minerals in certain circumstances. For instance, a field test in Mississippi (RC Trautz et al. 2013) showed that the dissolution of plagioclase (which reacts much slower than calcite) started to release calcium and subsequently trigger the increase in concentrations of Sr and Ba after the injection of CO₂-saturated water stopped, which illustrated that when the groundwater flow rate is fairly low, slow reacting minerals could also have significant impacts on the release of trace metals.

Third, dissolution/precipitation of minerals can alter the pore structure of sediments and, subsequently, the flow pathways. However, such an effect is more important for the mineral trapping of CO₂ in the storage formation than for the impact of the CO₂ and brine leakage on groundwater. Although in the last decade studies have shown fast reacting minerals, such as carbonate and sulfide minerals, and a few slow reacting minerals, such as plagioclase, play a major role in controlling the response of aquifers to the leakage of CO₂ and brine, these reactions are chains of complex reaction networks. It is therefore necessary to take into account all of the minerals phases when developing a reactive transport model, despite the fact that most of the time a subset of these minerals is selected due to pragmatic reasons, such as computation time. In this report, because it is not possible to have an exhaustive list of minerals, we focus on the mineral phases that are related to two aquifers: the Edwards and High Plains Aquifers. Table 3.15 shows the minerals for the Edwards Aquifer and their kinetic reaction rates.

Table 3.15. Kinetic Mineral Reactions and Neutral Mechanism Rates (Palandri and Kharaka, 2004) for the Edwards Aquifer at 25°C

Kinetic Reaction	Equilibrium Coefficient at 25°C, log	Forward Rate at 25°C, mol/m ² /s	Activation Energy, kJ/mol
Calcite + H ⁺ = HCO ₃ ⁻ + Ca ⁺²	1.847	1.5e-6	23.5
Dolomite + 2H ⁺ = 2HCO ₃ ⁻ + Ca ⁺² + Mg ⁺²	3.533	2.9e-8	52.2
Strontianite = CO ₃ ⁻ + Sr ⁺²	-9.271	Same as calcite	Same as calcite

Table 3.16. Equilibrium Constants of the Major Rock-Forming Minerals for the High Plains Aquifer. Chemical reactions for the minerals in the first column are written as the chemical species in the first row with stoichiometric coefficients listed under each species.

Minerals	logK (25°C)
Calcite + H ⁺ = Ca ⁺² + HCO ₃ ⁻	1.853
Illite + 6.3 H ₂ O = H ⁺ + 0.25Mg ⁺² + 0.85K ⁺ + 3.4 H ₄ SiO ₄ (aq) + 2.35AlO ₂ ⁻	-43.490
Kaolinite + 3H ₂ O = 2H ⁺ + 2H ₄ SiO ₄ (aq) + 2AlO ₂ ⁻	-39.262
Smectite + 7.32 H ₂ O = 0.68H ⁺ + 0.17Ca ⁺² + 0.335Mg ⁺² + 3.99 H ₄ SiO ₄ (aq) + 1.68AlO ₂ ⁻	-32.834
goethite + 3H ⁺ = 2H ₂ O + Fe ⁺³	0.363
Albite + 6H ₂ O = Na ⁺ + 3H ₄ SiO ₄ (aq) + AlO ₂ ⁻	-20.126
Quartz + 2H ₂ O = H ₄ SiO ₄ (aq)	-3.740
K-Feldspar + 6H ₂ O = K ⁺ + 3H ₄ SiO ₄ (aq) + AlO ₂ ⁻	-22.394
Dolomite + 2H ⁺ = Ca ⁺² + Mg ⁺² + HCO ₃ ⁻	3.545
Magnesite + H ⁺ = Mg ⁺² + HCO ₃ ⁻	1.420
Dawsonite = H ⁺ + Na ⁺ + HCO ₃ ⁻ + 2.35AlO ₂ ⁻	-18.535
Muscovite + 6H ₂ O = 2H ⁺ + K ⁺ + 3H ₄ SiO ₄ (aq) + 3AlO ₂ ⁻	-57.264
Ferrihydrite + 3H ⁺ = 3H ₂ O + Fe ⁺³	3.404
Gibbsite = H ₂ O + H ⁺ + AlO ₂ ⁻	-15.129

Table 3.16 lists all the major rock-forming minerals for the High Plains Aquifer. Kinetic rate parameters for most rock-forming minerals for the High Plains Aquifer were taken from J Palandri and YK Kharaka (2004), which are based mainly on experimental studies conducted under far-from-equilibrium conditions. The overall rate equation is tied to mineral equilibria through Q/K with a pH dependent rate consisting of acid, neutral, and base mechanisms as indicated below:

$$r = \pm k A \left[1 - \left(\frac{Q}{K} \right)^\theta \right]^\eta \quad (3.7)$$

and

$$k = k_2^n \exp \left[\frac{-E_a^{nu}}{R} \left(\frac{1}{T} - \frac{1}{29815} \right) \right] + k_2^H \exp \left[\frac{-E_a^H}{R} \left(\frac{1}{T} - \frac{1}{29815} \right) \right] a_H^{n_H} + k_2^{OH} \exp \left[\frac{-E_a^{OH}}{R} \left(\frac{1}{T} - \frac{1}{29815} \right) \right] a_{OH}^{n_{OH}} \quad (3.8)$$

where

- r = the kinetic rate,
- k = the rate constant,
- A = the specific reactive surface area,
- K = the equilibrium constant for the mineral–water reaction,
- Q = the reaction quotient.
- nu = neutral mechanism,

- H = acid mechanism
 OH = base mechanisms,
 E_a = activation energy that accounts for the dependence of the rate on temperature,
 T = absolute temperature,
 a_H = hydrogen ion activity
 a_{OH} = hydroxyl ion activity, and
 n = an empirical constant.

The parameters θ and η are assumed equal to unity. The mineral reactive surface areas were taken from T Xu et al. (2006), based on the work of E Sonnenthal et al. (2005). A thorough review and discussion of the kinetic rates for arsenian pyrite, pyrite, and galena was given in L Zheng et al. (2009). The kinetic properties for the minerals in the High Plains Aquifer are given in Table 3.17.

Table 3.17. Kinetic Properties for Minerals Considered in the Model (see text for data sources). “Primary” minerals are initially present in the aquifer. “Secondary” minerals are formed by precipitation.

Mineral	Parameters for Kinetic Rate Law									
	A (cm ² /g)	Neutral Mechanism			Acid Mechanism			Base Mechanism		
		k ₂₅ mol/m ² /s	E _a KJ /mol		k ₂₅	E _a	n(H ⁺)	k ₂₅	E _a	n(OH ⁻)
Primary:										
Calcite	3.05	1.6×10 ⁻⁶	62.76							
Illite	151.60	1.66×10 ⁻¹³	35.00	1.05×10 ⁻¹¹	23.60	0.34	3.02×10 ⁻¹⁷	58.9	-0.40	
Kaolinite	151.60	6.91×10 ⁻¹⁴	22.20	4.89×10 ⁻¹²	65.90	0.78	8.91×10 ⁻¹⁸	17.9	-0.47	
Smectite	151.60	1.66×10 ⁻¹³	35.00	1.05×10 ⁻¹¹	23.60	0.34	3.02×10 ⁻¹⁷	58.9	-0.4	
Goethite	12.90	2.51×10 ⁻¹⁵	66.20	4.07×10 ⁻¹⁰	66.20	1.00				
Albite	9.80	3.89×10 ⁻¹³	38.00	8.71×10 ⁻¹¹	51.70	0.50	6.31×10 ⁻¹²	94.1	-0.82	
Quartz	9.80	3.98×10 ⁻¹⁴	87.7							
K-feldspar	9.80	3.89×10 ⁻¹³	38.00	8.71×10 ⁻¹¹	51.70	0.50	6.31×10 ⁻¹²	94.1	-0.82	
Secondary:										
Dolomite	12.90	2.95×10 ⁻⁸	62.76	2.34×10 ⁻⁷	43.54	1.00				
Magnesite	9.80	4.57×10 ⁻¹⁰	23.50	4.17×10 ⁻⁷	14.40	1.00				
Dawsonite	9.80	3.89×10 ⁻¹³	38.00	8.71×10 ⁻¹¹	51.70	0.50	6.31×10 ⁻¹²	94.1	-0.82	
Muscovite	9.80	3.89×10 ⁻¹³	38.00	8.71×10 ⁻¹¹	51.70	0.50	6.31×10 ⁻¹²	94.1	-0.82	

Mineral	Parameters for Kinetic Rate Law								
	Neutral Mechanism			Acid Mechanism			Base Mechanism		
	A (cm ² /g)	k ₂₅ mol/m ² /s	E _a KJ/mol	k ₂₅	E _a	n(H ⁺)	k ₂₅	E _a	n(OH ⁻)
Gibbsite	9.80	3.89×10 ⁻¹³	38.00	8.71×10 ⁻¹¹	51.70	0.50	6.31×10 ⁻¹²	94.1	-0.82
Pyrite	12.90	2.52×10 ⁻¹²	62.76						

3.4.3 Redox Reactions

Redox potential is very important in determining the fate of redox-sensitive trace metals and organic compounds when groundwater in a shallow aquifer is affected by the leakage of CO₂. For example, it is known that As(III) has much higher mobility and is of more environmental concern than As(V). Also, the biodegradation rate for an organic compound is much higher in oxidizing than reducing conditions. When CO₂ or CO₂-saturated brine leaks into the aquifer, it primarily causes a decrease of pH. Meanwhile, Eh will change as well due to the interrelation of pH and Eh. It is therefore critical to determine the background redox condition in the aquifer and the change of redox condition after the intrusion of CO₂.

For confined aquifers, because of the fairly low redox potential, a sufficient increase in redox potential to cause a shift of speciation of redox-sensitive species, such as As, is unlikely. For unconfined aquifers, changes in redox potential are more likely and could shift the speciation and key parameters of potential contaminants (e.g., degradation rate for organic compounds). However, in either case, redox reactions have to be included in the reactive transport models and redox potentials have to be evaluated. The most prevalent redox reactions are those involving the following pairs of redox couples: Fe(II)/Fe(III), HS⁻/SO₄⁻², and As(III)/As(V).

3.5 Development of Conceptual and Reduced Order Models

The development of a ROM requires multiple runs of the reactive transport models that simulate the leakage of CO₂ and brine into a shallow aquifer. The core of the reactive transport model is the geochemical conceptual model. The following work is helpful, and sometime necessary, to build a defensible conceptual model.

First, it is necessary to gather detailed water and mineral composition data. This basic information, with the help of geochemical equilibrium calculations, can reveal which mineral phase controls the major and trace elements and which reactions are important for pH and Eh. It is also necessary to measure the cation exchange capacity (CEC) and sorption capacity of the aquifer sediments.

Second, batch experiments that typically involve the release of CO₂ into a pre-equilibrated water-sediment environment are very useful in two ways. First, the batch experiment is a great screening tool to determine which elements could be released. Such experiments have features, including the well mixing of sediment with water, that lead to a very aggressive release of trace elements (L Zheng, N Spycher, et al. 2015), and they therefore provide the upper bound of the type of elements and their concentrations that could be caused by the introduction of CO₂ into an aquifer. In other words, if a given element is not released by the batch experiment, it is unlikely to show up in the aquifer in a large scale CO₂ leakage scenario, although one should pay attention to the heterogeneity issue and make sure to do a series of

batch experiments with sediments from different locations of the aquifer. Secondly, the batch experiment, integrated with geochemical modeling, is very useful for determining the chemical reactions that control the release of trace elements. Because of the aggressiveness of the batch experiment, some reactions that are relevant for the batch experiment may become less important, or even irrelevant, for the real condition.

Third, it is desirable to have a column test to evaluate transport processes, such as the column test with High Plains Aquifer sediments (A Lawter et al. 2016). Such tests give us more realistic estimates of the type of elements and their concentrations that could result from the introduction of CO₂ into aquifer, and provide an insight of the interaction of chemicals with transport processes. A reactive transport model for the column test (L Zheng et al. 2016) can further narrow down the key reactions and parameters and lay a strong foundation for a reactive transport model at appropriate field scales.

After the establishment of the conceptual model, simulations can be conducted for the time steps and spatial resolution needed. A sensitivity analysis, which can be performed by manually tuning some key parameters, is useful to double-check the model setup.

The development of the Gen III hydrology ROM (SA Carroll et al. 2014) is an example of the procedure to develop a ROM. First, we need to know parameter ranges for the development of the aquifer model, hydrologic flow, leakage flux, brine concentrations, and geochemical parameters. Second, these parameters are sampled to design a number of simulations. For example, for the Gen III hydrology ROM (SA Carroll et al. 2014), 1000 simulations were designed. Third, model results are processed to calculate the entities used to build the ROM. Then the ROM is derived. Depending on the nature of the ROM (e.g., polynomial-based ROMs, lookup tables, etc.), the derivation method is different. The ROM should be able to emulate the outcome of the numerical model, but with less complexity, more thorough sampling of the parameter space, and significantly faster simulation times to generate risk-based profiles that can be used in decision making processes.

Development of the groundwater ROMs required the following data:

- Threshold values,
- Initial groundwater concentrations,
- Rock mineralogy,
- Thermodynamic data (log K's) for rock mineral and aqueous complexes,
- Surface complexation reactions for trace metals, and
- Koc and biodegradation rates for organics.

Parameters needed to drive the Gen II and III ROMs can be grouped in three categories: parameters that are related to the source term, parameters to define the hydrological properties of the aquifer, and parameters used to define the chemical properties of the aquifer. In the GEN III ROM (SA Carroll et al. 2014), the leakage models and variable parameters are illustrated in Figure 3.8. Variability in the CO₂ leakage profile was generated using four parameters:

1. q_{CO_2} – the peak flux
2. T_{1C} – the time needed to reach peak flux
3. dT_{2C} – the duration of the peak flux
4. dT_{3C} – the duration of the transition to zero flux after injection has stopped

Brine leakage profiles are different from that of CO₂. Brine leakage was characterized with a maximum and constant flux during injection, which falls off to a final flux after injection stops. Uncertainty in the brine leakage profile was generated using four parameters:

1. q_{BRN} – the initial and maximum flux.
2. λq_{BRN} – the final flux.
3. T_{1B} – the injection time.
4. dT_{2B} – the duration of the transition between the maximum and final flux.

An additional parameter, T_M , was included to represent wellbore mitigation time. The ranges of these parameters are given in Table 3.18 (SA Carroll et al. 2014). Another set of the parameters that are related to the source term are the concentrations of major ions (i.e., Na and Cl), trace metals, and organic compounds, which are listed in Table 3.19. Note that in Table 3.19, chloride concentration is assumed to be the same as sodium concentration and there is no barium in the leaking brine.

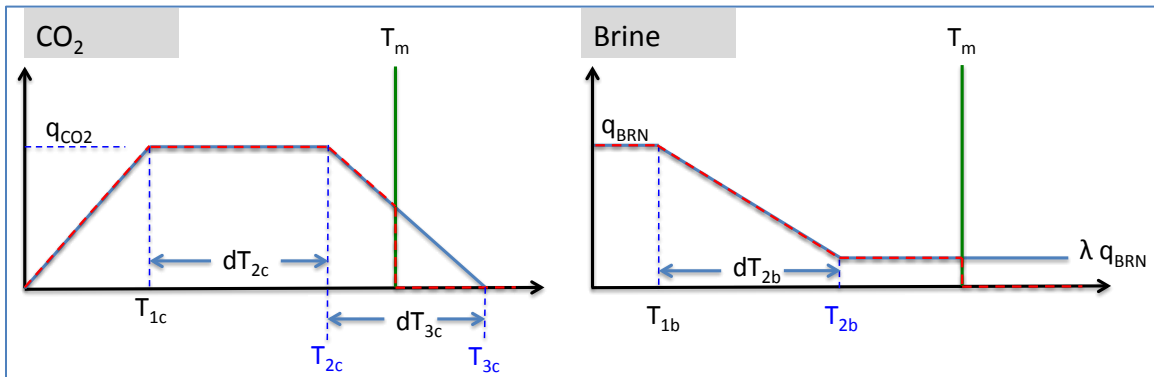


Figure 3.8. Schematic of the CO₂ and Brine Leakage Model Parameters and Profiles in the Generalized Model

Table 3.18. Proposed Parameter Ranges for Generalized CO₂ and Brine Leakage Models

Parameter	Min	Max	Notes
q_{CO_2}	-3.000	-0.301	$\text{Log}_{10}(0.001 - 0.5) \text{ kg s}^{-1}$
q_{BRN}	-2.301	-1.125	$\text{Log}_{10}(0.005 - 0.075) \text{ kg s}^{-1}$
λ	0.200	0.300	Ratio for brine leakage tail
T_{1c}	5.000	50.000	yr
dT_{2c}	0	100.000	yr
dT_{3c}	5.000	50.000	yr
T_{1b}	1.000	50.000	yr
dT_{2b}	1.000	10.000	yr
T_m	50.000	200.000	Mitigation time, yr

Table 3.19. Sodium, Trace Metals and Organics Concentrations Considered in the Groundwater Simulations and ROM. Trace metals are based on experiments (AK Karamalidis et al. 2013) and organic concentrations are based on L Zheng et al. (2010).

Trace Metal	Minimum	Maximum	Unit
Sodium Molality	-3	1	Log ₁₀ [mol kg ⁻¹]
Barium			Log ₁₀ [mol kg ⁻¹]
Cadmium	-8.87	-6.43	Log ₁₀ [mol kg ⁻¹]
Chromium	-6.42	-4.02	Log ₁₀ [mol kg ⁻¹]
Iron	-6.07	-2.79	Log ₁₀ [mol kg ⁻¹]
Lead	-8.12	-4.74	Log ₁₀ [mol kg ⁻¹]
Manganese	-5.13	-2.10	Log ₁₀ [mol kg ⁻¹]
Benzene	-10	-3.2	Log ₁₀ [mol kg ⁻¹]
Naphthalene	-10	-3.7	Log ₁₀ [mol kg ⁻¹]
Phenol	-10	-4.1	Log ₁₀ [mol kg ⁻¹]

Five parameters are needed to define the hydrological conditions in the aquifers, which are listed in Table 3.20. Table 3.21 lists the parameters related to the chemical properties of the aquifer.

Table 3.20. Parameter Definition and Ranges for Hydrologic Simulations and Emulations

Parameter	Minimum	Maximum	Unit
1 Sand volume fraction	0.35	0.65	-
2 Correlation length in X-direction	200	2500	[m]
3 Correlation length in Z-direction	0.5	25	[m]
4 Permeability in sand	-14	-10	Log ₁₀ [m ²]
5 Permeability in clay	-18	-15	Log ₁₀ [m ²]

Table 3.21. Input Parameters of the Development of the Scaling Functions

Parameter	Range
Calcite volume fraction	0.0 to 0.2
Goethite volume fraction	0.0 to 0.2
Illite volume fraction	0.0 to 0.3
Kaolinite volume fraction	0.0 to 0.2
Montmorillonite volume fraction	0.0 to 0.5
Cation exchange capacity (CEC meq/100)	0.1 to 40.0
Benzene concentration in the leaking brine (mol/L)	-10.0 to -3.2 ^a
Phenol concentration in the leaking brine (mol/L)	-10.0 to -3.7 ^a
Naphtalene concentration in the leaking brine (mol/L)	-10.0 to -4.1 ^a
Benzene distribution coefficient (L/kg)	-4.5 to 0.69 ^a

Parameter	Range
Phenol distribution coefficient (L/kg)	-6.0 to 0.15 ^a
Naphtalene distribution coefficient (L/kg)	-3.1 to 1.98 ^a
Benzene degradation constant (1/s)	0 to -6.1 ^a
Phenol degradation constant (1/s)	0 to -5.63 ^a
Naphtalene degradation constant (1/s)	0 to -6.45 ^a
Time (years)	0 to 200

(a) indicates log10 values

4.0 Potential Risk for Groundwater Pollution Due to CO₂ Gas and Brine Intrusion

This section of the report establishes the overall potential risk for groundwater pollution of CO₂/brine leakage based on literature review and data from modeling, laboratory, and field experiments conducted at PNNL and LBNL.

4.1 The Effects on TDS and pH

4.1.1 High Plains Aquifer

4.1.1.1 Experimental Results

Results from a series of batch and column experiments revealed important differences in pH and TDS that will be discussed in detail in the following section on modeling. Briefly, some of the sediment samples have detectable amounts of calcite, while some other samples had no XRD detectable calcite. In these latter samples, the pH remained lower than the pH measured in experiments conducted with calcite-containing sediments, mainly due to reduced buffering capacity of sediments that had no calcite. The pH for the calcite-containing sediments decreased to no less than ~6, while the pH for calcite-free sediments decreased to ~5. Aqueous samples from the calcite-free sediment showed a greater release of elements, including several regulated by the EPA, such as As, Cr, and Pb.

Contaminants, such as As and Cd present in saline brines, could travel upward with leaking CO₂ into the overlying aquifer. Batch and column experiments were conducted with As and Cd spikes (114 µg/L and 40 µg/L, respectively) to determine the fate of these contaminants if this were to happen. These solutions had no significant effect on pH.

Methane can also be transported upward with a CO₂ plume, so experiments were conducted with a 1% CH₄ and 99% CO₂ gas mix. These experiments revealed that the effect on pH was not significant.

4.1.1.2 Modeling

In this section the discussion is focused on input and fitted modeling parameters, sensitive and non-sensitive parameters, the impact of site-specific data on modeling, and whether the changes are short- or long-term.

The assessment of the risk of CO₂ and brine leakage on groundwater overlying a CO₂ sequestration site relies heavily on numerical models. Correct geochemical conceptual models and reliable key parameters are critical for the predictability of a numerical model. In light of modeling the impact of CO₂ and brine leakage on groundwater, conceptual models look at the chemical reactions that control the release of trace metals and the fate of organic compounds. Therefore, the most important parameters are those needed to describe these reactions. Model interpretation of the laboratory and field experiments is an effective way to develop the right conceptual model and calibrate key parameters.

A series of batch and column tests were conducted for the sediments from the High Plains Aquifer (A Lawter et al. 2016). In the column experiments, CO₂ saturated synthetic groundwater (which mimics the water composition of the High Plains Aquifer) was injected through a column packed with material from the High Plains Aquifer to simulate the impact of a gradual leak of CO₂ on a shallow aquifer. A reactive

transport model was developed to interpret the observed concentration changes in the column effluent water (L Zheng et al. 2016), attempting to shed light on the chemical reactions and key parameters that control the concentration changes of some constituents.

The geochemical conceptual model used in the reactive transport model for the column test was consistent with those revealed by modeling two field tests (L Zheng et al. 2012; RC Trautz et al. 2013): the Montana State University-Zero Emissions Research and Technology (MSU-ZERT) field test in Montana (YK Kharaka et al. 2010), and a field test conducted in Plant Daniel, Mississippi (RC Trautz et al. 2013). Note that both of these tests were conducted on a sandstone aquifer, for which the composition of key minerals in the aquifer sediments were similar to that of the High Plains Aquifer. Due to similarities between the two aquifer systems, it is not a surprise that the geochemical conceptual model developed for the field test in Mississippi is applicable to the model for the column test with High Plains Aquifer materials (A Lawter et al. 2016). In these models, dissolution of calcite is the primary pH buffering process, with the dissolution of magnesite and surface protonation playing a secondary role. Figure 4.1 shows the comparison of the model results with experimental data.

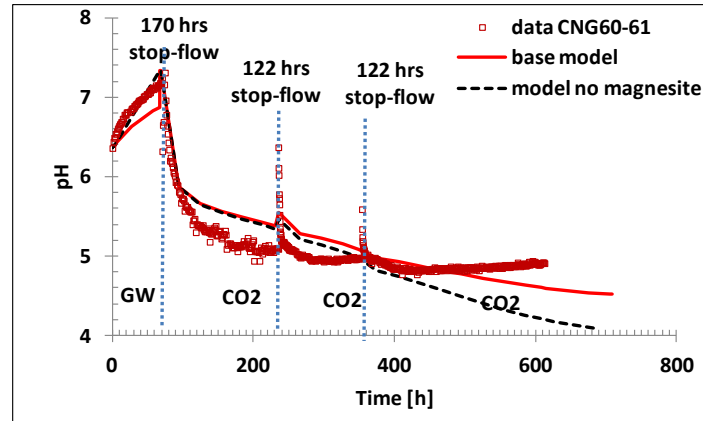


Figure 4.1. Simulated and Observed Breakthrough Curves of pH for the Column Test of Sample CNG60

4.1.2 Edwards Aquifer

4.1.2.1 Experimental Results

Materials from the Edwards Aquifer in Texas were used to represent a potential unconfined carbonate aquifer overlying a CO₂ sequestration site. As with the High Plains Aquifer sediments, both column and batch experiments were conducted using samples from the Edwards Aquifer. Unlike the unconsolidated sand and gravel aquifer sediments, the unweathered or slightly weathered rocks of the Edwards aquifer were ground by mortar and pestle and used in these experiments in the form of powder. Column studies were conducted with a steady CO₂ flow rate of 0.5 mL/min into the SGW, which was pumped through the columns at 0.03 mL/min. Because of the high calcite content and buffering capacity of these sediments, the effect on pH was similar in all tested materials. The pH of all experiments did not decrease below pH ~ 6 due to the high carbonate content and buffering capacity of these materials. Data from these experiments are presented in a previously published report (N Qafoku et al. 2013) and will be also discussed in the following section on modeling.

4.1.2.2 Modeling

Results from mineralogical analyses show that the limestone consists almost entirely of calcite (G Wang et al. 2016). Previous publications indicate that the predominant mineral in this limestone is calcite with a small amount of dolomite (RW Maclay and TA Small 1994); and a minor amount of the mineral strontianite was included in solid solution with calcite (AJ Tesoriero and JF Pankow 1996) (Table 4.1).

Table 4.1. Mineral Reactions

Kinetic Reaction	Equilibrium Coefficient at 25°C, log	Forward Rate at 25°C, mol/m ² /s	Activation Energy, kJ/mol
Calcite + H ⁺ = HCO ₃ ⁻ + Ca ⁺²	1.847	1.5e-6	23.5
Dolomite + 2H ⁺ = 2HCO ₃ ⁻ + Ca ⁺² + Mg ⁺²	3.533	2.9e-8	52.2
Strontianite = CO ₃ ⁻ + Sr ⁺²	-9.271	Same as calcite	Same as calcite

Modeling of the batch experiments was conducted using PHREEQC (DL Parkhurst and CAJ Appelo 1999) and the thermo.com.V8.R6 database (TW Wolery and RL Jarek 2003). Modeling of the column experiments was conducted using the multiphase flow and reactive transport solver STOMP-CO₂-R (MD White et al. 2012) with ECKEChem (MD White and BP McGrail 2005). The STOMP simulations used a smaller subset of equilibrium aqueous complexation reactions extracted from PHREEQC simulations of the batch experiments and groundwater samples (M Musgrove et al. 2010) taken from the unconfined/urban portion of the Edwards Aquifer (Table 4.2).

Table 4.2. Aqueous Complexation Reactions

Equilibrium Reaction	Equilibrium Coefficient at 25°C, log
HCO ₃ ⁻ + H ⁺ = CO ₂ + H ₂ O	6.3447
HCO ₃ ⁻ + Ca ⁺² = CaHCO ₃ ⁺	1.0467
HPO ₄ ⁻² + Ca ⁺² = CaHPO ₄	2.7400
HPO ₄ ⁻² + Ca ⁺² = CaPO ₄ ⁻ + H ⁺	-5.8618
SO ₄ ⁻² + Ca ⁺² = CaSO ₄	2.1111
Cl ⁻ + Cd ⁺² = CdCl ⁺	2.7059
HCO ₃ ⁻ + Cd ⁺² = CdHCO ₃ ⁺	1.5000
HPO ₄ ⁻² + H ⁺ = H ₂ PO ₄ ⁻	7.2054
Mg ⁺² + HCO ₃ ⁻ = MgHCO ₃ ⁺	1.0357
Mg ⁺² + HPO ₄ ⁻² = MgHPO ₄	2.9100
SO ₄ ⁻² + Mg ⁺² = MgSO ₄	2.4117
H ₂ O = OH ⁻ + H ⁺	-13.9951
Na ⁺ + HCO ₃ ⁻ = NaHCO ₃	0.1541
Pb ⁺² + HCO ₃ ⁻ = PbCO ₃ + H ⁺	-3.7488
Pb ⁺² + H ₂ O = PbOH ⁺ + H ⁺	-7.6951
Sr ⁺² + SO ₄ ⁻² = SrSO ₄	2.3000
2H ₂ O + Cr ⁺³ = Cr(OH) ₂ ⁺ + 2H ⁺	-9.7000
3H ₂ O + Cr ⁺³ = Cr(OH) ₃ + 3H ⁺	-18.0000
H ₂ O + Cr ⁺² = CrOH ⁺² + H ⁺	-4.0000
HCO ₃ ⁻ + Cu ⁺² = CuCO ₃ + H ⁺	-3.3735
H ₂ O + Cu ⁺² = CuOH ⁺ + H ⁺	-7.2875

Equilibrium Reaction	Equilibrium Coefficient at 25°C, log
$\text{SeO}_3^{-2} + \text{H}^+ = \text{HSeO}_3^-$	7.2861

The column experiments utilizing unweathered rock samples were modeled by including calcite and dolomite, and adjusting the amount of strontium in solid solution with calcite. For the first sample, the concentration of dissolved CO_2 in the inlet water was adjusted to match the observed pH (Figure 4.2), which decreases to a value of around 6.5. TDS was calculated based on major ion concentrations (Figure 4.2), and increased from a value of 161 mg/L at the beginning of the experiment to a value of 353 mg/L at the end of the column experiment. The reported median value of TDS in the urban, unconfined portion of the Edwards Aquifer is 329 mg/L (M Musgrove et al. 2010). The experimentally observed TDS is lower than the reported 75th percentile value of 360 mg/L.

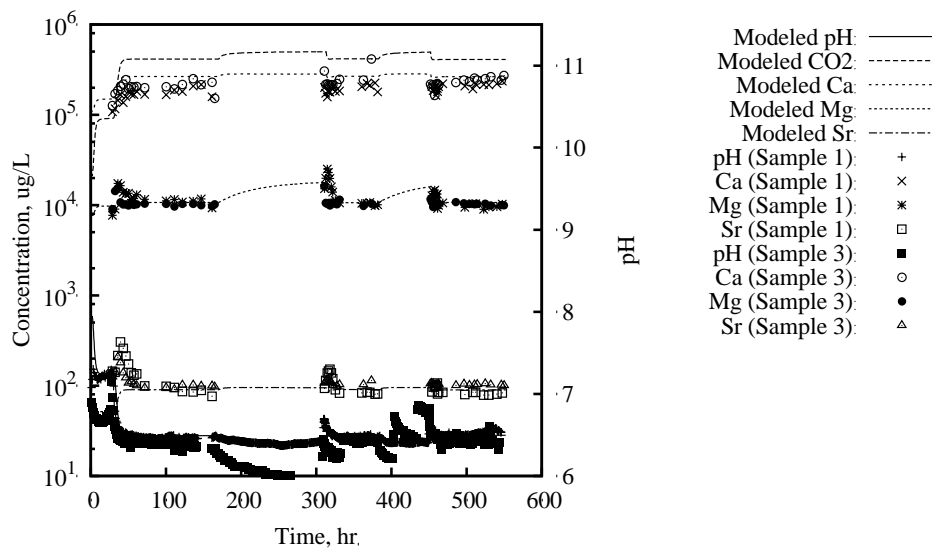


Figure 4.2. Major Ion Modeling Results Compared to Column Experiment Results

4.2 Changes in Major, Minor, and Trace Element Concentration

4.2.1 High Plains Aquifer

4.2.1.1 Experimental Results

The release of major, minor, and trace elements from sediments exposed to CO_2 gas streams was studied in a series of batch and column experiments. The data will be presented in the modeling section that follows.

As mentioned previously, contaminants, such as As and Cd, could travel upward with the leaking CO_2 into the overlying aquifer. Batch and column experiments were conducted with an As and Cd spike (114 $\mu\text{g/L}$ and 40 $\mu\text{g/L}$, respectively) to determine contaminant fate if this were to happen. Results showed the sandstone aquifer sediments had a large adsorption capacity for these contaminants, with a 90-95 % reduction of Cd and a 60-70% reduction of As within 4 hours in the gas injected reactors and a greater

reduction in the blank (no gas) reactors. Cd concentrations fell below detection limits and As fell below 73%.

Methane can also be transported upward with a CO₂ plume, so experiments were conducted with a 1% CH₄ and 99% CO₂ gas mix. Calcite-free sediments and sediments containing calcite were used in batch and column experiments. Results show little effect of CH₄ on contaminant release and again confirmed the large adsorption capacity for As and Cd in these sediments.

4.2.1.2 Modeling

The effluent water from the column test (Lawter et al., 2016) has high concentrations of major elements (e.g., Si, Ca, Mg, Na, K), minor elements (e.g., Al, Fe, Mn), and trace elements (e.g., Sb, Sr, Ba, Cr, Se, As, Pb, Cs, Cu, and Zn). Reactive transport models were developed to interpret the concentration change of the alkali and alkaline earth metals, As and Pb. In these models, calcite dissolution and Ca-driven cation exchange are responsible for the release of alkali and alkaline earth metals, including Ca, Mg, Na, K, Sr, Cs, and Ba; adsorption/desorption are the reactions that control the release of As and Pb. Because Pb, As, and Ba are included in the Gen III ROM, the reactive transport models for the column are very helpful to define the key reactions that control Pb, As, and Ba. Note that Cd is considered in the Gen III ROM, but the Cd was not detected in the column test; the reactive transport model for the column test thus cannot help to define the reactions for Cd. The details of these reactions are listed in Zheng et al. (2016).

Model interpretation of the column test also helped us to constrain key parameters. The parameters that were calibrated based on experimental data were calcite volume fraction, CEC, and the volume fraction of adsorbent (goethite). A limited amount of calcite that would be depleted after the intrusion of CO₂ was key to reproducing the pulse-like breakthrough curve of the concentration of alkali and alkaline earth metals in the effluent of the column test. A volume fraction of 0.045% and a specific surface area of 60 cm²/g were used for calcite, which led to a decent fit of the measured breakthrough curve of pH and Ca (Figure 4.1 and Figure 4.3). Calcite was not observed by XRD because the volume fraction was well below the detection limit of 1%, but a Ca bearing coating was detected in CNG 60 by SEM/EDS analysis. It is also noteworthy that a volume fraction of calcite below the XRD detection limit was also used in the model for the field test described in RC Trautz et al. (2013), where the presence of calcite in the sediments was later confirmed by micro-X ray spectroscopy. When deriving the Gen III ROM, a range of 0–20% was used for calcite volume fraction, which covers the value calibrated based on the column test data.

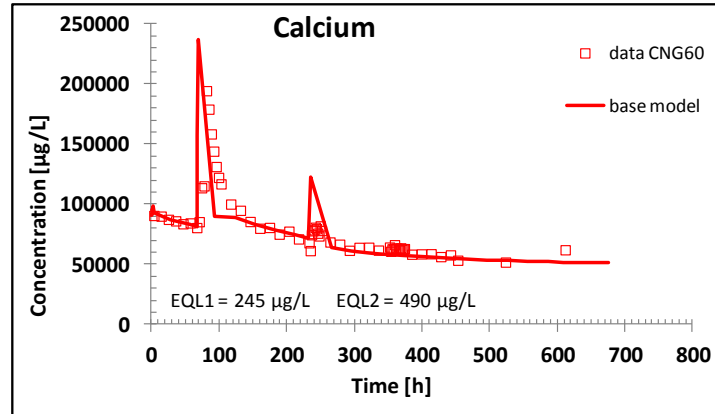


Figure 4.3. Simulated and Observed Breakthrough Curves of Ca for the Column Test of Sample CNG60

The key parameter relevant to Ba is the cation exchange capacity of the sediment; the calibrated CEC is 1.55 meq/100 g, which falls in the range of CECs that were used in the Gen III ROM. Another parameter is related to the adsorption/desorption reactions that control the release of As and Pb. In the reactive transport model that was used to derive the Generation III ROM, the adsorption capacity depends on the product of the amount of adsorbent and the surface area of the adsorbent. Therefore, the amount of adsorbent is considered as an input parameter in the ROM, while the surface area of adsorbent is fixed. Using a surface area of 40 m²/g, the calibrated amount of adsorbent (volume fraction of the goethite in this case) is 0.019 based on the column test data, which leads to a decent fit of measured data (Figure 4.4).

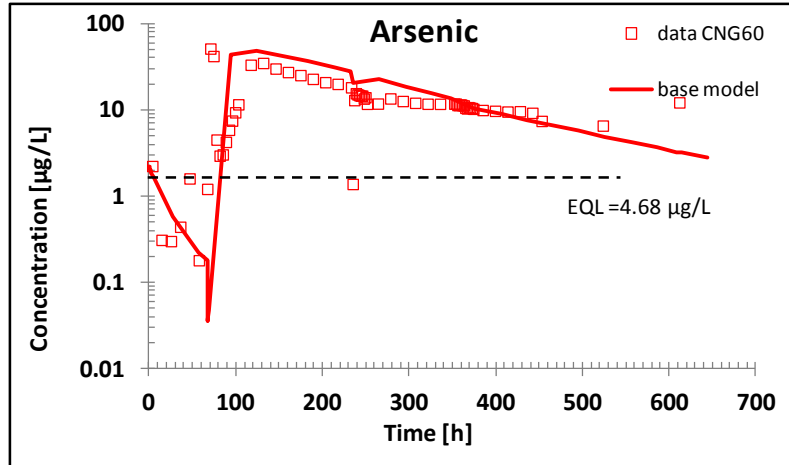


Figure 4.4. Simulated and Observed Breakthrough Curves of As for the Column Test of Sample CNG60

In summary, laboratory experiments integrated with reactive transport model simulations are very useful to find out the key chemical reactions and parameters that control the response of an aquifer to the leakage of CO₂. Regarding the Gen III ROM that is based on the conditions of the High Plains Aquifer, the reactive transport models for the column tests confirm the reactions taken into account in the ROM and parameter ranges for reactions related to Pb, As, and Ba. Because Cd and organic compounds were not detected or measured in the column test, reactions and parameters for these constituents cannot be evaluated via a reactive transport model for the column tests.

4.2.2 Edwards Aquifer

4.2.2.1 Experimental Results

The outcomes of the column experiments relative to the aquifer maximum concentrations and MCLs are summarized in Table 4.3. Concentrations are generally higher during the stop-flow periods. At the end of the first stop-flow period, all of the trace metals except for Cr exceed the maximum aquifer-observed values, and As, Pb, Sb, and Se exceed the MCL limits. However, concentrations of the trace metals generally decrease during the flow periods, and at the end of the second stop-flow period, Ba and Cr exceed the observed aquifer maximums and only As, Pb, and Sb exceed the MCL. By the last flow period, only Sb and Se exceed the aquifer maximum threshold and no trace metals exceed their respective MCLs.

Table 4.3. Summary of Column Experiment Trace Metal Concentrations at the End of Each Experimental Stage, Relative to Aquifer Maximum Concentrations and MCL Regulatory Limits (grey background indicates aquifer maximum exceeded, black background indicates MCL exceeded)

Experiment Stage	As	Ba	Cr	Cu	Pb	Sb	Se
Flow 1	1.00	19.5	0.590	1.52	1.32	0.690	3.01
Stop-Flow 1	44.7	203	2.03	58.2	817	17.8	150
Flow 2	0.460	10.8	0.580	1.80	0.180	0.170	1.07
Stop-Flow 2	10.1	88.2	18.1	10.9	45.0	8.64	34.5
Flow 3	0.750	5.66	0.460	0.660	0.150	0.210	2.56
Threshold	As	Ba	Cr	Cu	Pb	Sb	Se
Aquifer Max, µg/L	1.11	69.9	5.57	57.3	0.15	0.06	1.40
MCL, µg/L	10	2000	100	1300	15	6	50

4.2.2.2 Modeling

Figure 4.5 through Figure 4.11 show the model predictions for trace metal concentrations compared to column experimental results for Samples 1 and 3, and are compared to aquifer median and maximum concentrations, as well as the EPA MCL values. The release of the trace metals with time is very different in shape than that of the major ions. Whereas the major ions increase to a stable value with time and show small spikes during the stop-flow events, the trace metal concentrations generally decrease with time and show relatively large spikes during the stop-flow events. Arsenic concentrations during the flow periods are relatively stable, decreasing slightly between the first and second flow periods and increasing again during the third flow period, spiking above the MCL during the first stop-flow period, and reaching the MCL at the start of the second stop-flow period (Figure 4.5). Barium concentrations spike above the aquifer maximum during the stop-flow periods, but fall below the aquifer median during the flow periods (Figure 4.6). Chromium concentrations spike above the aquifer maximum during the stop-flow periods, but fall below the aquifer median during the flow periods (Figure 4.7). Copper concentrations remain between the aquifer median and maximum for the duration of the experiment (**Error! Reference source not found.**). Lead concentrations spike above the MCL threshold initially and during both stop-flow events, finally falling beneath the aquifer maximum near the end of the experiment (Figure 4.9). Antimony concentrations spike above the MCL thresholds during the two stop-flow events, and remain above the aquifer maximum for the duration of the experiment (Figure 4.10). Selenium concentrations

spike above the MCL threshold during the two stop-flow events and average close to the aquifer maximum for the duration of the experiment (Figure 4.11).

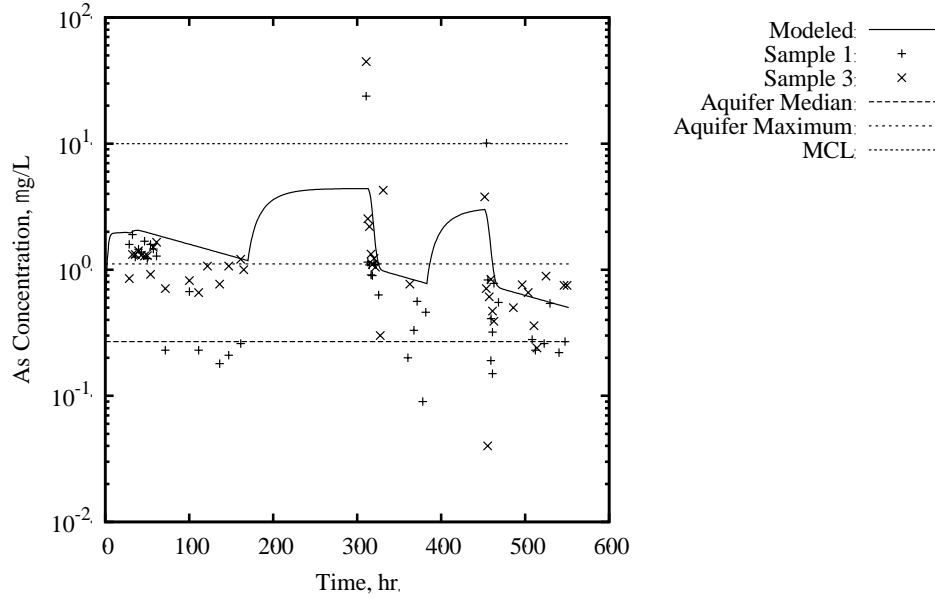


Figure 4.5. As Modeling Results Compared to Column Experiment Results and Aquifer Concentrations

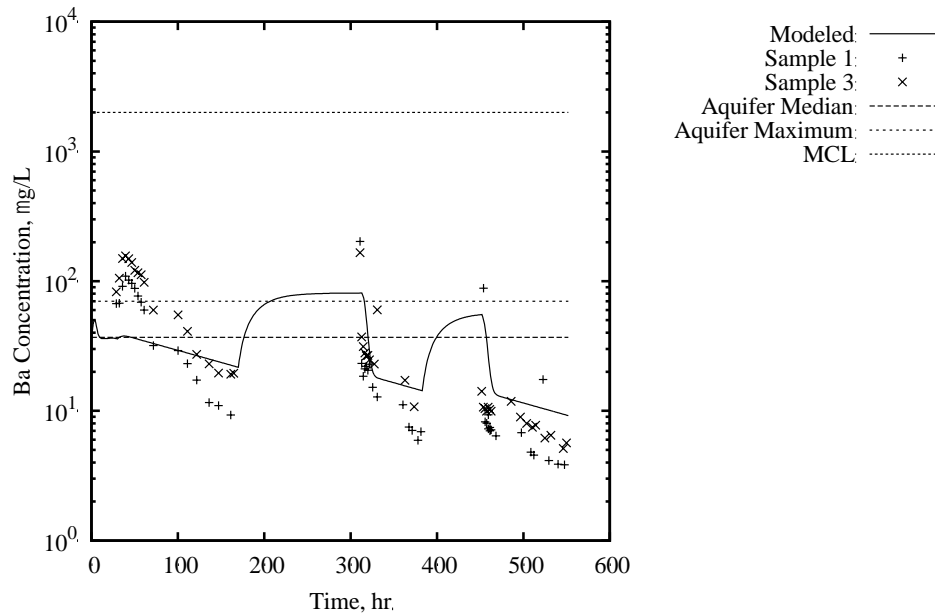


Figure 4.6. Ba Modeling Results Compared to Experimental Results and Aquifer Concentrations

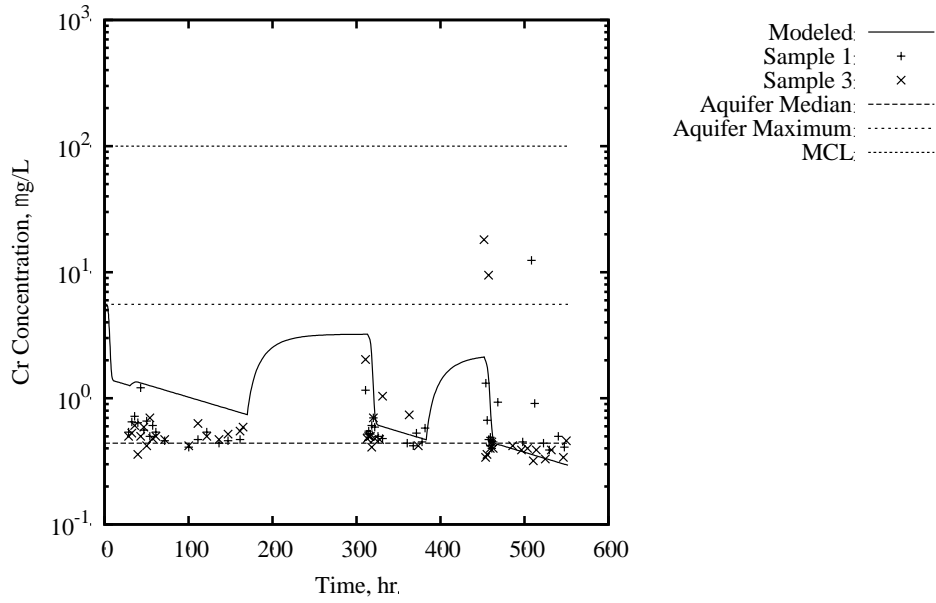


Figure 4.7. Cr Modeling Results Compared to Experimental Results and Aquifer Concentrations

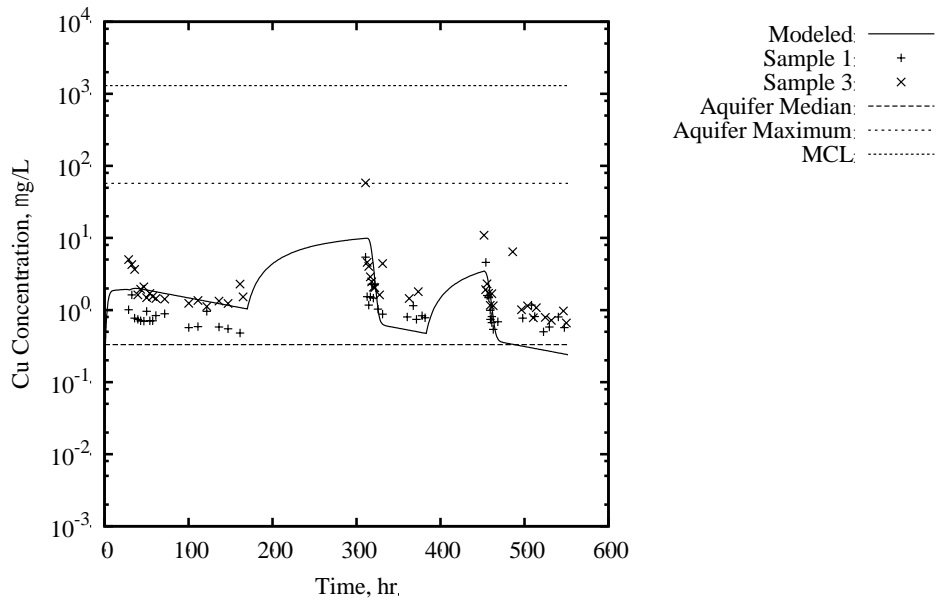


Figure 4.8. Cu Modeling Results Compared to Experimental Results and Aquifer Concentrations

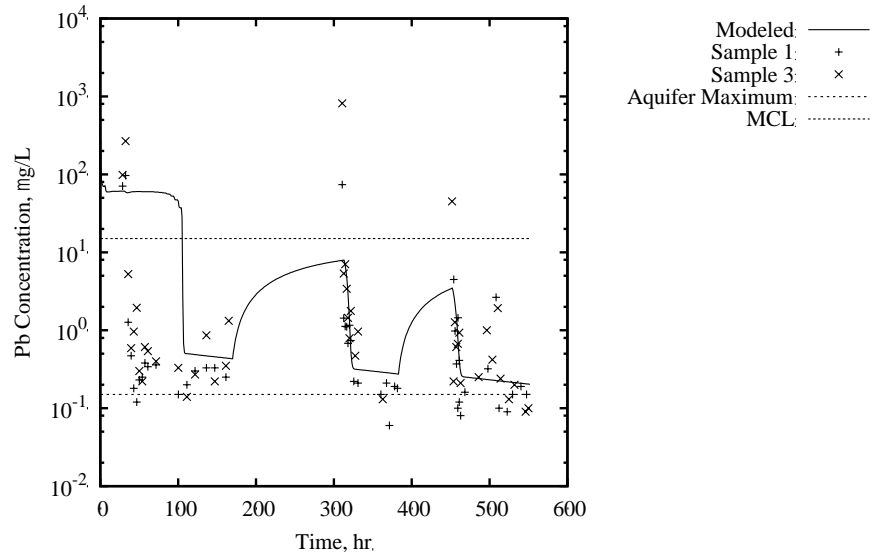


Figure 4.9. Pb Modeling Results Compared to Experimental Results and Aquifer Concentrations. Aquifer median concentrations are below detection.

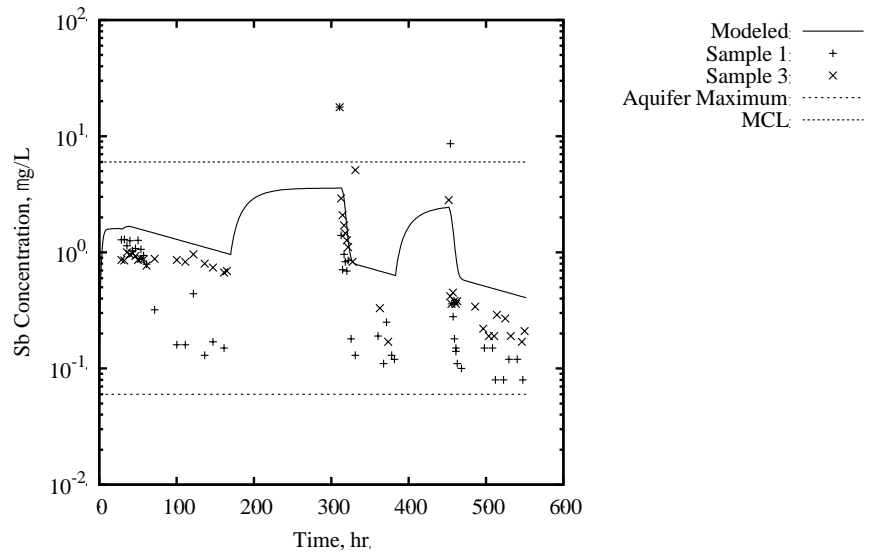


Figure 4.10. Sb Modeling Results Compared to Experimental Results and Aquifer Concentrations. Aquifer median concentrations are below detection.

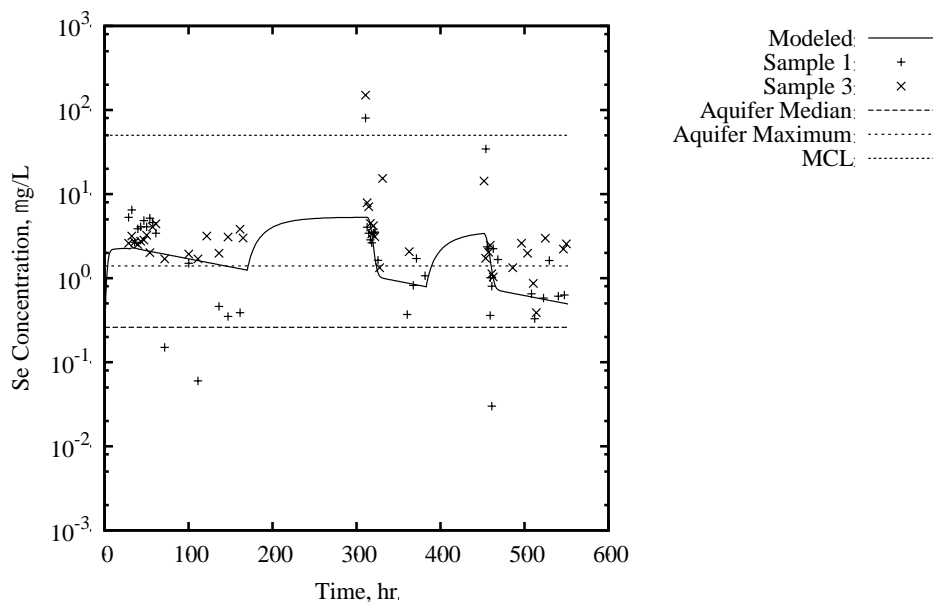


Figure 4.11. Se Modeling Results Compared to Experimental Results and Aquifer Concentrations

4.2.3 Other Aquifers

Despite detectable contaminant concentrations in their batch study, K Kirsch et al. (2014) concluded that the low level of released contaminants during experiments also indicates a low risk for impacting groundwater quality. PJ Mickler et al. (2013) conducted laboratory batch experiments as well as a single-well push-pull field test and found that several of the elements initially mobilized after introduction of CO₂ (Mo, V, Zn, Se, and Cd) were removed from solution by the end of the experiment. PJ Mickler et al. (2013) observed several other elements increase in concentration, but only Mn exceeded EPA MCLs.

In addition to experimental work, numerical modeling has been used to conduct a generic evaluation of the potential groundwater quality changes as a result of the hypothetical leakage of CO₂ (JA Apps et al. 2010; S Carroll, Y Hao and R Aines 2009; S Wang and PR Jaffe 2004; RT Wilkin and DC Digiulio 2010; L Zheng et al. 2009; CQ Vong et al. 2011; AS Altevogt and PR Jaffe 2005; N Jacquemet et al. 2011), and also to understand the chemical processes that control the CO₂-induced release of metals via model interpretation of laboratory experiments (K Kirsch et al. 2014; H Viswanathan et al. 2012; A Wunsch et al. 2014) and field tests (RC Trautz et al. 2013; L Zheng et al. 2012). In general, these models predicted the release of trace metals such as Pb and As (S Wang and PR Jaffe 2004; JA Apps et al. 2010; L Zheng et al. 2009), which is largely consistent with the observations from laboratory experiments (RC Smyth et al. 2009; J Lu et al. 2010; MG Little and RB Jackson 2010; P Humez et al. 2013; A Wunsch et al. 2014; H Viswanathan et al. 2012; C Varadharajan et al. 2013; K Kirsch et al. 2014), although the type of metal being released and the severity of release vary among these experiments.

However, release of trace metals, especially those of environmental relevance such as As, Pb, Ba, and Cd, have not been observed in field tests (A Peter et al. 2012; CB Yang et al. 2013; RC Trautz et al. 2013; LH Spangler et al. 2010; AG Cahill and R Jakobsen 2013; YK Kharaka et al. 2010). The difference between the observation of laboratory and field tests in terms of the release of trace metals is likely because the laboratory experiments are more aggressive in leaching out trace metals due to the use of DI water, manipulation of the particle size of material tested, oxidation, high water/solid ratios, and longer reaction time. However, release of alkali and alkaline earth metals, including Na, K, Ca, Mg, Sr, and Ba, were

commonly observed in both the laboratory and field experiments, although the degree of release is different in the laboratory versus the field tests. The rise in concentrations of dissolved constituents observed during field tests is typically much less pronounced than in laboratory experiments—field tests show increases of about an order of magnitude or less compared to pre-CO₂ levels (20% to 700% in the studies cited above), while orders-of-magnitude increases have been observed in laboratory tests.

Despite potential trace metal release, most current research results show releases below the EPA MCL requirements for drinking water, resulting in a small potential risk for groundwater aquifers due to CO₂ leakage when considering current water quality regulations. However, if studies used a “no-impact” threshold, as discussed in Section 3.1, the risk might be larger. In addition, studies thus far have focused on aquifer variability; very few have been published on variables in the injected or upward migrating gas stream or aquifer brine composition. A variety of compositions may be present in the gas stream due to the presence of trace contaminants remaining after the CO₂ capture process. Methane, for example, can be present as an impurity in the injection gas (ST Blanco et al. 2012; S Mohd Amin et al. 2014). Methane can also be present as a native gas within the reservoir (I Taggart 2010; CM Oldenburg and C Doughty 2011; SA Hosseini et al. 2012), or could be produced through methanogenesis either in the reservoir or after CO₂ enters the aquifer (JY Leu et al. 2011). Inclusion of methane prior to injection can lead to several challenges, including increased pressure needed for transport and reduced CO₂ capacity during transport and storage due to the buoyancy of methane (ST Blanco et al. 2012; SA Hosseini, SA Mathias and F Javadpour 2012). Despite problematic properties of methane, presence of this gas has also been shown to be beneficial. Modeling by S Mohd Amin, DJ Weiss and MJ Blunt (2014) showed reduced transportation of acidic CO₂ saturated brine, resulting in reduced dissolution of the storage reservoir caprock. I Taggart (2010) created a model showing CO₂ driving out dissolved methane from reservoir brine, creating a leading CH₄ plume that could be useful for monitoring leakage. I Taggart (2010) also suggests the methane could be recovered for energy production.

4.3 Changes in Organic Contaminant Concentrations

4.3.1 High Plains Aquifer

In the experiments conducted with the High Plains Aquifer sediments (A Lawter et al. 2016), no measurements were conducted to determine the organic compounds in the aqueous phase of the batch experiments or in the column effluents, although the organic matter concentration in these sediments seems to be low based on visual observations. However, when CO₂ and brine move up from the storage reservoir, they can carry organic compounds, especially if the CO₂ is stored in a depleted oil reservoir. Therefore, in the Gen III ROM for High Plains Aquifers, organic compounds were included in reactive transport models, and subsequently in the derived ROM.

When organic compounds were included in the reactive transport models, we needed to determine which compounds to include and what their prospective concentrations in the leaking CO₂ and brine were. Although the organic compounds present in deep saline aquifers were seldom reported, their compositions in waters produced from oil fields have been extensively studied (TI RøeUtvik 1999; AE Witter and AD Jones 1999). The most common dissolved hydrocarbons are benzene, toluene, ethylbenzene, xylenes BTEX, PAHs, and phenols. To simplify the model, benzene is used to represent BTEX, naphthalene to represent PAHs, and phenol to represent phenols. The respective maximum concentrations in the brine were taken from L Zheng et al. (2010) (Table 4.4), which were largely based on the concentration of these compounds in the production water (YK Kharaka and JS Hanor 2007). The minimum concentrations were arbitrary.

Table 4.4. Organics Concentrations in Brine Considered in the Reactive Transport Model (L Zheng et al. 2010)

Organic Compounds	Minimum	Maximum	Unit
Benzene	-10	-3.2	Log ₁₀ [mol kg ⁻¹]
Naphthalene	-10	-3.7	Log ₁₀ [mol kg ⁻¹]
Phenol	-10	-4.1	Log ₁₀ [mol kg ⁻¹]

Oxidation of the organics was calculated with first-order degradation kinetics:

$$\frac{dC}{dt} = -KC \quad (4.1)$$

where C is the concentration of the organic compound and K is the first-order rate constant, which was treated as a variable parameter.

Linear adsorption isotherms are used to model the adsorption of organic compounds; the key parameter is the distribution coefficient, K_d. The range for the distribution coefficient and degradation constant are listed in Table 4.5.

Table 4.5. Distribution Coefficient and Degradation Constant for Organic Compounds

Parameter	Range
Benzene distribution coefficient (L/kg)	-4.5* to 0.69 ^a
Phenol distribution coefficient (L/kg)	-6.0* to 0.15 ^a
Naphthalene distribution coefficient (L/kg)	-3.1* to 1.98 ^a
Benzene degradation constant (1/s)	0 to -6.1 ^a
Phenol degradation constant (1/s)	0 to -5.63 ^a
Naphthalene degradation constant (1/s)	0 to -6.45 ^a

(a) indicates log₁₀ values

Around 500 simulations have been conducted to account for the uncertainties of both flow and chemical parameters. The following graphs show results from one of the simulations to illustrate the spatial distribution of organic compounds after 200 years of leakage. For details of other conditions of the model, refer to SA Carroll et al. (2014). The key parameters used in this particular simulation are listed in Table 4.6.

Table 4.6. Flow and Chemical Parameters used in Simulations that Model Results

Parameter	Value
Benzene concentration in the leaking brine (mol/L)	2.51E-7
phenol concentration in the leaking brine (mol/L)	1.41E-7
Naphthalene concentration in the leaking brine (mol/L)	8.9E-8
Benzene distribution coefficient (L/kg)	1.24E-2
phenol distribution coefficient (L/kg)	1.18E-3
Naphthalene distribution coefficient (L/kg)	2.75E-1
Benzene degradation constant (1/s)	0
phenol degradation constant (1/s)	3.7E-7
Naphthalene degradation constant (1/s)	0

Figure 4.12 shows the plume of pH, which can be used to approximate the movement of CO₂. In comparison, the plumes for organic compounds are very small. Figure 4.13 and Figure 4.14 show the spatial distribution of benzene. Despite the continuous leakage of brine that contained a high concentration of benzene, the plume was fairly small and always surrounded the leakage point. The plume for naphthalene (Figure 4.15 and Figure 4.16) was smaller than that of benzene because of stronger adsorption of naphthalene by aquifer sediments as manifested by the higher distribution coefficient for naphthalene. Phenol (Figure 4.17 and Figure 4.18) had the smallest plume in comparison with that of benzene and naphthalene because phenol undergoes both adsorption and biodegradation.

In summary, the model results suggest that in comparison to the plume of pH or dissolved CO₂, the plumes for organic compounds were very small, and if the leakage stops, the plumes could quickly disappear due to adsorption and biodegradation.

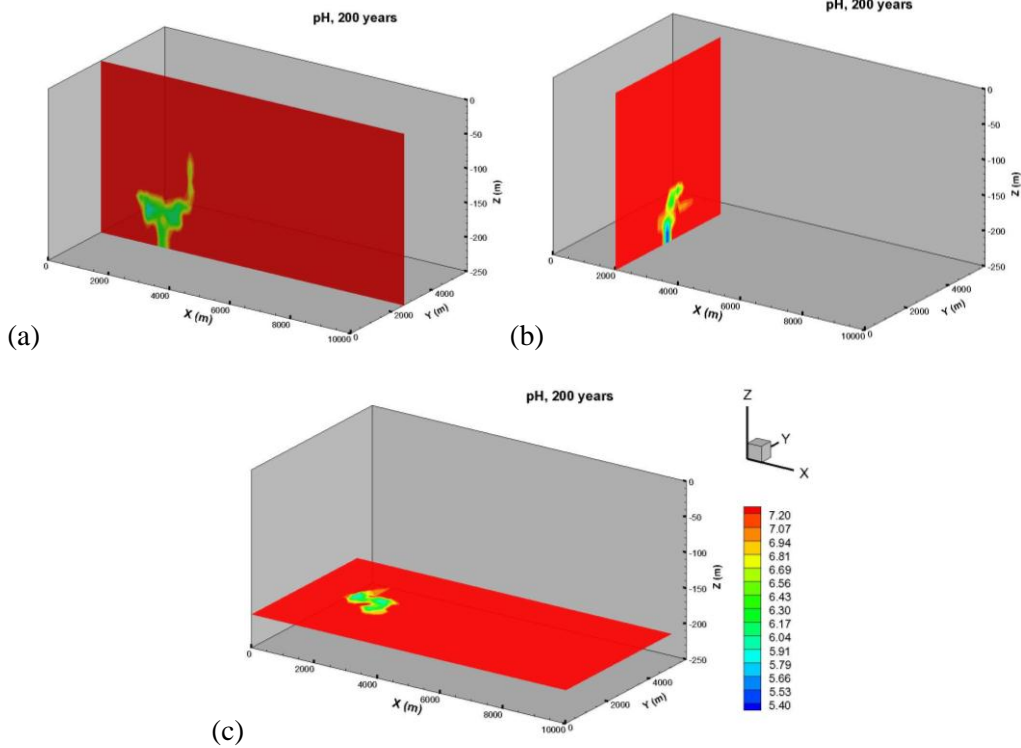


Figure 4.12. Cross Section Views of the Spatial Distribution of pH at 50, 200 years. (a) at $y=2600$ m, (b) at $x=2000$ m, and (c) at $z=-202.5$ m

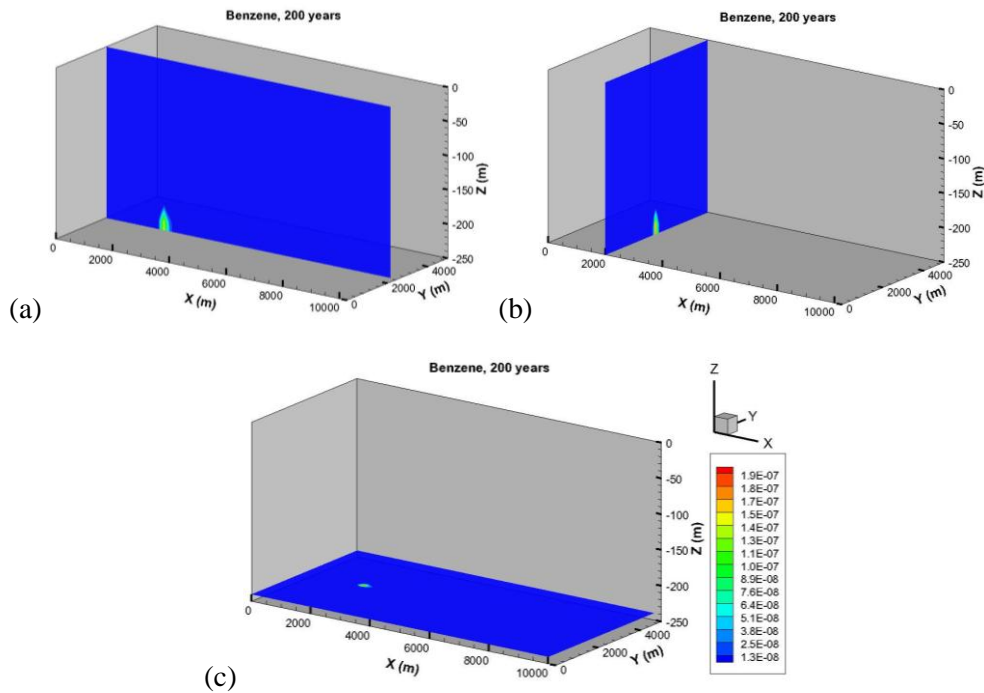


Figure 4.13. Cross Section Views of the Spatial Distribution of Total Aqueous Benzene Concentration at 200 Years: (a) at $y=2600$ m, (b) at $x=2000$ m, and (c) at $z=-202.5$ m

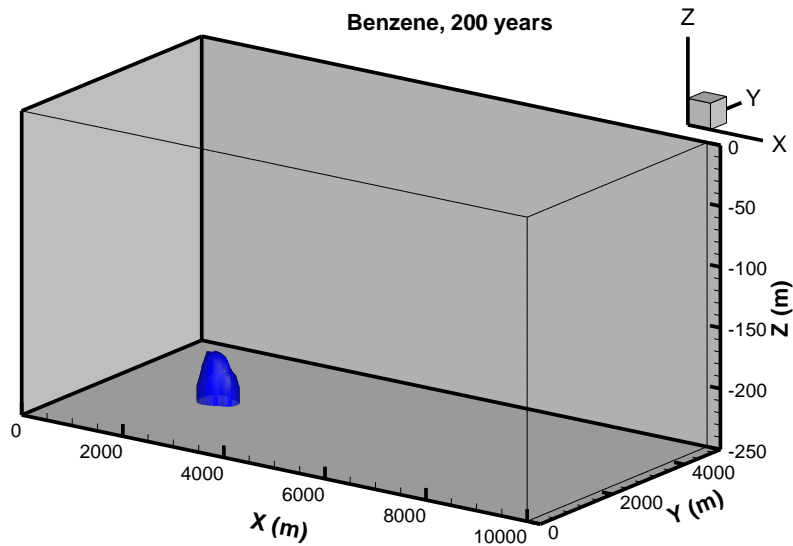


Figure 4.14. An Iso-Surface at Benzene Concentration of 3.84×10^{-10} mol/L ($0.03 \mu\text{g/L}$, threshold value)

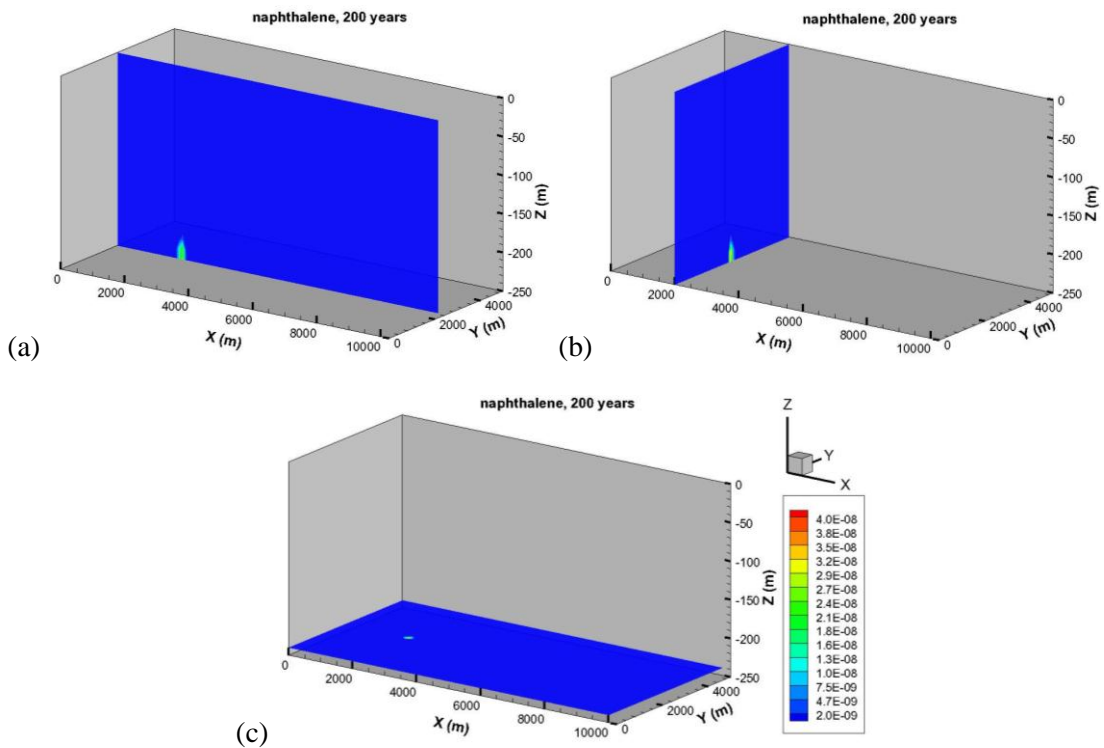


Figure 4.15. Cross Section Views of the Spatial Distribution of Total Aqueous Naphthalene Concentration at 200 Years: (a) at $y = 2600$ m, (b) at $x = 2000$ m, and (c) at $z = -202.5$ m

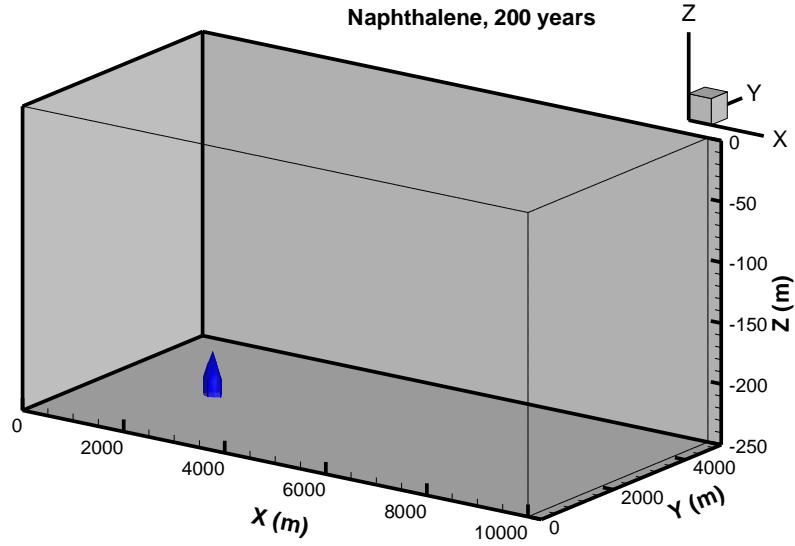


Figure 4.16. An Iso-Surface at Naphthalene Concentration of $1.53\text{e-}9$ mol/L ($0.2 \mu\text{g/L}$, threshold value)

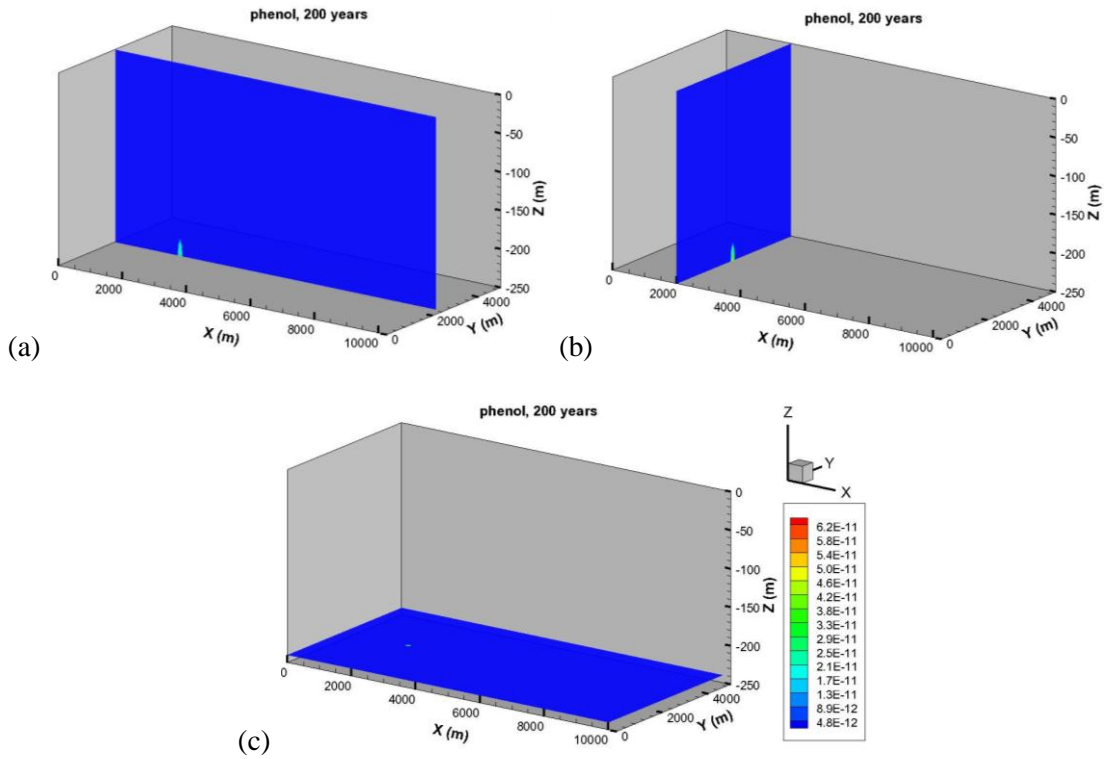


Figure 4.17. Cross Section Views of the Spatial Distribution of Total Aqueous Phenol Concentration at 200 Years: (a) at $y=2600$ m, (b) at $x = 2000$ m, and (c) at $z = -202.5$ m

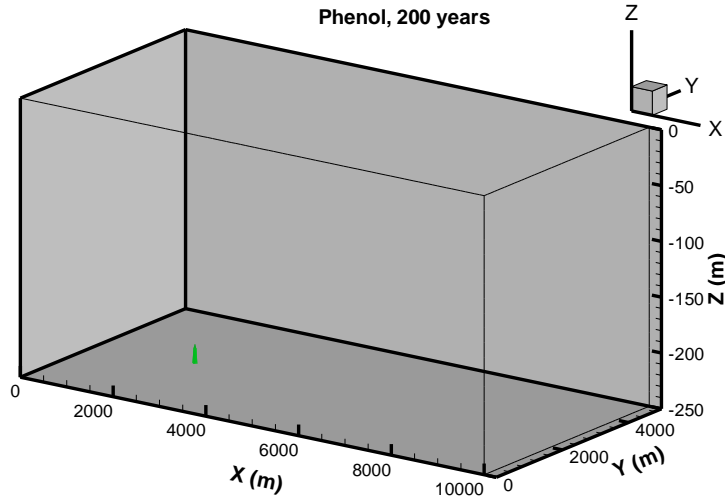


Figure 4.18. An Iso-Surface at Naphthalene Concentration of 3.19×10^{-11} mol/L ($0.003 \mu\text{g/L}$, threshold value)

4.3.2 Edwards Aquifer

4.3.2.1 Modeling

The impact of organic compounds leaking into the Edwards Aquifer has been developed by DH Bacon et al. (2014). Three organic compounds (benzene, naphthalene, and phenol) are included in the model. As with the modeling of organic compounds in the High Plains Aquifer, benzene was included as a representative of BTEX; naphthalene as a representative of PAHs; and phenol as a representative of phenols. BTEX, phenols, and PAHs have been identified as the organic compounds that are most likely to be leached out along with CO_2 as well as pose threats on the quality of shallow groundwater (L Zheng et al. 2013). The adsorption of the organic compounds was assumed to be controlled by a linear adsorption isotherm, proportional to the organic carbon content of the aquifer material. The organic carbon content of the limestone aquifer was assumed to range between 0.1 and 1% by volume. Input parameters for organic adsorption and biodegradation, along with the source of the inputs, are listed in Table 4.7.

Table 4.7. Input Parameters for Organic Adsorption and Biodegradation

Description	Minimum	Maximum	Units	Reference
Organic carbon volume fraction	1.00E-03	1.00E-02	—	Estimated
Benzene organic carbon partition coefficient	3.09E+01	5.37E+01	L/kg	(SJ Lawrence 2006)
Naphthalene organic carbon partition coefficient	9.93E+00	9.55E+02	L/kg	(SJ Lawrence 2006)
Phenol organic carbon partition coefficient	1.61E+01	3.02E+01	L/kg	(SA Boyd et al. 1983; GC Briggs 1981)
Benzene aerobic biodegradation rate	1.00E-03	4.95E-01	day ⁻¹	(D Aronson et al. 1999)
Naphthalene aerobic biodegradation rate	6.40E-03	5.00E+00	day ⁻¹	(D Aronson et al. 1999)
Phenol aerobic biodegradation rate	6.00E-03	1.00E+01	day ⁻¹	(D Aronson et al. 1999)

The concentrations of organics in the leaking brine were assumed to be uncertain variables, with ranges shown in Table 4.8.

Table 4.8. Organic Concentration Ranges in Brine

Species in Brine	Minimum	Maximum	Units
Benzene	1.00E-10	6.31E-04	mol/L
Naphthalene	1.00E-10	7.94E-05	mol/L
Phenol	1.00E-10	2.00E-04	Mol/L

Initial concentrations of the organics in the aquifer were assumed to be zero, based on average aqueous concentrations for the 90 groundwater samples from the shallow, urban, unconfined portion of the Edwards Aquifer (M Musgrove et al. 2010). This set of water samples was used to examine methodologies for establishing baseline data sets and statistical protocols for determining statistically significant changes between background concentrations and predicted concentrations that would be used to represent a contamination plume in the modeling presented in this report (GV Last et al. 2013). No-impact threshold values were determined that could be used to identify potential areas of contamination predicted by numerical models of carbon sequestration storage reservoirs (Table 4.9). Initial values of these concentrations were also determined using selected statistical methods. For comparison, the EPA MCL is also shown.

Table 4.9. Initial Values, Tolerance Limits, and Regulatory Standards for Each Variable

Analyte	Initial Value	“No-Impact” Threshold	Maximum Contaminant Level	Units
Benzene	0.000	0.016	5	µg/L
Naphthalene	0.000	0.400	0.2	µg/L
Phenol	0.000	0.005	10000	µg/L

The volume of groundwater exceeding the threshold values for organic compounds is influenced significantly by biodegradation. Volumes of groundwater with concentrations greater than the benzene, naphthalene and phenol no-impact threshold values are relatively small (Figure 4.19). By comparison, for the same set of simulations, the median pH-impacted aquifer volumes ranged from $1e^5 \text{ m}^3$ at 10 years to $1e^7 \text{ m}^3$ at 200 years.

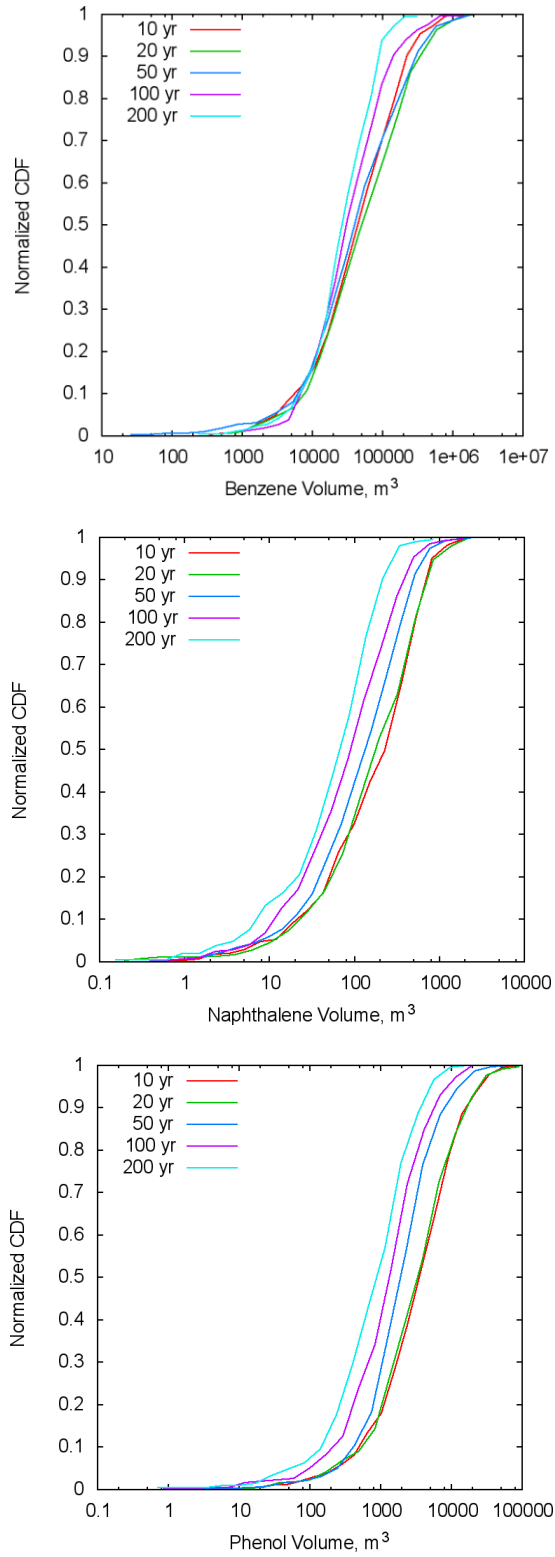


Figure 4.19. Cumulative Density Function of Aquifer Volume Exceeding Organic No-Impact Thresholds during 200 Years of Well Leakage

4.3.3 Reservoirs as a Source Term for Organic Compounds

Mobilization of toxic organic compounds, including BTEX, and PAHs by scCO₂, has been reported in laboratory experiments for rock samples from depleted oil reservoirs, coal deposits (LR Zhong et al. 2014), and sandstones (AK Scherf et al. 2011). Groundwater monitoring results from GCS demonstration sites have shown increased concentrations of BTEX, PAHs, phenols, and other toxic compounds in groundwater after CO₂ injection (YK Kharaka et al. 2009; YK Kharaka, P Campbell, et al. 2010; YK Kharaka et al. 2010; AK Scherf et al. 2011). L Zhong et al. (2014) focused on the transport and fate of toxic organic compounds mobilized by supercritical CO₂ from organic rich storage reservoirs such as unmineable coal seams and depleted oil reservoirs. Column experiments were conducted using a water wetted sandstone core installed in a tri-axial core holder to study the potential for toxic organic compounds mobilized from coal by supercritical CO₂ under simulated geologic carbon storage conditions to impact groundwater. The concentrations of the organic compounds in the column effluent and their distribution within the sandstone core were monitored. Results indicated that the mobility through the core sample was much higher for BTEX compounds than for naphthalene. Retention of organic compounds from the vapor phase to the core appeared to be primarily controlled by partitioning from the vapor phase to the aqueous phase according to Henry's Law. Accordingly, reduced temperature and elevated pressure resulted in greater partitioning of the mobilized organic contaminants into pore water. Adsorption to the surfaces of the wetted sandstone was also significant for naphthalene.

KJ Cantrell and CF Brown (2014) conducted a modeling study and found that when CO₂ is introduced into a reservoir with 90wt.% CO₂ and 10 wt.% oil, a significant fraction of the oil dissolves into the vapor phase. As the vapor phase moves up through the stratigraphic column, pressures and temperatures decrease, resulting in significant condensation of oil components. The heaviest organic components condense early in this process (at higher pressures and temperatures), while the lighter components tend to remain in the vapor phase until much lower pressures and temperatures are reached. The final concentrations to reach an aquifer at 1,520kPa and 25°C were quite significant for benzene and toluene, indicating that these compounds could adversely impact groundwater quality (benzene in particular) in the event of a leak of CO₂ stored in a depleted oil reservoir. Conversely, it was determined that CO₂ was unlikely to transport significant concentrations of PAHs to near surface depths, limiting their potential impact to groundwater. This is particularly true for the most carcinogenic of the PAH compounds, which are relatively heavy, making them prone to condensation from the vapor phase at much higher pressures and temperatures.

5.0 Conclusive Remarks

GCS is a global carbon emission reduction strategy involving the capture of CO₂ emitted from fossil fuel burning power plants, as well as the subsequent injection of the captured CO₂ gas into deep subsurface reservoirs, such as saline aquifers or depleted oil and gas reservoirs. A critical question that arises from the proposed GCS is the potential impacts of CO₂ injection on the quality of drinking-water systems overlying CO₂ sequestration storage sites.

Although storage reservoirs are evaluated and selected based on their ability to safely and securely store emplaced fluids, leakage of CO₂ from storage reservoirs is a primary risk factor and a potential barrier to the widespread acceptance of geologic CO₂ sequestration. Therefore, a systematic understanding of how CO₂ leakage would affect the geochemistry of potable aquifers, and subsequently control or affect contaminant release via dissolution, desorption, and/or redox reactions, is vital.

This report was written with the overall objective to identify the set of geochemical data and reactions and the hydrological processes required to assess and predict aquifer responses to CO₂ and brine leakage, to gather important site-specific data required to evaluate impacts, and to present and discuss potential risks for groundwater pollution due to CO₂ gas and brine exposure.

5.1 Crucial Site-Specific Data

Establishing the mean and variance of background groundwater concentrations is necessary to determining whether there will be an impact due to leaking CO₂ and brine in groundwater aquifers. The resulting no-impact threshold values can be used to inform a “no change” scenario with respect to groundwater impacts. In some cases, the calculated no-impact threshold values may exceed regulatory standards. For instance, in the High Plains Aquifer, the no-impact threshold of 1,300 mg/L is significantly higher than the regulatory standard of 500 mg/L for TDS. Also, if there is little variability in background values there will be a higher likelihood that the threshold values will be exceeded. For instance, in the Edwards Aquifer, the mean value of pH (6.9) is only a few tenths of a pH point above the “no-impact” threshold of pH 6.6.

Determining the salinity, trace metal, and organic content of reservoir fluids is necessary to make accurate predictions of the impact to groundwater due to leaking brine. The contaminants of concern will depend on the characteristics of the reservoir brine, and whether there are significant differences between the reservoir pore water composition and the drinking water aquifer.

In order to make accurate predictions of the impact of leaking CO₂ on aquifer materials, calcite content in the sediment and/or aquifer rocks should be determined. There is a significant difference in the impact to pH on the High Plains Aquifer samples with and without calcite present. The Edwards Aquifer limestone, which consists mainly of calcite, shows a strong capacity to buffer pH changes due to interaction with CO₂.

It should also be determined whether there are other minerals in the aquifer that could dissolve under low pH conditions and contribute to increased TDS or trace metal concentrations. For instance, the dissolution of calcite can cause significant increases in dissolved calcium, raising TDS above background levels. Similarly, the dissolution of galena could cause increases in lead concentrations above background levels.

Measuring the amount and type of clays and the amount of calcite is important for estimating adsorption capacity and coefficients for trace metals. In the Edwards Aquifer, adsorption on calcite controls the release of trace metals after exposure to a lowered pH due to CO₂ exposure. In a sand and gravel aquifer

like the High Plains, Fe oxides and hydroxides (such as, goethite and HFO), and clay minerals (such as illite, kaolinite, and montmorillonite) are important adsorbents.

If organic contaminants are mobilized from the injection reservoir and transported by the leaking CO₂ or brine, then determining the amount of organic matter and biodegradation potential in the aquifer is necessary in order to predict the persistence of organic contaminants in the aquifer. Establishing the redox potential of the aquifer is important, because measured biodegradation rates tend to be higher in oxidizing environments.

5.2 Potential Risk to Groundwater

Over the last decade, a number of studies have been undertaken to assess the impacts of potential CO₂ leakage from deep storage reservoirs on the quality of overlying freshwater aquifers. These studies include natural analogs, field-scale in-situ CO₂ injection, and laboratory-scale column and batch studies. However, the results of the studies are contradictory, as some indicate CO₂ leaks pose a serious risk and some indicate low levels of risk, while others have found possible benefits related to CO₂ leakage into groundwater. In an effort to reconcile these differing conclusions and to generate additional sets of data on this subject, experimental and modeling studies were conducted as part of the NRAP to define conditions under which impacts to groundwater may be significant.

Data presented in the literature and data collected from laboratory-scale experimental and modeling work conducted at PNNL and LBNL and supported by NRAP show that the aquifer responses are site-specific. Results from laboratory experimental work show that data generated from batch experiments often over predict total changes in the aquifer systems. This is due to the importance of leakage and flow rates, and because the reactions that control aqueous trace metal concentrations are time dependent (these concentrations were significantly lower during the flow portions of the column experiments but increased during stop-flows, indicating dependency on the fluid residence time and/or pH; pH also increased during the stop-flows). Additionally, both batch and columns experiments tend to be performed with size-segregated material that is more reactive due to its higher surface area to volume ratio; therefore, both types of experiments tend to provide more conservative estimates of aquifer impacts.

In this report, we also show that the development of site-specific conceptual and ROMs to describe and predict aquifer responses is possible. These models can then be used to estimate the degree of impact in terms of changes in the pH, major, minor, and trace element releases based on aquifer properties (e.g., initial aqueous concentration, mineralogy, etc.), changes in solid phase chemistry and mineralogy, changes in the extent and rate of reactions and processes and the establishment of a new network of reactions and processes affecting or controlling the overall response, leaking plume characteristics (gas composition, such as pure CO₂ and/or CO₂-CH₄-H₂S mixtures), and brine concentration and composition.

These models are also able to predict the degree of impact, whether the changes in aquifer are significant or insignificant, the fate of the elements released from sediments or transported with brine, and the extent and rate of reactions such as precipitation/incorporation into minerals (calcite and other minerals), adsorption, electron transfer reactions, and the role of natural attenuation.

Some modeling Application of these models (SA Carroll et al. 2014) and various field studies (Table 3.4) indicate that results presented in this report and data from the literature estimate that there are cases where there are may be measurable, long-term impacts to groundwater due to CO₂ or brine leaks.

Field-scale models of CO₂ and brine leakage, driven by models of CO₂ injection into a reservoir and leakage via abandoned wellbores of varying permeability, for the High Plains Aquifer and shallow, urban

unconfined portion of the Edwards Aquifer, were used to calculate the volume of the aquifer above background thresholds due to CO₂ leaks of different rates. The volume of the impacted aquifer is very sensitive to the threshold values assumed; in most cases the regulatory threshold (EPA MCL) is significantly less limiting than the threshold value indicated by the background variability in aquifer concentrations, and so groundwater impacts are more pronounced when utilizing these no-impact thresholds.

When comparing the volumes of each of the two aquifers impacted by elevated trace metal concentrations, we find that although initial adsorbed trace metal concentrations are lower in the Edwards sediments than the High Plains sediments, the background variability of the shallow, urban unconfined portion of the Edwards Aquifer is low compared to the High Plains Aquifer, leaving it more vulnerable to changes in groundwater quality due to CO₂ or brine leakage. A parameter sensitivity analysis shows that groundwater impacts are more sensitive to the leak rates of CO₂ and brine and hydraulic aquifer characteristics, such as permeability and groundwater flow rate, than to geochemical parameters, such as mineral dissolution rate, with the exception of the presence of calcite in the aquifer sediments.

A remaining question is whether trace metal releases due to leaking CO₂ are harmful. It could be argued that a small increase in lead concentrations above the “no-impact” threshold values in an aquifer will not have a measureable health impact. However, EPA MCL thresholds have been established to protect human health. Long-term increases above the MCL thresholds could therefore have the potential for negative impacts on human health.

Clearly, the scientific community has not yet reached an agreement on the important issue of deciding whether the impacts are negative, insignificant, or positive. One reason could be that the degree of perturbation and response to induced changes is site-specific and a function of inherent aquifer properties as well as the characteristics of the leaking plume (i.e., gas composition and brine concentration) at the specific site.

We have considered the risk to groundwater due to changes in pH, TDS, trace metals, and organics. The risk to groundwater is directly proportional to the mass of CO₂ or brine leaked. In many simulations considered in the NRAP risk analyses, the leaked mass is relatively small and plumes are not likely to be detected by the pumping of existing groundwater wells (E Keating et al. 2014). However, zones of lowered pH and elevated TDS and trace metals may persist for decades. Based on biodegradation rates and sorption coefficients from the literature, organic plumes are not expected to persist in groundwater; further experimental research is needed to confirm this under site-specific conditions.

5.3 Future Efforts

Over the last two decades, a number of laboratory and field experiments as well as modeling work have been conducted to study the impact of CO₂ and brine leakage on groundwater quality; this greatly enhances our understanding on the magnitude of such impact and the controlling processes. However, questions remain and further investigations are required.

One of the remaining questions to be addressed as investigations move to the post-injection site care period is whether trace metals released during the leakage phase will recover to the background level of the aquifer and at what times scales this would happen when compared with the recovery of pH and dissolved CO₂ if the leakage were to be detected and stopped. Once the leakage stops, the plume of high CO₂ (dissolved or gaseous) and low pH will be diluted due to mixing with groundwater. As a result, the gaseous CO₂ will dissolve, and eventually, dissolved CO₂ will have a very low concentration. While it may not reach pre-leakage conditions, concentrations may become low enough to make aqueous pH

return to values close to neutral (or, at least, higher than the EPA MCL of 6.5). Nevertheless, modeling studies (L Zheng et al. 2015) and laboratory experiments (PM Fox et al. 2014) show that trace metals have fairly complex behavior in terms of recovery. Further studies are certainly warranted. Numerical models supported with laboratory experiments should be conducted to address this issue.

Organic contaminants mobilized from the injection reservoir were considered in development of the groundwater impact models for the High Plains and Edwards Aquifers. However, it is not known how these contaminants may partition between the CO₂ saturated aqueous and air phases as they travel up a borehole or other leakage path. Experiments are needed to determine how changes in pressure and temperature along the leakage path will affect phase partitioning of these contaminants. This will impact their long-term persistence once they arrive in the aquifer. Studies are also needed to determine the extent and rate of major and minor element release in the leakage pathway (i.e., from deep reservoirs to aquifers) under conditions of decreasing temperature and pressure.

While ROMs have been demonstrated as an effective tool to evaluate the risk associated with groundwater, the development of such models is challenging mainly because of the highly non-linear response of the impacted volume to the change of chemical parameters. For example, if the aquifer sediments are low in calcite content and calcite is removed due to dissolution, the volume of pH greater than the threshold changes sharply; this process is difficult to be emulated by ROMs. One potential solution is to further categorize aquifer conditions and develop ROMs for each condition. Currently, NRAP has two groundwater ROMs that are based on the Edward and High Plains Aquifers; both are designed for aquifers with appreciable pH buffering capacity. In the future, a ROM should be developed for aquifers with limited pH buffering capacity.

6.0 References

- Altevogt AS, and PR Jaffe. 2005. "Modeling the Effects of Gas Phase CO₂ Intrusion on the Biogeochemistry of Variably Saturated Soils." *Water Resources Research* 41.
- Annunziatellis A, SE Beaubien, S Bigi, G Ciotoli, M Coltella, and S Lombardi. 2008. "Gas Migration Along Fault Systems and through the Vadose Zone in the Latera Caldera (Central Italy): Implications for CO₂ Geological Storage." *Int. J. Greenhouse Gas Control* 2:353-72.
- Appelo CJA, and D Postma. 1994. *Geochemistry, Groundwater and Pollution*. A.A.Balkema, Rotterdam, Netherlands.
- Apps JA, L Zheng, Y Zhang, T Xu, and JT Birkholzer. 2010. "Evaluation of Potential Changes in Groundwater Quality in Response to CO₂ Leakage from Deep Geologic Storage." *Transport Porous Med.* 82:215-46.
- Apps JA, LG Zheng, N Spycher, JT Birkholzer, Y Kharaka, J Thordsen, E Kakouros, and R Trautz. 2011. "Transient Changes in Shallow Groundwater Chemistry During the MSU ZERT CO₂ Injection Experiment." *10th International Conference on Greenhouse Gas Control Technologies* 4:3231-38.
- Aronson D, M Citra, K Shuler, H Printup, and PH Howard. 1999. *Aerobic Biodegradation of Organic Chemicals in Environmental Media: A Summary of Field and Laboratory Studies*. Technical, U.S. EPA, North Syracuse, New York.
- Arthur J, A Dabous, and J Cowart. 2002. "Mobilization of Arsenic and Other Trace Elements During Aquifer Storage and Recovery, Southwest Florida." in U.S. Geological Survey artificial recharge workshop, eds. GR Aiken and EL Kuniandy. USGS, Sacramento, California.
- Bachu S. 2008. "CO₂ Storage in Geological Media: Role, Means, Status, and Barriers to Deployment." *Progress in Energy and Combustion Science* 34:254-73.
- Bacon D. 2013. "Reduced Order Model for the Geochemical Impacts of Carbon Dioxide, Brine, and Trace Metal Leakage into an Unconfined, Oxidizing Carbonate Aquifer, Version 2.1." NRAP REPORT PNNL-22285, Pacific Northwest National Laboratory.
- Bacon D, N Qafoku, Z Dai, E Keating, and C Brown. 2016. "Modeling the Impact of Carbon Dioxide Leakage into an Unconfined, Oxidizing Carbonate Aquifer." *International Journal of Greenhouse Gas Control* 44:290-99.
- Bacon DH, Z Dai, and L Zheng. 2014. "Geochemical Impacts of Carbon Dioxide, Brine, Trace Metal and Organic Leakage into an Unconfined, Oxidizing Limestone Aquifer." *Energy Procedia* 63:4684-707.

Birkholzer JT, J Apps, L Zheng, Y Zhang, T Xu, and C-F Tsang. 2008. Research Project on CO₂ Geological Storage and Groundwater Resources, Quality Effects Caused by CO₂ Intrusion into Shallow Groundwater, Technical Report. Technical, Earth Sciences Division, Lawrence Berkeley National Laboratory, Berkeley, CA.

Blanco ST, C Rivas, J Fernandez, M Artal, and I Velasco. 2012. "Influence of Methane in CO₂ Transport and Storage for CCS Technology." *Environmental Science & Technology* 46:13016-23.

Boyd SA, DR Shelton, D Berry, and JM Tiedje. 1983. "Anaerobic Biodegradation of Phenolic-Compounds in Digested-Sludge." *Appl Environ Microb* 46:50-54.

Briggs GC. 1981. "Theoretical and Experimental Relationships between Soil Adsorption, Octanol-Water Partition- Coefficients, Water Solubilities, Bioconcentration Factors, and the Parachor." *J. Agric. Food Chem.* 29:1050-59.

Cahill AG, and R Jakobsen. 2013. "Hydro-Geochemical Impact of CO₂ Leakage from Geological Storage on Shallow Potable Aquifers: A Field Scale Pilot Experiment." *International Journal of Greenhouse Gas Control* 19:678-88.

Cahill AG, R Jakobsen, TB Mathiesen, and CK Jensen. 2013. "Risks Attributable to Water Quality Changes in Shallow Potable Aquifers from Geological Carbon Sequestration Leakage into Sediments of Variable Carbonate Content." *International Journal of Greenhouse Gas Control* 19:117-25.

Cantrell KJ, and CF Brown. 2014. "Source Term Modeling for Evaluating the Potential Impacts to Groundwater of Fluids Escaping from a Depleted Oil Reservoir Used for Carbon Sequestration." *International Journal of Greenhouse Gas Control* 27:139-45.

Caritat Pd, A Hortle, M Raistrick, C Stalvies, and C Jenkins. 2013. "Monitoring Groundwater Flow and Chemical and Isotopic Composition at a Demonstration Site for Carbon Dioxide Storage in a Depleted Natural Gas Reservoir." *Applied Geochemistry* 30:16-32.

Carroll S, Y Hao, and R Aines. 2009. "Geochemical Detection of Carbon Dioxide in Dilute Aquifers." *Geochem.Trans.* 10:<http://www.geochemicaltransactions.com/content/10/1/4>.

Carroll SA, M Bianchi, K Mansoor, L Zheng, Y Sun, N Spycher, and J Birkholtzer. 2014. Reduced-Order Model for Estimating Impacts from Co₂ Storage Leakage to Alluvium Aquifers: Third-Generation Combines Physical and Chemical Processes. Technical, NRAP Technical Report Series; U.S. Department of Energy, National Energy Technology Laboratory: Morgantown, WV, 2014; p XX.

Carroll SA, E Keating, K Mansoor, Z Dai, Y Sun, W Trainor-Guitton, C Brown, and D Bacon. 2014. "Key Factors for Determining Groundwater Impacts Due to Leakage from Geologic Carbon Sequestration Reservoirs." *International Journal of Greenhouse Gas Control* 29:153-68.

Celia MA, and JM Nordbotten. 2009. "Practical Modeling Approaches for Geological Storage of Carbon Dioxide." *Ground Water* 47:627-38.

Costagliola P, F Bardelli, M Benvenuti, F Di Benedetto, P Lattanzi, M Romanelli, M Paolieri, V Rimondi, and G Vaggelli. 2013. "Arsenic-Bearing Calcite in Natural Travertines: Evidence from Sequential Extraction, Mu Xas, and Mu Xrf." *Environmental Science & Technology* 47:6231-38.

Dafflon B, YX Wu, SS Hubbard, JT Birkholzer, TM Daley, JD Pugh, JE Peterson, and RC Trautz. 2013. "Monitoring Co2 Intrusion and Associated Geochemical Transformations in a Shallow Groundwater System Using Complex Electrical Methods." *Environmental Science & Technology* 47:314-21.

Damen K, A Faaij, F van Bergen, J Gale, and E Lysen. 2005. "Identification of Early Opportunities for Co2 Sequestration-Worldwide Screening for CO2-EOR and CO2-ECBM Projects." *Energy* 30:1931-52.

DeSimone LA. 2009. Quality of Water from Domestic Wells in Principal Aquifers of the United States, 1991–2004. Technical Rpt. Scientific Investigations Report 2008–5227, U.S. Geological Survey, Reston, Virginia.

Di Benedetto F, P Costagliola, M Benvenuti, P Lattanzi, M Romanelli, and G Tanelli. 2006. "Arsenic Incorporation in Natural Calcite Lattice: Evidence from Electron Spin Echo Spectroscopy." *Earth and Planetary Science Letters* 246:458-65.

Dixit S, and JG Hering. 2003. "Comparison of Arsenic(V) and Arsenic(III) Sorption onto Iron Oxide Minerals: Implications for Arsenic Mobility." *Environ. Sci. Technol.* 37:4182-89.

DOE. 2007. Carbon Sequestration Technology Roadmap and Program Plan. Technical, U.S. DOE and NETL, Washington DC.

Donahue RB, SL Barhour, and JV Headley. 1999. "Diffusion and Adsorption of Benzene in Regina Clay." *Can. Geotech. J.* 36:430-42.

Dzombak DA, and FMM Morel. 1990. *Surface Complexation Modeling-Hydrous Ferric Oxide*. John Wiley & sons, New York.

Fox PM, PS Nico, JA Davis, and N Spycher. 2014. "Impact of Elevated CO2 on Release of Trace Elements from Aquifer Sediments of the San Joaquin Valley, Ca." in AGU fall meeting.

Frye E, C Bao, L Li, and S Blumsack. 2012. "Environmental Controls of Cadmium Desorption During CO2 Leakage." *Environmental Science & Technology* 46:4388-95.

Goldberg S. 2002. "Competitive Adsorption of Arsenate and Arsenite on Oxides and Clay Minerals." *SOIL SCI. SOC. AM. J.*, 66:413-21.

Gu X, and LJ Evans. 2007. "Modelling the Adsorption of Cd(II), Cu(II), Ni(II), Pb(II), and Zn(II) onto Fithian Illite." *Journal of Colloid and Interface Science* 307:317-25.

Gu X, and LJ Evans. 2008. "Surface Complexation Modelling of Cd(II), Cu(II), Ni(II), Pb(II) and Zn(II) Adsorption onto Kaolinite." *Geochimica et Cosmochimica Acta* 72:267-76.

Gu X, LJ Evans, and SJ Barabash. 2010. "Modeling the Adsorption of Cd (II), Cu (II), Ni (II), Pb (II) and Zn (II) onto Montmorillonite." *Geochimica et Cosmochimica Acta* 74:5718-28.

Harvey OR, NP Qafoku, KJ Cantrell, G Lee, GE Amonette, and CF Brown. 2013. "Geochemical Implications of Gas Leakage Associated with Geologic CO₂ Storage-a Qualitative Review." *Environ. Sci. Technol.* 47:23-26.

Hawthorne SB, and DJ Miller. 2003. "Evidence for Very Tight Sequestration of BTEX Compounds in Manufactured Gas Plant Soils Based on Selective Supercritical Fluid Extraction and Soil/Water Partitioning. ." *Environ. Sci. Technol.* 37:3578-94.

Holloway S, Pearce, J.M., Hards, V.L., Ohsumi, T., Gale, J. 2007. "Natural Emissions of CO₂ from the Geosphere and Their Bearing on the Geological Storage of Carbon Dioxide." *Energy* 32:1194-201.

Hosseini SA, SA Mathias, and F Javadpour. 2012. "Analytical Model for CO₂ Injection into Brine Aquifers-Containing Residual CH₄." *Transport in Porous Media* 94:795-815.

Hovorka SD, TA Meckel, RH Trevino, J Lu, J-P Nicot, J-W Choi, D Freeman, P Cook, TM Daley, JB Ajo-Franklin, BM Freifeild, C Doughty, CR Carrigan, D La Brecque, YK Kharaka, JJ Thordsen, TJ Phelps, C Yang, KD Romanak, T Zhang, RM Holt, JS Lindler, and RJ Butsch. 2011. "Monitoring a Large Volume CO₂ Injection: Year Two Results from SECARB Project at Denbury's Cranfield, Mississippi, USA." *10th International Conference on Greenhouse Gas Control Technologies* 4:3478-85.

Humez P, V Lagneau, J Lions, and P Negrel. 2013. "Assessing the Potential Consequences of CO₂ Leakage to Freshwater Resources: A Batch-Reaction Experiment Towards an Isotopic Tracing Tool." *Applied Geochemistry* 30:178-90.

Jacquemet N, G Picot-Colbeaux, CQ Vong, J Lions, O Bouc, and R Jeremy. 2011. "Intrusion of CO₂ and Impurities in a Freshwater Aquifer-Impact Evaluation by Reactive Transport Modelling." *10th International Conference on Greenhouse Gas Control Technologies* 4:3202-09.

Jean J-S, C-L Tsai, S-H Ju, C-W Tsao, and S-M Wang. 2002. "Biodegradation and Transport of Benzene, Toluene, and Xylenes in a Simulated Aquifer: Comparison of Modelled and Experimental Results." *HYDROLOGICAL PROCESSES* 16:3151-68.

Jordan P, Benson, S. 2009. "Well Blowout Rates and Consequences in California Oil and Gas District 4 from 1991 to 2005: Implications for Geological Storage of Carbon Dioxide." *Environ. Geol.* 57:1103-23.

Jun Y-S, DE Giammar, and CJ Werth. 2013. "Impacts of Geochemical Reactions on Geologic Carbon Sequestration." *Environ. Sci. Technol.* 47:3-8.

Karamalidis AK, SG Torres, JA Hakala, H Shao, KJ Cantrell, and S Carroll. 2013. "Trace Metal Source Terms in Carbon Sequestration Environments." *Environmental Science & Technology* 47:322-29.

Karickhoff SW, DS Brown, and TA Scott. 1979. "Sorption of Hydrophobic Pollutants on Natural Sediments." *Water Research* 13:241-48.

Keating E, Z Dai, D Dempsey, and R Pawar. 2014. "Effective Detection of Co₂ Leakage: A Comparison of Groundwater Sampling and Pressure Monitoring." *Energy Procedia* 63:4163-71.

Keating E, D Newell, D Dempsey, and R Pawar. 2014. "Insights into Interconnections between the Shallow and Deep Systems from a Natural CO₂ Reservoir near Springerville, Arizona." *International Journal of Greenhouse Gas Control* 25:162-72.

Keating EH, J Fessenden, N Kanjorski, DJ Koning, and R Pawar. 2010. "The Impact of CO₂ on Shallow Groundwater Chemistry: Observations at a Natural Analog Site and Implications for Carbon Sequestration." *Environmental Earth Sciences* 60:521-36.

Keating EH, JA Hakala, H Viswanathan, JW Carey, R Pawar, GD Guthrie, and J Fessenden-Rahn. 2013. "CO₂ Leakage Impacts on Shallow Groundwater: Field-Scale Reactive-Transport Simulations Informed by Observations at a Natural Analog Site." *Applied Geochemistry* 30:136-47.

Keating EH, DL Newell, H Viswanathan, JW Carey, G Zvoloski, and R Pawar. 2013. "Co₂/Brine Transport into Shallow Aquifers Along Fault Zones." *Environmental Science & Technology* 47:290-97.

Kharaka YK, P Campbell, JJ Thorden, PB Thomas, DR Cole, and SD Hovorka. 2010. "Geologic Storage of Carbon Dioxide: Potential Environmental Impacts of CO₂-Organic Interactions." *Geochimica et Cosmochimica Acta* 74:A511-A11.

Kharaka YK, DR Cole, SD Hovorka, WD Gunter, KG Knauss, and BM Freifeld. 2006. "Gas-Water-Rock Interactions in Frio Formation Following CO₂ Injection: Implications for the Storage of Greenhouse Gases in Sedimentary Basins." *Geology* 34:577-80.

Kharaka YK, DR Cole, JJ Thordsen, E Kakouros, and HS Nance. 2006. "Gas-Water-Rock Interactions in Sedimentary Basins: Co2 Sequestration in the Frio Formation, Texas, USA." *Journal of Geochemical Exploration* 89:183-86.

Kharaka YK, and JS Hanor. 2007. "Deep Fluids in the Continents: I. Sedimentary Basins." in *Surface and Ground Water, Weathering and Soils*, ed. JI Drever, Vol 5, pp. 1-48. Elsevier, *Treatise on Geochemistry*.

Kharaka YK, JJ Thordsen, SD Hovorka, HS Nance, DR Cole, TJ Phelps, and KG Knauss. 2009. "Potential Environmental Issues of CO2 Storage in Deep Saline Aquifers: Geochemical Results from the Frio-I Brine Pilot Test, Texas, USA." *Applied Geochemistry* 24:1106-12.

Kharaka YK, JJ Thordsen, E Kakouros, G Ambats, WN Herkelrath, SR Beers, JT Birkholzer, JA Apps, NF Spycher, LE Zheng, RC Trautz, HW Rauch, and KS Gullickson. 2010. "Changes in the Chemistry of Shallow Groundwater Related to the 2008 Injection of CO2 at the ZERT Field Site, Bozeman, Montana." *Environmental Earth Sciences* 60:273-84.

Kirsch K, AK Navarre-Sitchler, A Wunsch, and JE McCray. 2014. "Metal Release from Sandstones under Experimentally and Numerically Simulated CO2 Leakage Conditions." *Environmental Science & Technology* 48:1436-42.

Larsen T, PI Qeldsen, and TH Christensen. 1992. "Correlation of Benzene, 1,1,1-Trichloroethane, and Naphthalene Distribution Coefficients to the Characteristics of Aquifer Materials with Low Organic Carbon Content." *Chemosphere* 24:979-91.

Last GV, CF Brown, CJ Murray, DH Bacon, NP Qafoku, M Sharma, and PD Jordan. 2013. *Determining Threshold Values for Identification of Contamination Predicted by Reduced Order Models*. Technical, Pacific Northwest National Laboratory, Richland, WA.

Lawrence SJ. 2006. *Description, Properties, and Degradation of Selected Volatile Organic Compounds Detected in Ground Water — a Review of Selected Literature*. Technical, U.S. Geological Survey, Reston, Virginia.

Lawter A, N Qafoku, H Shao, D Bacon, and C Brown. 2015. "Evaluating Impacts of CO2 and CH4 Gas Intrusion into an Unconsolidated Aquifer: Fate of as and Cd." *Frontiers in Environmental Science* 3:49.

Lawter A, NP Qafoku, G Wang, H Shao, and CF Brown. 2016. "Evaluating Impacts of CO2 Intrusion into an Unconsolidated Aquifer: I. Experimental Data." *International Journal of Greenhouse Gas Control* 44:323-33.

Lazareva O, G Druschel, and T Pichler. 2014. "Understanding Arsenic Behavior in Carbonate Aquifers: Implications for Aquifer Storage and Recovery (ASR)." *Applied Geochemistry*.

Leu JY, YH Lin, and FL Chang. 2011. "Conversion of CO₂ into CH₄ by Methane-Producing Bacterium FJ10 under a Pressurized Condition." *Chemical Engineering Research & Design* 89:1879-90.

Lewicki JL, J Birkholzer, and C-F Tsang. 2007. "Natural and Industrial Analogues for Leakage of CO₂ from Storage Reservoirs: Identification of Features, Events, and Processes and Lessons Learned." *Environ. Geol.* 52:457-67.

Little MG, and RB Jackson. 2010. "Potential Impacts of Leakage from Deep CO₂ Geosequestration on Overlying Freshwater Aquifers." *Environ. Sci. Technol.* 44:9225-32.

Lu J, JW Partin, SD Hovorka, and C Wong. 2010. "Potential Risks to Freshwater Resources as a Result of Leakage from CO₂ Geological Storage: A Batch-Reaction Experiment." *Environ. Earth Sci.* 60:335-48.

Mackay D, YS Wan, and CM Kuo. 1992. *Lustrated Handbook of Physical-Chemical Properties and Environmental Fate for Orgwric Chemicals. Volume 1. Monoaromatic Hydrocarbons, Chlorobenzenes, and Pcbs.* Lewis Boca Raton.

Maclay RW, and TA Small. 1994. *Carbonate Geology and Hydrology of the Edwards Aquifer in the San Antonio Area, Texas.* Technical Rpt. OFR 83-537, U.S. Geological Survey.

McGrath AE, GL Upson, and MD Caldwell. 2007. "Evaluation and Mitigation of Landfill Gas Impacts on Cadmium Leaching from Native Soils." *Ground Water Monitoring and Remediation* 27:99-109.

Mickler PJ, CB Yang, BR Scanlon, R Reedy, and JM Lu. 2013. "Potential Impacts of CO₂ Leakage on Groundwater Chemistry from Laboratory Batch Experiments and Field Push-Pull Tests." *Environmental Science & Technology* 47:10694-702.

Mohd Amin S, DJ Weiss, and MJ Blunt. 2014. "Reactive Transport Modelling of Geologic CO₂ Sequestration in Saline Aquifers: The Influence of Pure CO₂ and of Mixtures of CO₂ with CH₄ on the Sealing Capacity of Cap Rock at 37°C and 100 Bar." *Chemical Geology* 367:39-50.

Montes-Hernandez G, F Renard, and R Lafay. 2013. "Experimental Assessment of CO₂-Mineral-Toxic Ion Interactions in a Simplified Freshwater Aquifer: Implications for CO₂ Leakage from Deep Geological Storage." *Environmental Science & Technology* 47:6247-53.

Musgrove M, L Fahlquist, NA Houston, RJ Lindgren, and PB Ging. 2010. *Geochemical Evolution Processes and Water-Quality Observations Based on Results of the National Water-Quality Assessment Program in the San Antonio Segment of the Edwards Aquifer, 1996-2006.* Technical Rpt. Scientific Investigations Report 2010-5129, U.S. Geological Survey, Reston, Virginia.

Newmark RL, SJ Friedmann, and SA Carroll. 2010. "Water Challenges for Geologic Carbon Capture and Sequestration." *Environmental Management* 45:651-61.

Nicot J-P, CM Oldenburg, JE Houseworth, and J-W Choi. 2013. "Analysis of Potential Leakage Pathways at the Cranfield, MS, USA, CO₂ Sequestration Site." *International Journal of Greenhouse Gas Control* 18:388-400.

Nisi B, O Vaselli, F Tassi, J de Elio, AD Huertas, LF Mazadiego, and MF Ortega. 2013. "Hydrogeochemistry of Surface and Spring Waters in the Surroundings of the CO₂ Injection Site at Hontomin-Huermeces (Burgos, Spain)." *International Journal of Greenhouse Gas Control* 14:151-68.

Nordbotten JM, MA Celia, S Bachu, and HK Dahle. 2005. "Semianalytical Solution for CO₂ Leakage through an Abandoned Well." *Environ. Sci. Technol.* 39:602-11.

Oldenburg CM, and C Doughty. 2011. "Injection, Flow, and Mixing of CO₂ in Porous Media with Residual Gas." *Transport in Porous Media* 90:201-18.

Oldenburg CM, and AP Rinaldi. 2011. "Buoyancy Effects on Upward Brine Displacement Caused by CO₂ Injection." *Transport in Porous Media* 87:525-40.

Palandri J, and YK Kharaka. 2004. A Compilation of Rate Parameters of Water-Mineral Interaction Kinetics for Application to Geochemical Modeling. Technical, US Geol. Surv. Open File report 2004-1068.

Parkhurst DL, and CAJ Appelo. 1999. User's Guide to Phreeqc (Version 2) : A Computer Program for Speciation, Batch-Reaction, One-Dimensional Transport, and Inverse Geochemical Calculations. Technical Rpt. Water Resources Investigations Report 99-4259, U.S. Geological Survey, Washington, D.C.

Peter A, H Lamert, M Beyer, G Hornbruch, B Heinrich, A Schulz, H Geistlinger, B Schreiber, P Dietrich, U Werban, C Vogt, HH Richnow, J Grossmann, and A Dahmke. 2012. "Investigation of the Geochemical Impact of CO₂ on Shallow Groundwater: Design and Implementation of a CO₂ Injection Test in Northeast Germany." *Environmental Earth Sciences* 67:335-49.

Qafoku N, C Bown, G Wang, E Sullivan, A Lawter, O Harvey, and M Bowden. 2013. Geochemical Impacts of Leaking Co₂ from Subsurface Storage Reservoirs to Unconfined and Confined Aquifers. , Richland, Wa. . Technical Rpt. PNNL-22420.

RøeUtvik TI. 1999. "Chemical Characterisation of Produced Water from Four Offshore Oil Production Platforms in the North Sea." *Chemosphere* 39:2593-606.

Romanak KD, RC Smyth, C Yang, SD Hovorka, M Rearick, and J Lu. 2012. "Sensitivity of Groundwater Systems to CO₂: Application of a Site-Specific Analysis of Carbonate Monitoring Parameters at the SACROC CO₂-Enhanced Oil Field." *International Journal of Greenhouse Gas Control* 6:142-52.

Saleem ZA. 1999. *Anaerobic Biodegradation Rates of Organic Chemicals in Groundwater: A Summary of Field and Laboratory Studies*. Technical, U.S. Environmental Protection Agency, Office of Solid Waste, Washington, DC 20460.

Scherer GW, B Kutchko, N Thaulow, A Duguid, and B Mook. 2011. "Characterization of Cement from a Well at Teapot Dome Oil Field: Implications for Geological Sequestration." *Int. J. Greenhouse Gas Control* 5:115-24.

Scherf AK, C Zetzl, I Smirnova, M Zettlitzer, A Vieth-Hillebrand, and CO₂SINK Grp. 2011. "Mobilisation of Organic Compounds from Reservoir Rocks through the Injection of CO₂ - Comparison of Baseline Characterization and Laboratory Experiments." *Energy Procedia* 4:4524-31.

Shao H, N Qafoku, A Lawter, M Bowden, and C Brown. 2015. "Coupled Geochemical Impacts of Leaking CO₂ and Contaminants from Subsurface Storage Reservoirs on Groundwater Quality." *Environmental Science & Technology* 49(13): 8202-09.

Skinner L. 2003. *CO₂ Blowouts: An Emerging Problem : Well Control and Intervention*. 224, Gulf, Houston, TX, ETATS-UNIS.

Smyth RC, SD Hovorka, J Lu, KD Romanak, JW Partin, C Wong, and C Yang. 2009. "Assessing Risk to Fresh Water Resources from Long Term CO₂ Injection-Laboratory and Field Studies." *Energy Procedia* 1:1957-64.

Sø HU, D Postma, R Jakobsen, and F Larsen. 2008. "Sorption and Desorption of Arsenate and Arsenite on Calcite." *Geochimica et Cosmochimica Acta* 72:5871-84.

Sonnenthal E, A Ito, N Spycher, M Yui, J Apps, Y Sugita, M Conrad, and S Kawakami. 2005. "Approaches to Modeling Coupled Thermal, Hydrological, and Chemical Processes in the Drift Scale Heater Test at Yucca Mountain." *nt. J. Rock Mech. Min. Sci.* 42:6987-719.

Spangler LH, LM Dobeck, KS Repasky, AR Nehrir, SD Humphries, JL Barr, CJ Keith, JA Shaw, JH Rouse, AB Cunningham, SM Benson, CM Oldenburg, JL Lewicki, AW Wells, JR Diehl, BR Strazisar, JE Fessenden, TA Rahn, JE Amonette, JL Barr, WL Pickles, JD Jacobson, EA Silver, EJ Male, HW Rauch, KS Gullickson, R Trautz, Y Kharaka, J Birkholzer, and L Wielopolski. 2010. "A Shallow Subsurface Controlled Release Facility in Bozeman, Montana, USA, for Testing near Surface CO₂ Detection Techniques and Transport Models." *Environmental Earth Sciences* 60:227-39.

Swedlund PJ, JG Webster, and GM Miskelly. 2009. "Goethite Adsorption of Cu(II), Pb(II), Cd(II), and Zn(II) in the Presence of Sulfate: Properties of the Ternary Complex." *Geochimica et Cosmochimica Acta* 73:1548-62.

Taggart I. 2010. "Extraction of Dissolved Methane in Brines by CO₂ Injection: Implication for CO₂ Sequestration." *Spe Reservoir Evaluation & Engineering* 13:791-804.

Tesoriero AJ, and JF Pankow. 1996. "Solid Solution Partitioning of Sr²⁺, Ba²⁺, and Cd²⁺ to Calcite." *Geochimica Et Cosmochimica Acta* 60:1053-63.

Trautz RC, JD Pugh, C Varadharajan, LG Zheng, M Bianchi, PS Nico, NF Spycher, DL Newell, RA Esposito, YX Wu, B Dafflon, SS Hubbard, and JT Birkholzer. 2013. "Effect of Dissolved CO₂ on a Shallow Groundwater System: A Controlled Release Field Experiment." *Environmental Science & Technology* 47:298-305.

U.S. Environmental Protection Agency. 2009. Statistical Analysis of Groundwater Monitoring Data at RCRA Facilities, Unified Guidance. Technical Rpt. EPA 530/R-09-007, Washington, D.C.

Underschultz J, C Boreham, T Dance, L Stalker, B Freifeld, D Kirste, and J Ennis-King. 2011. "CO₂ Storage in a Depleted Gas Field: An Overview of the CO₂CRC Otway Project and Initial Results." *International Journal of Greenhouse Gas Control* 5:922-32.

Varadharajan C, RM Tinnacher, JD Pugh, RC Trautz, LG Zheng, NF Spycher, JT Birkholzer, H Castillo-Michel, RA Esposito, and PS Nico. 2013. "A Laboratory Study of the Initial Effects of Dissolved Carbon Dioxide (CO₂) on Metal Release from Shallow Sediments." *International Journal of Greenhouse Gas Control* 19:183-211.

Viswanathan H, ZX Dai, C Lopano, E Keating, JA Hakala, KG Scheckel, LG Zheng, GD Guthrie, and R Pawar. 2012. "Developing a Robust Geochemical and Reactive Transport Model to Evaluate Possible Sources of Arsenic at the CO₂ Sequestration Natural Analog Site in Chimayo, New Mexico." *International Journal of Greenhouse Gas Control* 10:199-214.

Vong CQ, N Jacquemet, G Picot-Colbeaux, J Lions, J Rohmer, and O Bouc. 2011. "Reactive Transport Modeling for Impact Assessment of a CO₂ Intrusion on Trace Elements Mobility within Fresh Groundwater and Its Natural Attenuation for Potential Remediation." *10th International Conference on Greenhouse Gas Control Technologies* 4:3171-78.

Wang G, N Qafoku, A Lawter, M Bowden, O Harvey, C Sullivan, and C Brown. 2016. "Geochemical Impacts of Leaking CO₂ from Subsurface Storage Reservoirs to an Unconfined Oxidizing Carbonate Aquifer." *International Journal of Greenhouse Gas Control* 44:310-22.

Wang S, and PR Jaffe. 2004. "Dissolution of a Mineral Phase in Potable Aquifers Due to CO₂ Releases from Deep Formations; Effect of Dissolution Kinetics." *Energy Convers. manage.* 45:2833-48.

Wei Y, M Maroto-Valer, and MD Steven. 2011. "Environmental Consequences of Potential Leaks of CO₂ in Soil." *Energy Procedia* 4:3224–30.

White MD, DH Bacon, BP McGrail, DJ Watson, SK White, and ZF Zhang. 2012. STOMP Subsurface Transport over Multiple Phases: STOMP-CO₂ and STOMP-CO₂e Guide: Version 1.0, PNNL-21268. Technical, Pacific Northwest National Laboratory, Richland, WA.

White MD, and BP McGrail. 2005. Stomp, Subsurface Transport over Multiple Phases, Version 1.0, Addendum: Ekechem, Equilibrium-Conservation-Kinetic Equation Chemistry and Reactive Transport. Technical Rpt. PNN-15482, Pacific Northwest National Laboratory, Richland, Washington.

Wilkin RT, and DC Digiulio. 2010. "Geochemical Impacts to Groundwater from Geologic Carbon Sequestration: Controls on pH and Inorganic Carbon Concentrations from Reaction Path and Kinetic Modeling." *Environ. Sci. Technol.* 44:4821-27.

Witter AE, and AD Jones. 1999. "Chemical Characterization of Organic Constituents from Sulfide-Rich Produced Water Using Gas Chromatography/Mass Spectrometry." *Environ. Toxicol. Chem.* 18:1920-26.

Wolery TW, and RL Jarek. 2003. Software User's Manual, Eq3/6, Version 8.0. Technical, Sandia National Laboratories, Albuquerque, New Mexico.

Wunsch A, AK Navarre-Sitchler, J Moore, and JE McCray. 2014. "Metal Release from Limestones at High Partial-Pressures of CO₂." *Chemical Geology* 363:40-55.

Wunsch A, AK Navarre-Sitchler, J Moore, A Ricko, and JE McCray. 2013. "Metal Release from Dolomites at High Partial-Pressures of CO₂." *Applied Geochemistry* 38:33-47.

Xu T, E Sonnenthal, N Spycher, and K Pruess. 2006. "Toughreact: A Simulation Program for Non-Isothermal Multiphase Reactive Geochemical Transport in Variably Saturated Geologic Media." *Computers and Geosciences* 32:145-65.

Yang C, Z Dai, KD Romanak, SD Hovorka, and RH Trevino. 2014. "Inverse Modeling of Water-Rock-CO₂ Batch Experiments: Potential Impacts on Groundwater Resources at Carbon Sequestration Sites." *Environ Sci Technol* 48:2798-806.

Yang CB, PJ Mickler, R Reedy, BR Scanlon, KD Romanak, JP Nicot, SD Hovorka, RH Trevino, and T Larson. 2013. "Single-Well Push-Pull Test for Assessing Potential Impacts of CO₂ Leakage on Groundwater Quality in a Shallow Gulf Coast Aquifer in Cranfield, Mississippi." *International Journal of Greenhouse Gas Control* 18:375-87.

Yokoyama Y, K Tanaka, and Y Takahashi. 2012. "Differences in the Immobilization of Arsenite and Arsenate by Calcite." *Geochimica Et Cosmochimica Acta* 91:202-19.

Zheng L, JA Apps, N Spycher, JT Birkholzer, YK Kharaka, J Thordsen, SR Beers, WN Herkelrath, E Kakouros, and RC Trautz. 2012. "Geochemical Modeling of Changes in Shallow Groundwater Chemistry Observed During the MSU-ZERT CO₂ Injection Experiment." *International Journal of Greenhouse Gas Control* 7:202-17.

Zheng L, JA Apps, Y Zhang, T Xu, and JT Birkholzer. 2009. "On Mobilization of Lead and Arsenic in Groundwater in Response to CO₂ Leakage from Deep Geological Storage." *Chemical geology* 268:281-97.

Zheng L, NP Qafoku, A Lawter, G Wang, H Shao, and CF Brown. 2016. "Evaluating Impacts of CO₂ Intrusion into an Unconsolidated Aquifer: Ii. Modeling Results." *International Journal of Greenhouse Gas Control* 44:300-09.

Zheng L, N Spycher, J Birkholtzer, T Xu, J Apps, and Y Kharaka. 2013. "On Modeling the Potential Impacts of CO₂ Sequestration on Shallow Groundwater: Transport of Organics and Co-Injected H₂s by Supercritical CO₂ to Shallow Aquifers." *International Journal of Greenhouse Gas Control* 14:113-27.

Zheng L, N Spycher, J Birkholzer, T Xu, and J Apps. 2010. Modeling Studies on the Transport of Benzene and H₂S in CO₂-Water Systems. Technical, Lawrence Berkeley National Laboratory, Berkeley, California.

Zheng L, N Spycher, C Varadharajan, RM Tinnachera, JD Pugh, M Bianchi, J Birkholzer, PS Nico, and RC Trautz. 2015. "On the Mobilization of Metals by CO₂ Leakage into Shallow Aquifers: Exploring Release Mechanisms by Modeling Field and Laboratory Experiments " *Greenhouse Gases: Science and Technology* 5:403-18.

Zhong L, KJ Cantrell, DH Bacon, and J Shewell. 2014. "Transport of Organic Contaminants Mobilized from Coal through Sandstone Overlying a Geological Carbon Sequestration Reservoir." *International Journal of Greenhouse Gas Control* 21:158-64.

Zhong LR, K Cantrell, A Mitroshkov, and J Shewell. 2014. "Mobilization and Transport of Organic Compounds from Reservoir Rock and Caprock in Geological Carbon Sequestration Sites." *Environmental Earth Sciences* 71:4261-72.



Pacific Northwest
NATIONAL LABORATORY

*Proudly Operated by **Battelle** Since 1965*

902 Battelle Boulevard
P.O. Box 999
Richland, WA 99352
1-888-375-PNNL (7665)

U.S. DEPARTMENT OF
ENERGY

www.pnnl.gov